Basic Physics

Structure of Matter

1-1 THE ATOM

All matter is composed of individual entities called elements. Each element is distinguishable from the others by the physical and chemical properties of its basic component—the atom. Originally thought to be the "smallest" and "indivisible" particle of matter, the atom is now known to have a substructure and can be "divided" into smaller components. Each atom consists of a small central core, the nucleus, where most of the atomic mass is located and a surrounding "cloud" of electrons moving in orbits around the nucleus. Whereas the radius of the atom (radius of the electronic orbits) is approximately 10^{-10} m, the nucleus has a much smaller radius, namely, about 10^{-15} m. Thus, for a high-energy electron, photon, or a particle of size comparable to nuclear dimensions, it will be quite possible to penetrate several atoms of matter before a collision happens. As will be pointed out in the chapters ahead, it is important to keep track of those particles or photons that have not interacted with the atoms and those that have suffered collisions.

1-2 THE NUCLEUS

The properties of atoms are derived from the constitution of their nuclei and the number and the organization of the orbital electrons.

The nucleus contains two kinds of fundamental particles: protons and neutrons. Whereas protons are positively charged, neutrons have no charge. Because the electron has a negative unit charge (1.602×10^{-19} C) and the proton has a positive unit charge, the number of protons in the nucleus is equal to the number of electrons outside the nucleus of an electrically neutral atom.

An atom is completely specified by the formula ${}^{A}_{Z}X$, where X is the chemical symbol for the element; A is the mass number, defined as the number of nucleons (neutrons and protons in the nucleus); and Z is the atomic number, denoting the number of protons in the nucleus (or the number of electrons outside the nucleus). An atom represented in such a manner is also called a nuclide. For example, ${}^{1}H$ and ${}^{4}_{2}He$ represent atoms or nuclei or nuclides of hydrogen and helium، respectively.

On the basis of different proportions of neutrons and protons in the nuclei, atoms have been classified into the following categories: isotopes, atoms

having nuclei with the same number of protons but different number of neutrons; isotones, atoms having the same number of neutrons but different number of protons; isobars, atoms with the same number of nucleons but different number of protons; and isomers, atoms containing the same number of protons as well as neutrons. The last category, namely isomers, represents identical atoms except that they differ in their nuclear energy states. For example, ${}^{131m}_{54}Xe$ (m stands for metastable state) is an isomer of ${}^{131}_{54}Xe$.

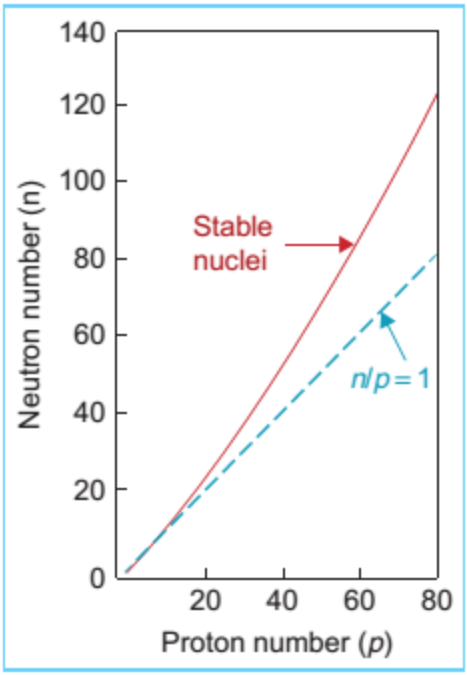

Figure 1.1. a plot of neutrons versus protons in stable nuclei.

Certain combinations of neutrons and protons result in stable (nonradioactive) nuclides than others. For instance, stable elements in the low atomic number range have an almost equal number of neutrons, N, and protons, Z. However, as Z increases beyond about 20, the neutron to-proton ratio for stable nuclei becomes greater than 1 and increases with Z. This is evident in

Figure 1.1, which shows a plot of the number of neutrons versus protons in stable nuclei.

Nuclear stability has also been analyzed in terms of even and odd numbers of neutrons and protons. of about 300 different stable isotopes, more than half have even numbers of protons.

1.3 ATOMIC MASS AND ENERGY UNITS

Masses of atoms and atomic particles are conveniently given in terms of atomic mass unit (amu). An amu is defined as 1/12 of the mass of a ${}^{12}_{6}C$ atom. Thus, the ${}^{12}_{6}C$ atom is arbitrarily assigned the mass equal to 12 amu. In basic units of mass 1 amu = 1.66×10^{-27} kg

The mass of an atom expressed in terms of amu is known as atomic mass or atomic weight.

Another useful term is gram atomic weight, which is defined as the mass in grams numerically equal to the atomic weight. According to Avogadro's law, every gram atomic weight of a substance contains the same number of atoms. The number, referred to as Avogadro number or Avogadro constant (N_A), has been measured by many investigators, and its currently accepted value is 6.0221 X 10^{23} atoms per gram atomic weight (or mole).

From the previous definitions, one can calculate other quantities of interest such as the number of atoms per gram, grams per atom, and electrons per gram. Considering helium as an example, its atomic weight (A_W) is equal to 4.0026.

Therefore,

$$\text{Number of atoms/g} = \frac{N_A}{A_W} = 1.505 \times 10^{23}$$

$$\text{Grams/atom} = \frac{A_W}{N_A} = 6.646 \times 10^{-24}$$

$$\text{Number of electrons/g} = \frac{N_A \cdot Z}{A_W} = 3.009 \times 10^{23}$$

The masses of atomic particles, according to the amu, are electron = 0.000548 amu, proton= 1.00727 amu, and neutron = 1.00866 amu.

Because the mass of an electron is much smaller than that of a proton or neutron and protons and neutrons have nearly the same mass, equal to approximately 1 amu, all the atomic masses in units of amu are very nearly equal to the mass number. However, it is important to point out that the mass of an atom is not exactly equal to the sum of the masses of constituent particles.

The reason for this is that, when the nucleus is formed, a certain mass is destroyed and converted into energy that acts as a "glue" to keep the nucleons together. This mass difference is called the mass defect. Looking at it from a different perspective, an amount of energy equal to the mass

defect must be supplied to separate the nucleus into individual nucleons. Therefore, this energy is also called the binding energy of the nucleus.

The basic unit of energy is joule (J) and is equal to the work done when a force of 1 newton acts through a distance of 1 m. The newton, in turn, is a unit of force given by the product of mass (1 kg) and acceleration (1 m/s^2). However, a more convenient energy unit in atomic and nuclear physics is electron volt (eV), defied as the kinetic energy acquired by an electron in passing through a potential difference of 1 V. It can be shown that the work done in this case is given by the product of potential difference and the charge on the electron. Therefore, we have:

$1eV = 1\ V \times 1.602 \times 10^{-19}\ C = 1.602 \times 10^{-19}\ J$

Multiples of this unit are 1keV = 1,000 eV

1million eV (MeV) = 1,000,000 eV

According to Einstein's principle of equivalence of mass and energy, a mass m is equivalent to energy E and the relationship is given by

$E = mc^2$

where c is the velocity of light (3×10^8 m/s). For example, a mass of 1 kg, if converted to energy، is equivalent to

$E = 1\ kg \times (3 \times 10^8\ m/s)^2$

$= 9X\ 10^{16}\ J = 5.62 \times 10^{29}\ MeV$

The mass of an electron at rest is sometimes expressed in terms of its energy equivalent (E_0). Because its mass is 9.1×10^{-31} kg, we have:

$E_0 = 0.511\ MeV$

Another useful conversion is that of amu to energy. It can be shown that

1amu = 931.5 MeV

we can see that the equivalent mass of any particle of total energy E (kinetic plus rest mass energy) is given by E/c^2. Accordingly, masses of particles may also be expressed in units of GeV/c^2. It can be shown that

$1GeV/c^2 = 1.0723$ amu

In the above examples, we have not considered the effect of particle velocity on its mass. Experiments with high-speed particles have shown that the mass of a particle depends on its velocity and that it increases with

velocity. The relationship between mass and velocity can be derived from Einstein's theory of relativity. If m is the mass of a particle moving with velocity υ and m_0 is its rest mass, then

$$m = \frac{m_0}{\sqrt{1 - v^2/c^2}}$$

The kinetic energy (E_k) is given by

$$E_k = mc^2 - m_0c^2 = m_0c^2\left[\frac{1}{\sqrt{1 - \frac{v^2}{c^2}}} - 1\right]$$

It should be noted that the relativistic effect of velocity on mass becomes important when a particle travels with a velocity comparable to that of light.

1.4: DISTRIBUTION OF ORBITAL ELECTRONS

According to the model proposed by Niels Bohr in 1913, the electrons revolve around the nucleus in specific orbits and are prevented from leaving the atom by the centripetal force of attraction between the positively charged nucleus and the negatively charged electron.

On the basis of classical physics, an accelerating or revolving electron must radiate energy.

This would result in a continuous decrease of the radius of the orbit with the electron eventually spiraling into the nucleus. However, the data on the emission or absorption of radiation by elements reveal that the change of energy is not continuous but discrete. To explain the observed line spectrum of hydrogen, Bohr theorized that the sharp lines of the spectrum represented electron jumps from one orbit down to another with the emission of light of a particular frequency or a quantum of energy. He proposed two fundamental postulates: (a) electrons can exist only in those orbits for which the angular momentum of the electron is an integral multiple of $h/2\pi$، where h is the Planck's constant (6.626×10^{-34} J-sec); and (b) no energy is gained or lost while the electron remains in any one of the permissible orbits.

The arrangement of electrons outside the nucleus is governed by the rules of quantum mechanics and the Pauli exclusion principle (not discussed here). Although the actual configuration of electrons is rather complex and dynamic, one may simplify the concept by assigning electrons to specific orbits. The innermost orbit or shell is called the K shell. The next shells are

L, M, N, and O. The maximum number of electrons in an orbit is given by 2n2, where n is the orbit number.

For example, a maximum of 2 electrons can exist in the first orbit, 8 in the second, and 18 in the third. Figure 1.2 shows the electron orbits of hydrogen, helium, and oxygen atoms.

A shell need not be completely filed before the electrons begin to fil the next shell.

For most atoms, when the number of electrons in the outermost shell reaches 8, additional electrons begin to fil the next level to create a new outermost shell before more electrons are added to the lower shell. For example, an atom of calcium has 20 electrons, with 2 in the K shell، 8 in the L shell, 8 in the M shell, and the remaining 2 in the N shell. Electrons in the outermost orbit are called the valence electrons. The chemical properties of an atom depend on the number of electrons in the outermost orbit.

Electron orbits can also be considered as energy levels. The energy in this case is the potential energy of the electrons. With the opposite sign it may also be called the binding energy of the electron.

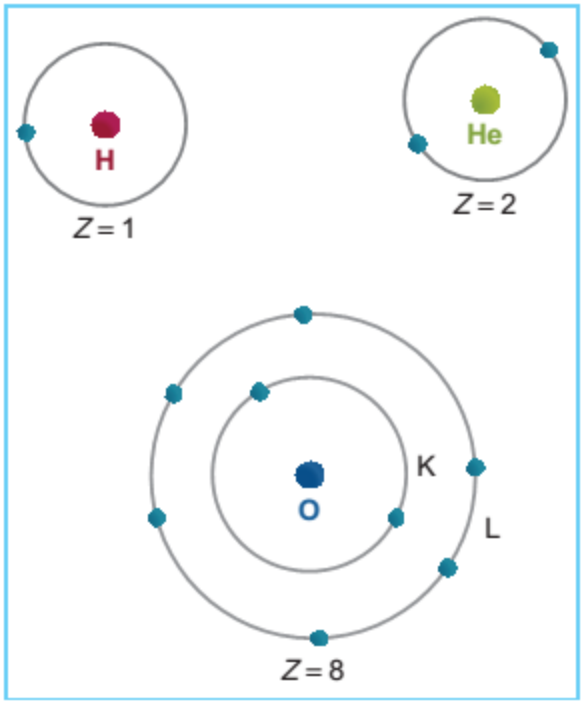

Figure 1.2. electron orbits for hydrogen, helium, and oxygen.

1.5 ATOMIC ENERGY LEVELS

It is customary to represent the energy levels of the orbital electrons by what is known as the energy level diagram (Fig. 1.3). The binding energies of the electrons in various shells depend on the magnitude of Coulomb force of attraction between the nucleus and the orbital electrons.

Thus the binding energies for the higher Z atoms are greater because of the greater nuclear charge. In the case of tungsten (Z = 74), the electrons in the K, L, and M shells have binding energies of about 69,500, 11,000, and 2,500 eV, respectively. The so-called valence electrons، which are responsible for chemical reactions and bonds between atoms as well as the emission of optical radiation spectra, normally occupy the outer shells. If energy is imparted to one of these valence electrons to raise it to a higher energy (higher potential energy but lower binding energy) orbit, this will create a state of atomic instability. The electron will fall back to its normal position with the emission of energy in the form of optical radiation. The energy of the emitted radiation will be equal to the energy difference of the orbits between which the transition took place.

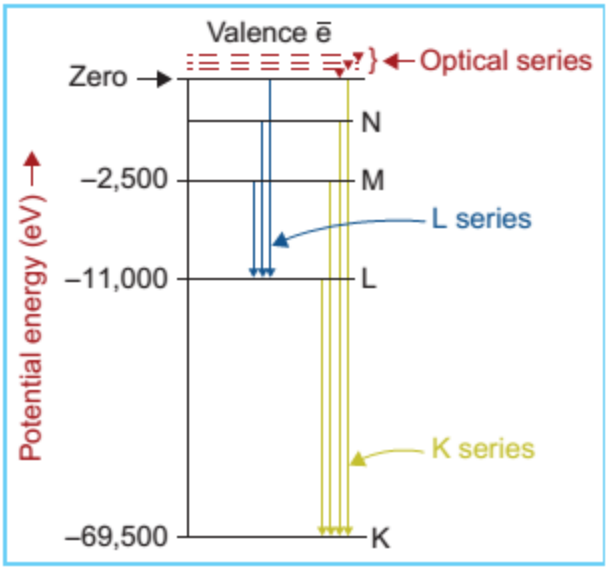

Figure 1.3. A simplified energy level diagram of the tungsten atom (not to scale). Only few possible transitions are shown for illustration. Zero of the energy scale is arbitrarily set at the position of the valence electrons when the atom is in the unexcited state.

If the transition involved inner orbits, such as K, L, and M shells where the electrons are more tightly bound (because of larger Coulomb forces), the absorption or emission of energy will involve higher energy radiation. Also, if sufficient energy is imparted to an inner orbit electron so that it is

completely ejected from the atom, the vacancy or the hole created in that shell will be almost instantaneously filed by an electron from a higher level orbit. To conserve energy، this transition would be accompanied either by an emission of radiation, such as characteristic x-rays, or the ejection of an outer shell electron, known as the Auger electron.

1.6 NUCLEAR FORCES

As discussed earlier, the nucleus contains neutrons that have no charge and protons with positive charge. But how are these particles held together, in spite of the fact that electrostatic repulsive forces exist between particles of similar charge? Earlier, in Section 1.3, the terms mass defect and binding energy of the nucleus were mentioned. It was then suggested that the energy required to keep the nucleons together is provided by the mass defect. However, the nature of the forces involved in keeping the integrity of the nucleus is quite complex and will be discussed here only briefly. There are four different forces in nature. These are, in the order of their strengths: (a) strong nuclear force, (b) electromagnetic force, (c) weak nuclear force, and (d) gravitational force. Of these, the gravitational force involved in the nucleus is very weak and can be ignored. The electromagnetic force between charged nucleons is quite strong, but it is repulsive and tends to disrupt the nucleus. A force much larger than the electromagnetic force is the strong nuclear force that is responsible for holding the nucleons together in the nucleus. The weak nuclear force is much weaker and appears in certain types of radioactive decay (e.g., b decay).

The strong nuclear force is a short-range force that comes into play when the distance between the nucleons becomes smaller than the nuclear diameter ($\sim 10^{-15}$ m). If we assume that a nucleon has zero potential energy when it is an infinite distance apart from the nucleus, then as it approaches close enough to the nucleus to be within the range of nuclear forces, it will experience strong attraction and will "fall" into the potential well (Fig. 1.4A). This potential well is formed as a result of the mass defect and provides the nuclear binding energy. It acts as a potential barrier against any nucleon escaping the nucleus.

In the case of a positively charged particle approaching the nucleus, there will be a potential barrier due to the Coulomb forces of repulsion, preventing the particle from approaching the nucleus. If, however, the particle is able to get close enough to the nucleus so as to be within the range of the strong nuclear forces, the repulsive forces will be overcome

and the particle will be able to enter the nucleus. Figure 1.4B illustrates the potential barrier against a charged particle such as an α particle (traveling $^{4}_{2}He$ nucleus) approaching a $^{238}_{92}U$ nucleus. Conversely, the barrier serves to prevent an α particle escaping from the nucleus. Although it appears, according to the classical ideas, that an α particle would require a minimum energy equal to the height of the potential barrier (30 MeV) in order to penetrate the 23892U nucleus or escape from it, the data show that the barrier can be crossed with much lower energies. This has been explained by a complex mathematical theory known as wave mechanics, in which particles are considered associated with de Broglie waves.

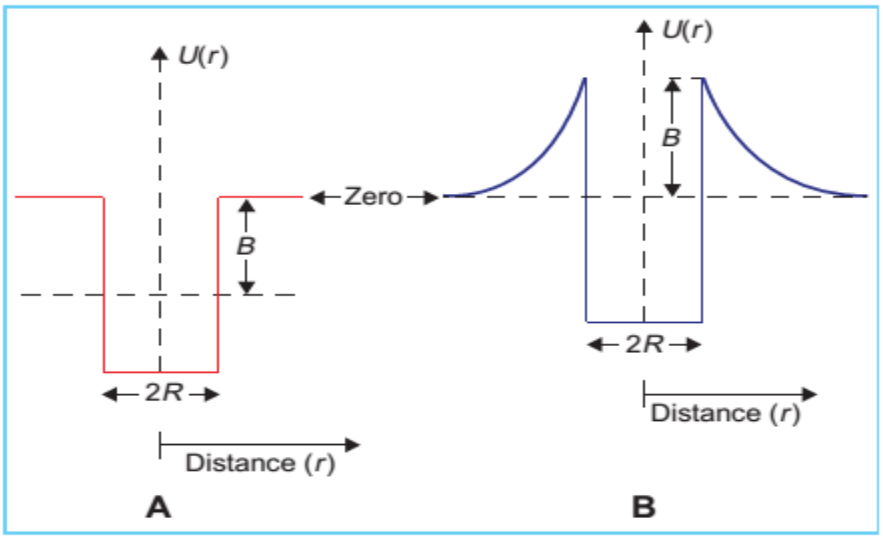

Figure 1.4. Energy level diagram of a particle in a nucleus: A: Particle with no charge; B: Particle with positive charge; U(r) is the potential energy as a function of distance r from the center of the nucleus. B is the barrier height R is the nuclear radius.

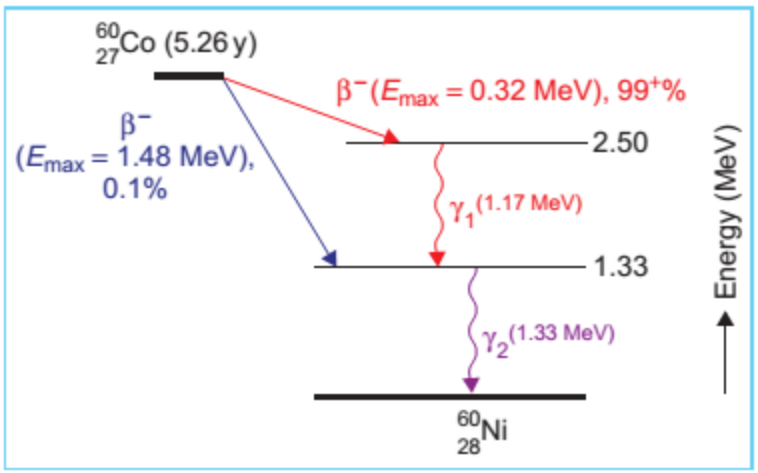

Figure 1.5. Energy level diagram for the decay of $^{60}_{27}Co$ nucleus.

1.7 NUCLEAR ENERGY LEVELS

The shell model of the nucleus assumes that the nucleons are arranged in shells, representing discrete energy states of the nucleus similar to the atomic energy levels. If energy is imparted to the nucleus, it may be raised to an excited state, and when it returns to a lower energy state, it will give off energy equal to the energy difference of the two states. Sometimes the energy is radiated in steps, corresponding to the intermediate energy states, before the nucleus settles down to the stable or ground state.

Figure 1.5 is an example of a decay scheme which shows the decay of excited states of nuclei.

In these diagrams, energy is plotted in the vertical axis and the atomic number is plotted on the horizontal axis. This figure shows a decay scheme of a cobalt-60 $^{60}_{27}Co$ nucleus which has been made radioactive in a reactor by bombarding stable $^{59}_{27}Co$ atoms with neutrons. The excited $^{60}_{27}Co$ nucleus fist emits a particle, known as β^- particle, and then, in two successive jumps, emits packets of energy, known as photons. The emission of a β^- particle is the result of a nuclear transformation in which one of the neutrons in the nucleus disintegrates into a proton, an electron، and a neutrino. The electron and neutrino are emitted instantaneously and share the released energy with the recoiling nucleus. The process of b decay will be discussed in the next chapter.

1.8 PARTICLE RADIATION

The term radiation applies to the emission and propagation of energy through space or a material medium. By particle radiation, we mean energy propagated by traveling corpuscles that have a definite rest mass and within limits have a definite momentum and defined position at any instant. However, the distinction between particle radiation and electromagnetic waves, both of which represent modes of energy travel, became less sharp when, in 1925, de Broglie introduced a hypothesis concerning the dual nature of matter. He theorized that not only do photons (electromagnetic waves) sometimes appear to behave like particles (exhibit momentum) but also material particles such as electrons, protons, and atoms have some type of wave motion associated with them (show refraction and other wave-like properties).

Besides protons, neutrons, and electrons discussed earlier, many other atomic and subatomic particles have been discovered. These particles can travel with high speeds, depending on their kinetic energy, but never attain

exactly the speed of light in a vacuum. Also, they interact with matter and produce varying degrees of energy transfer to the medium.

1.9 ELEMENTARY PARTICLES

Elementary or fundamental particles are particles that are not known to have substructure. In the past, the name was given to protons, neutrons, and electrons. With the discovery that protons and neutrons have substructure (quarks), they are no longer considered fundamental particles. The following discussion of elementary particles is presented here for general interest.

There are two classes of particles: fermions and bosons. Fermion is a general name given to a particle of matter or antimatter that is characterized by spin in odd half integer quantum units of angular momentum (1/2, 3/2, 5/2,…). Boson is a general name for any particle with a spin of an integer number (1, 2, 3, …).

The fundamental particles of matter (fermions) are of two kinds: quarks and leptons. There are six types of each, as listed below:

•Quarks: up (u), down (d), charm (c), strange (s), top (t), and bottom (b)؛

•Leptons: electron (e), electron neutrino (ν_e) ، muon (μ), muon neutrino (ν_μ) ،tau (τ), and tau neutrino (ν_τ).

Besides the above 12 elementary particles of matter, there are 12 corresponding elementary particles of antimatter. This follows the principle discovered by Paul Dirac (1928) which states that for every particle of matter there must be another particle of antimatter with the same mass but opposite charge. So there are six antiquarks and six antileptons.

Quarks are the building blocks of heavier particles, called hadrons (neutrons, protons، mesons, etc.). For example, it takes three quarks (u, u, d) to make a proton and three quarks (u, d, d) to make a neutron. These quarks are held together by field particles called gluons, the messenger particles of the strong nuclear force.

The class of particles called the messenger particles are the carriers of force in a force field according to the quantum electrodynamics (QED) theory. These particles of force are not material particles but quanta of the field. Thus, the force between any two interacting matter particles is transmitted by the messenger particles traveling at the speed of light, which is the speed with which all photons travel.

There are 13 messenger particles or bosons that mediate the four forces of nature. They are listed below:

Electromagnetism	photon (γ)
Strong force	eight gluons
Weak force	W^+, W^-, Z^o
Gravity	graviton (not yet detected)

Whereas matter particles (fermions) can attain high energy or speeds, they cannot quite attain the speed of light. When their speed reaches close to that of light, further acceleration increases their energy through an increase in their mass rather than their speed. So the ultrahigh energy particles produced in accelerators (e.g., Tevatron at Fermi Lab and CERN in Geneva) have greater mass but are not as swift as light. The messenger particles (bosons), on the other hand، can have high quantum energies but they all travel with the speed of light. They can also transform themselves into material particles, whereby their high energy is converted into high-energy material particles. For example, W^+ to electron (e^-) and neutrino (ν), W^- to electron (e^-) and antineutrino (n), and Z° to e^+ and e^- or a pair of mesons ($\mu^+ + \mu-$). W+ or W^- have a quantum energy of about 79 GeV and Z° about 91 GeV. Another mysterious particle has been added to the above list. It is called the Higgs boson, after Peter Higgs, who postulated its existence in 1964. Particle physicists believe that our universe is pervaded with Higgs bosons. The Higgs field is thought to permeate all space and is the same everywhere. All the rest mass of matter is generated by the Higgs field. In other words, particles acquire their mass through interaction with Higgs field. The sea of Higgs bosons produces a drag effect on the particles, thereby manifesting properties of inertia. The resistance to motion defies their mass.

It should be mentioned that Higgs idea was used by theoretical physicists Steven Weinberg and Abdus Salam to combine electromagnetic and weak forces into a unified electroweak force، mediated by messenger particles, photon, W^+, W^-, and Z_0.

Back to the Higgs field, the term field in physics is defined as lines of force. For example, a magnet is surrounded by its magnetic field. A particle of iron placed in the field will be attracted toward the magnetic pole and follow a path or a line of magnetic force. The forces are transmitted in a field by the exchange of force carriers such as photons, W or Z bosons, and gluons. For the Higgs field, the force carrier is the Higgs particle (a boson).

The Higgs boson was tentatively observed in July 2012. The announcement came on the basis of research findings from the large hadron collider (LHC) at CERN. Further analysis of the LHC's 2012 data showed that the observed particle is a Higgs boson of spin zero. The scientists announced their tentative confirmation on March 14, 2013.

Figure 1.6 is a chart of fundamental particles. It provides a glimpse of the current knowledge in particle physics.

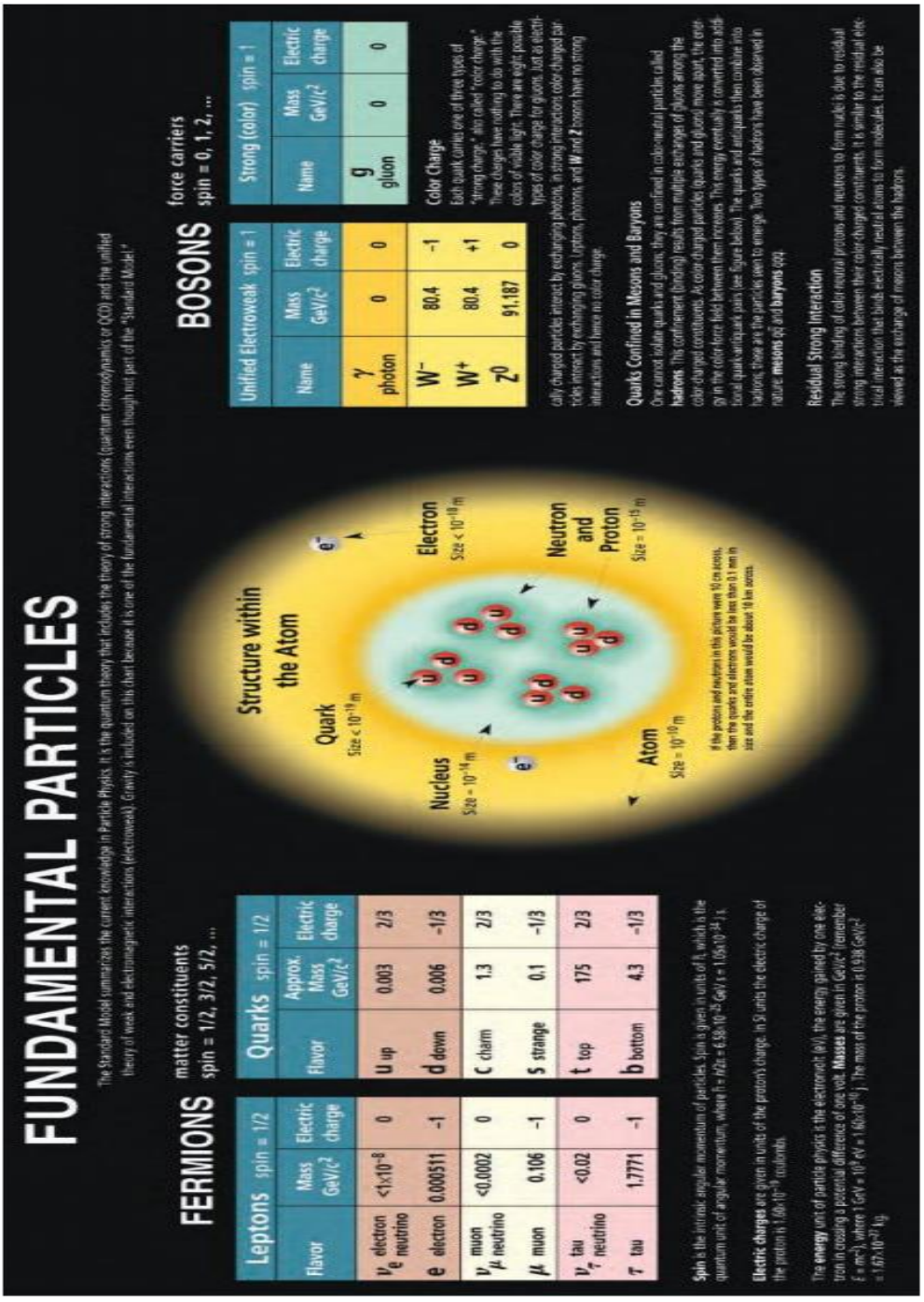

Figure 1.6. A chart of fundamental particles and interactions.

1.10 ELECTROMAGNETIC RADIATION

A. WAVE MODEL

Electromagnetic radiation constitutes the mode of energy propagation for such phenomena as light waves, heat waves, radio waves, microwaves, ultraviolet rays, x-rays, and γ rays. These radiations are called "electromagnetic" because they were fist described, by Maxwell, in terms of oscillating electric and magnetic fields. As illustrated in Figure 1.7, an electromagnetic wave can be represented by the spatial variations in the intensities of an electric field (E) and a magnetic field (H), the fields being at right angles to each other at any given instant. Energy is propagated with the speed of light (3×10^8 m/s in vacuum) in the Z direction. The relationship between wavelength (l), frequency (n), and velocity of propagation (c) is given by $c = n\lambda$

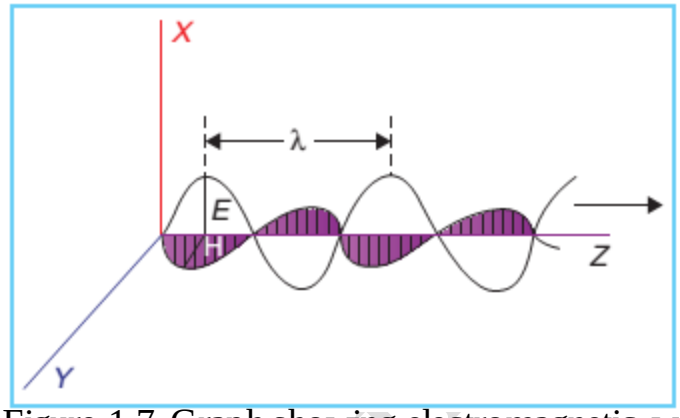

Figure 1.7. Graph showing electromagnetic wave at a given instant of time. E and H are, respectively, the peak amplitudes of electric and magnetic fields. The two fields are perpendicular to each other.

In the above equation, c should be expressed in meters per second; l, in meters; and ν, in cycles per second or hertz.

Figure 1.8 shows a spectrum of electromagnetic radiations with wavelengths ranging anywhere from 10^7 (radio waves) to 10^{-13} m (ultrahigh-energy x-rays). Since wavelength and frequency are inversely related, the frequency spectrum corresponding to the above range will be 3×10^1 to 3×10^{21} cycles/s. Only a very small portion of the electromagnetic spectrum constitutes visible light bands. The wavelengths of the wave to which the human eye responds range from 4×10^{-7} (blue light) to 7×10^{-7} m (red).

The wave nature of the electromagnetic radiation can be demonstrated by experiments involving phenomena such as interference and diffraction of

light. Similar effects have been observed with x-rays using crystals which possess interatomic spacing comparable to the x-ray wavelengths. However, as the wavelength becomes very small or the frequency becomes very large, the dominant behavior of electromagnetic radiations can only be explained by considering their particle or quantum nature.

B. QUANTUM MODEL

To explain the results of certain experiments involving interaction of radiation with matter, such as the photoelectric effect and the Compton scattering, one has to consider electromagnetic radiations as particles rather than waves. The amount of energy carried by such a packet of energy, or photon, is given by $E = h\nu$

where E is the energy (joules) carried by the photon, h is the Planck's constant (6.626×10^{-34} J-sec) and ν is the frequency (cycles/s). By combining above Equations, we have

$$E = \frac{hc}{\lambda}$$

If E is to be expressed in electron volts (eV) and λ in meters (m), then, since 1 eV = 1.602×10^{-19}J:

$$E = \frac{1.24\,x\,10^{-6}}{\lambda}$$

The above equations indicate that as the wavelength becomes shorter or the frequency becomes larger, the energy of the photon becomes greater. This is also seen in Figure 1.8.

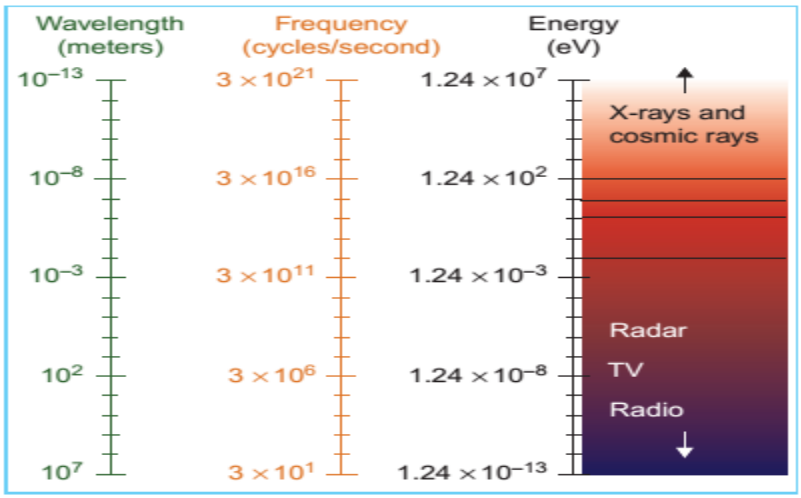

Figure 1.8. The electromagnetic spectrum. Ranges are approximate.

Nuclear Transformations

2.1 .Radioactivity

Radioactivity, first discovered by Antonio Henri Becquerel (1852 to 1908) in 1896, is a phenomenon in which radiation is given off by the nuclei of the elements. This radiation can be in the form of particles, electromagnetic radiation, or both.

Figure 2.1 illustrates a method in which radiation emitted by radium can be separated by a magnetic field. Since α particle (helium nuclei) are positively charged and β particles (electrons) are negatively charged, they are deflected in opposite directions. The difference in the radii of curvature indicates that α particles are much heavier than β particles. On the other hand، γ rays, which are similar to x-rays except for their nuclear origin, have no charge and, therefore، are unaffected by the magnetic field.

It was mentioned in Chapter 1 (Section 1.6) that there is a potential barrier preventing particles from entering or escaping the nucleus. Although the particles inside the nucleus possess kinetic energy, this energy, in a stable nucleus, is not sufficient for any of the particles to penetrate the nuclear barrier. However, a radioactive nucleus has excess energy that is constantly redistributed among the nucleons by mutual collisions. As a matter of probability, one of the particles may gain enough energy to escape from the nucleus, thus enabling the nucleus to achieve a state of lower energy. Also, the emission of a particle may still leave the nucleus in an excited state. In that case, the nucleus will continue stepping down to lower energy states by emitting particles or γ rays until the stable (ground) state has been achieved.

2.2 .Decay Constant

The process of radioactive decay or disintegration is a statistical phenomenon. Whereas it is not possible to know when a particular atom will disintegrate, one can accurately predict, in a large collection of atoms, the proportion that will disintegrate in a given time. The mathematics of radioactive decay is based on the simple fact that the change in the number of atoms per unit time, $(\Delta N/\Delta t)$, is proportional to the number of radioactive atoms, (N) present. Mathematically,

$$\frac{\Delta N}{\Delta t} \propto N \text{ or } \frac{\Delta N}{\Delta t} = -\lambda N \quad (2.1)$$

where λ is a constant of proportionality, called the decay constant. The minus sign indicates that the number of the radioactive atoms present decreases with time.

If ΔN and Δt are so small that they can be replaced by their corresponding differentials, dN and dt, then Equation 2.1 becomes a differential equation. The solution of this equation yields the following equation:

$$N = N_0 e^{-\lambda t} \quad (2.2)$$

where N_0 is the initial number of radioactive atoms and e is the number denoting the base of the natural logarithm (e ≈ 2.718). Equation 2.2 is the well-known exponential equation for radioactive decay.

2.3 .Activity

The number of disintegrations per unit time is referred to as the activity of a radioactive material. If ΔN/Δt in Equation 2.1 is replaced by A, the symbol for activity, then

$$A = \lambda N \quad (2.3)$$

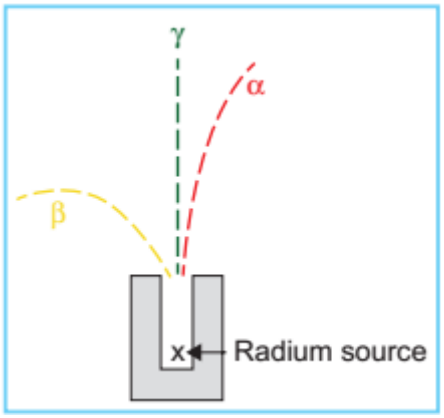

Figure 2.1. Diagrammatic representation of the separation of three types of radiation emitted by radium under the influence of magnetic field (applied perpendicular to the plane of the paper).

where the negative sign in Equation 2.1 has been left off because activity is the disintegration rate rather the change in the number of atoms. Similarly, Equation 2.2 can be expressed in terms of activity:

$$A = A_0 e^{-\lambda t} \quad (2.4)$$

where A is the activity remaining at time t, and A_0 is the original activity equal to λN_0.

The SI unit for activity is becquerel (Bq), defined as one disintegration per second (dps). In radiation therapy, a more common unit of activity is the curie (C_i), defined as

$$1 \text{ Ci} = 3.7 \times 10^{10} \text{ Bq}^1$$

Fractions of this unit are

$$1 \text{ mCi} = 10^{-3} \text{ Ci} = 3.7 \times 10^{7} \text{ Bq}$$
$$1 \ \mu\text{Ci} = 10^{-6} \text{ Ci} = 3.7 \times 10^{4} \text{ Bq}$$
$$1 \text{ nCi} = 10^{-9} \text{ Ci} = 3.7 \times 10^{1} \text{ Bq}$$
$$1 \text{ pCi} = 10^{-12} \text{ Ci} = 3.7 \times 10^{-2} \text{ Bq}$$

2.4 .The Half-Life and The Mean Life

The term half-life ($T_{1/2}$) of a radioactive substance is defined as the time required for either the activity or the number of radioactive atoms to decay to half the initial value. By substituting $N/N_0 = ½$ in Equation 2.2 or $A/A_0 = ½$ in Equation 2.4, at $t = T_{1/2}$, we have

$$\frac{1}{2} = e^{-\lambda \cdot T_{\frac{1}{2}}} \quad \text{or} \quad T_{\frac{1}{2}} = \frac{\ln 2}{\lambda}$$

where ln 2 is the natural logarithm of 2 having an approximate value of 0.693. By replacing ln 2 above by 0.693, we get

$$T_{\frac{1}{2}} = \frac{0.693}{\lambda} \tag{2.5}$$

Figure 2.2A illustrates the exponential decay of a radioactive sample as a function of time، expressed in units of half-life. It can be seen that after one half-life, the activity is ½ the initial value, after two half-lives, it is ¼, and so on. Thus, after n half-lives, the activity will be reduced to ½n of the initial value.

Although an exponential function can be plotted on a linear graph (Fig. 2.2A), it is better plotted on a semilog paper because it yields a straight line, as demonstrated in Figure 2.2B. This general curve applies to any radioactive material and can be used to determine the fractional activity remaining if the elapsed time is expressed as a fraction of half-life.

The mean or average life (T_a) is the average lifetime of a radioactive atom before it decays. It is the sum of the lifetimes of all the individual nuclei divided by the total number of nuclei involved. Although, in theory, it will take an infinite amount of time for all the atoms to decay، the concept of

average life can be understood in terms of an imaginary source that decays at a constant rate equal to the initial activity of the exponentially decaying source. Such a source would produce the same total number of disintegrations in time Ta as the given source decaying exponentially from time t = 0 to t = ∞. Because the initial activity = λN_0 (from Equation 2.3), the imaginary source would produce a total number of disintegrations = $T_a \lambda N_0$. Also because the total number of disintegrations must be equal to N_0, we have

$$T_a \lambda N_0 = N_0 \quad \text{or} \quad T_a = \frac{1}{\lambda} \tag{2.6}$$

Comparing Equations 2.5 and 2.6, we obtain the following relationship between half-life and average life:

$$T_a = 1.44\, T_{1/2} \tag{2.7}$$

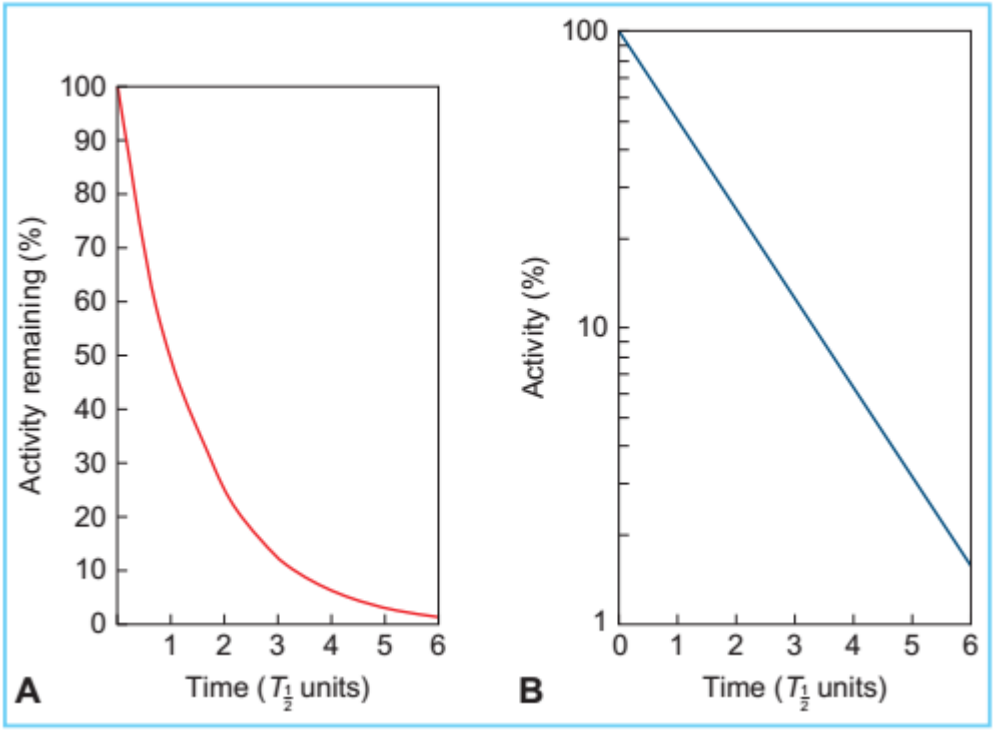

Figure 2.2. General decay curve. activity as a percentage of initial activity plotted against time in units of half-life. a: plot on linear graph; B: plot on semilogarithmic graph.

EXAMPLE 1

1. Calculate the number of atoms in 1 g of ^{226}Ra.
2. What is the activity of 1 g of ^{226}Ra (half-life = 1,622 years)?
   a. In Section 1.3, we showed that

$$\text{Number of atoms/g} = \frac{N_A}{A_W}$$

where N_A is Avogadro's number (6.02×10^{23} atoms per gram atomic weight) and A_W is the atomic weight. Also, we stated in the same section that A_W is very nearly equal to the mass number. Therefore, for ^{226}Ra

$$\text{Number of atoms/g} = \frac{6.02 \times 10^{23}}{226} = 2.66 \times 10^{21}$$

   b. Activity = λN (Equation 2.3). Since $N = 2.66 \times 10^{21}$ atoms/g (example above) and

$$\lambda = \frac{0.693}{T_{1/2}}$$
$$= \frac{0.693}{(1{,}622 \text{ years}) \times (3.15 \times 10^7 \text{ seconds/y})}$$
$$= 1.356 \times 10^{-11}/\text{s}$$

Therefore,

$$\text{Activity} = 2.66 \times 10^{21} \times 1.356 \times 10^{-11} \text{ dps/g}$$
$$= 3.61 \times 10^{10} \text{ dps/g}$$
$$= 0.975 \text{ Ci/g}$$

The activity per unit mass of a radionuclide is termed the specific activity. As shown in the previous example, the specific activity of radium is slightly less than 1 Ci/g, although the curie was originally defined as the decay rate of 1 g of radium. The reason for this discrepancy, as mentioned previously, is the current revision of the actual decay rate of radium without modification of the original definition of the curie.

High specific activity of certain radionuclides can be advantageous for a number of applications. For example, the use of elements as tracers in studying biochemical processes requires that the mass of the incorporated element should be so small that it does not interfere with the normal metabolism and yet it should exhibit measurable activity. Another example is the use of radioisotopes as teletherapy sources. One reason why cobalt-60 is preferable to cesium-137, in spite of its lower half-life (5.26 years for ^{60}Co vs. 30.0 years for ^{137}Cs), is its much higher specific activity. The interested reader may verify this fact by actual calculations. (It should be assumed in these calculations that the specific activities are for pure forms of the nuclides.)

EXAMPLE 2

1. Calculate the decay constant for cobalt-60 ($T_{1/2}$ = 5.26 years) in units of month^{-1}.
2. What will be the activity of a 5,000-Ci ^{60}Co source after 4 years?
   a. From Equation 2.5, we have

$$\lambda = \frac{0.693}{T_{\frac{1}{2}}}$$

since $T_{\frac{1}{2}}$ = 5.26 years = 63.12 months. Therefore,

$$\lambda = \frac{0.693}{63.12} = 1.0979 \times 10^{-2} \text{ month}^{-1}$$

   b. t = 4 years = 48 months. From Equation 2.4, we have

$$\begin{aligned} A &= A_0 e^{-\lambda t} \\ &= 5{,}000 \times e^{-1.0979 \times 10^{-2} \times 48} \\ &= 2{,}952 \text{ Ci} \end{aligned}$$

Alternatively,

$$t = 4 \text{ years} = \frac{4}{5.26} T_{\frac{1}{2}} = 0.760\, T_{\frac{1}{2}}$$

Therefore,

$$A = 5{,}000 \times \frac{1}{2^{0.760}} = 2{,}952 \text{ Ci}$$

Alternatively, reading the fractional activity from the universal decay curve given in Figure 2.2 at time = 0.760$T_{1/2}$ and then multiplying it with the initial activity, we get the desired answer.

EXAMPLE 3

When will 5 mCi of ^{131}I ($T_{1/2}$ = 8.05 days) and 2 mCi of ^{32}P ($T_{1/2}$ = 14.3 days) have equal activities? For ^{131}I,

$$A_0 = 5 \text{ mCi}$$

and

$$\lambda = \frac{0.693}{8.05} = 8.609 \times 10^{-2} \text{ day}^{-1}$$

For ^{32}P,

$$A_0 = 2 \text{ mCi}$$

and

$$\lambda = \frac{0.693}{14.3} = 4.846 \times 10^{-2} \text{ day}^{-1}$$

Suppose the activities of the two nuclides are equal after t days. Then, from Equation 2.4,

$$5 \times e^{-8.609 \times 10^{-2} \times t} = 2 \times e^{-4.846 \times 10^{-2} \times t}$$

Taking the natural log of both sides,

$$\ln 5 - 8.609 \times 10^{-2} \times t = \ln 2 - 4.846 \times 10^{-2} \times t$$

$$\text{or } 1.609 - 8.609 \times 10^{-2} \times t = 0.693 - 4.846 \times 10^{-2} \times t$$

$$\text{or } t = 24.34 \text{ days}$$

Alternatively, one may plot the activity of each sample as a function of time. The activities of the two samples will be equal at the time when the two curves intersect each other.

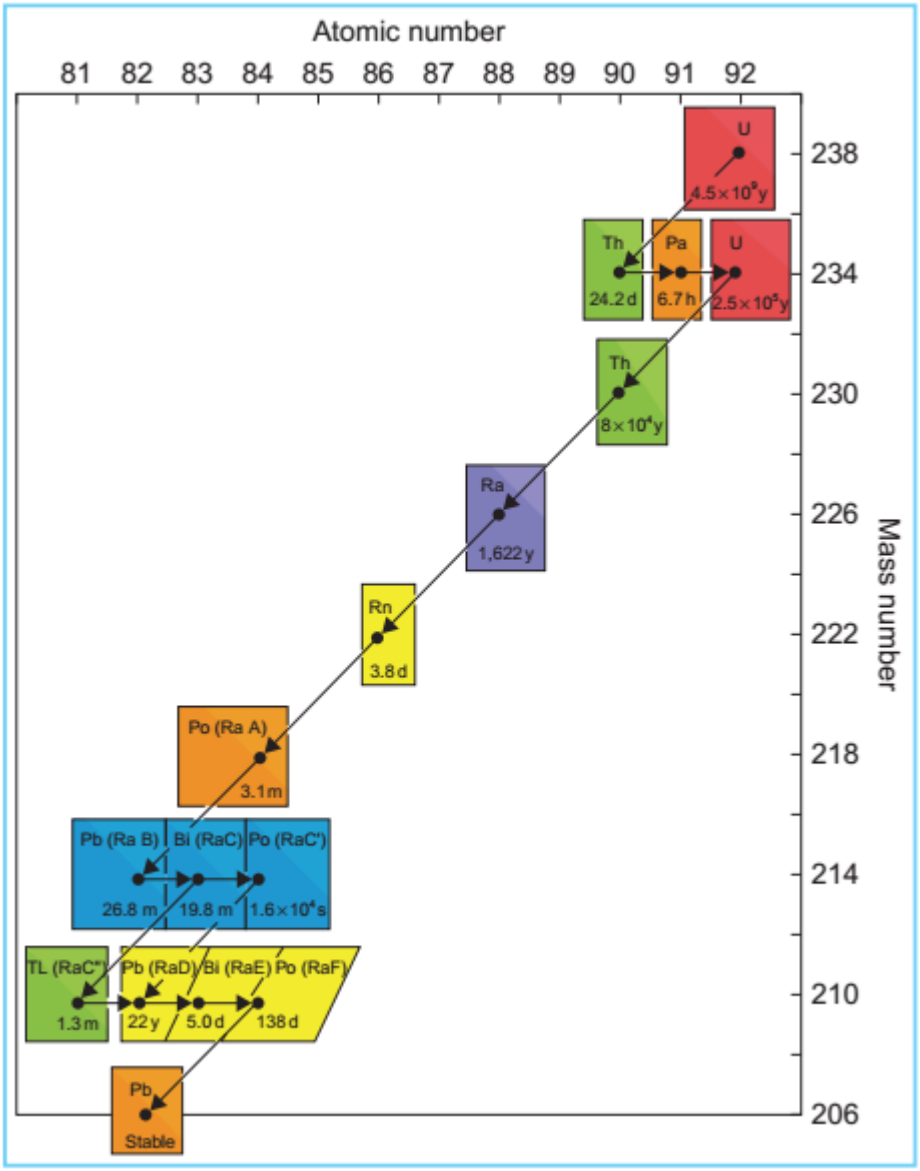

Figure 2.3. the uranium series.

2.5 .Radioactive Series

There are a total of 118 elements known today. Of these, the first 92 (from Z = 1 to Z = 92) occur naturally. The others have been produced artificially. In general, the elements with lower Z tend to be stable whereas the ones with higher Z are radioactive. It appears that as the number of particles inside the nucleus increases, the forces that keep the particles together become less effective and, therefore, the chances of particle emission are increased. This is suggested by the observation that all elements with Z greater than 82 (lead) are radioactive.

All naturally occurring radioactive elements have been grouped into three series: the uranium series, the actinium series, and the thorium series. The uranium series originates with ^{238}U having a half-life of 4.51×10^9 years and goes through a series of transformations involving the emission of a and β particles. γ rays are also produced as a result of some of these transformations. The actinium series starts from ^{235}U with a half-life of 7.13×10^8 years and the thorium series begins with ^{232}Th with half-life of 1.39×10^{10} years. All the series terminate at the stable isotopes of lead with mass numbers 206, 207, and 208, respectively. As an example, and because it includes radium as one of its decay products, the uranium series is represented in Figure 2.3.

2.6 .Radioactive Equilibrium

Many radioactive nuclides undergo successive transformations in which the original nuclide, called the parent, gives rise to a radioactive product nuclide, called the daughter. The naturally occurring radioactive series provides examples of such transitions. If the half-life of the parent is longer than that of the daughter, then after a certain time, a condition of equilibrium will be achieved, that is, the ratio of daughter activity to parent activity will become constant. In addition, the apparent decay rate of the daughter nuclide is then governed by the half-life or disintegration rate of the parent.

Two kinds of radioactive equilibria have been defined, depending on the relative half-lives of the parent and the daughter nuclides. If the half-life of the parent is not much longer than that of the daughter, then the type of equilibrium established is called the transient equilibrium. On the other hand, if the half-life of the parent is much longer than that of the daughter, then it can give rise to what is known as the secular equilibrium.

A general equation can be derived relating the activities of the parent and daughter:

$$A_2 = A_1 \frac{\lambda_2}{\lambda_2 - \lambda_1}(1 - e^{-(\lambda_2 - \lambda_1)t}) \tag{2.8}$$

where A_1 and A_2 are the activities of the parent and the daughter, respectively. λ_1 and λ_2 are the corresponding decay constants. In terms of the half-lives, T_1 and T_2, of the parent and daughter، respectively, the above equation can be rewritten as

$$A_2 = A_1 \frac{T_1}{T_1 - T_2}\left(1 - e^{-0.693\,\frac{T_1 - T_2}{T_1 T_2}\,t}\right) \tag{2.9}$$

Equation 2.9, when plotted, will initially exhibit a growth curve for the daughter before approaching the decay curve of the parent (Figures 2.4 and 2.5). In the case of a transient equilibrium, the time t to reach the equilibrium value is very large compared with the half-life of the daughter. This makes the exponential term in Equation 2.9 negligibly small. Thus, after the transient equilibrium has been achieved, the relative activities of the two nuclides are given by

$$\frac{A_2}{A_1} = \frac{\lambda_2}{\lambda_2 - \lambda_1} \tag{2.10}$$

or in terms of half-lives

$$\frac{A_2}{A_1} = \frac{T_1}{T_1 - T_2} \tag{2.11}$$

A practical example of the transient equilibrium is the ^{99}Mo generator producing ^{99m}Tc for diagnostic procedures. Such a generator is sometimes called “cow” because the daughter product, in this case ^{99m}Tc, is removed or “milked” at regular intervals. Each time the generator is completely milked, the growth of the daughter and the decay of the parent are governed by Equation 2.9. It may be mentioned that not all the ^{99}Mo atoms decay to ^{99m}Tc. Approximately 12% promptly decay to ^{99}Tc without passing through the metastable state of ^{99m}Tc (1). Thus the activity of ^{99}Mo should be effectively reduced by 12% for the purpose of calculating ^{99m}Tc activity, using any of Equations 2.8 to 2.11.

Since in the case of a secular equilibrium, the half-life of the parent is very long compared with the half-life of the daughter, λ_2 is much greater than λ_1. Therefore, λ_1 can be ignored in Equation 2.8:

$$A_2 = A_1(1 - e^{-\lambda_2 t}) \tag{2.12}$$

Equation 2.12 gives the initial buildup of the daughter nuclide, approaching the activity of the parent asymptotically (Fig. 2.5). At the secular equilibrium, after a long time, the product $\lambda_2 t$ becomes large and the exponential term in Equation 2.12 approaches zero. Thus at secular equilibrium and thereafter,

$$A_2 = A_1 \tag{2.13}$$

or

$$\lambda_2 N_2 = \lambda_1 N_1 \tag{2.14}$$

A radium source in a sealed tube or needle (to keep in the radon gas) is an excellent example of secular equilibrium. After an initial time (approximately 1 month), all the daughter products are in equilibrium with the parent and we have the relationship:

$$\lambda_1 N_1 = \lambda_2 N_2 = \lambda_3 N_3 = \cdots \tag{2.15}$$

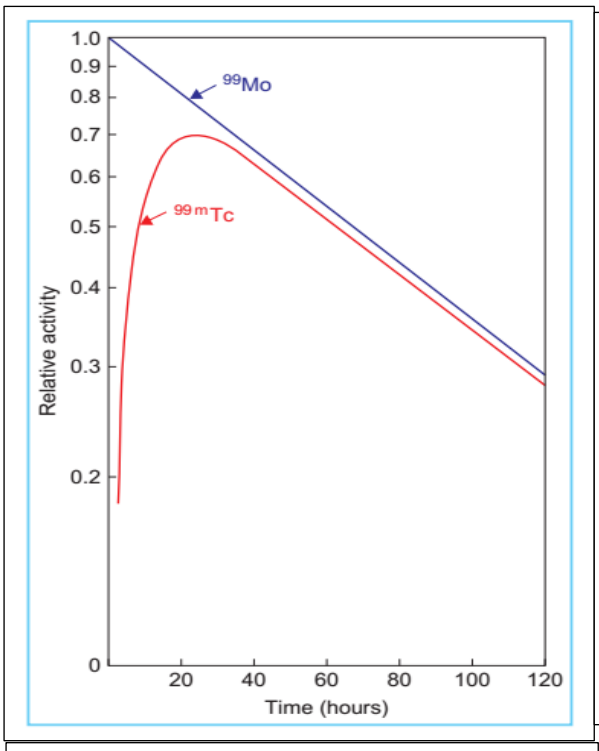

Figure 2.4. Illustration of transient equilibrium by the decay of ^{99}Mo to 99mtc. It has been assumed that only 88% of the ^{99}Mo atoms decay to ^{99m}Tc.

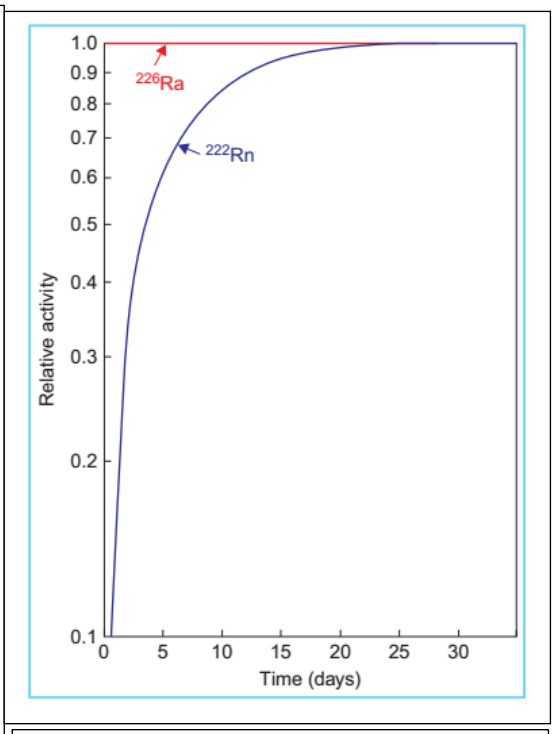

Figure 2.5. Illustration of secular equilibrium by the decay of ^{226}Ra to ^{222}Rn.

2.7. Modes of Radioactive Decay

a. α Particle Decay

Radioactive nuclides with very high atomic numbers (greater than 82) decay most frequently with the emission of an α particle. It appears that as the number of protons in the nucleus increases beyond 82, the Coulomb forces of repulsion between the protons become large enough to overcome the nuclear forces that bind the nucleons together. Thus the unstable nucleus emits a particle composed of two protons and two neutrons. This particle, which is in fact a helium nucleus, is called the α particle.

As a result of a decay, the atomic number of the nucleus is reduced by 2 and the mass number is reduced by 4. Thus, a general reaction for a decay can be written as

$$^{A}_{Z}X \rightarrow ^{A-4}_{Z-2}Y + ^{4}_{2}He + Q$$

where Q represents the total energy released in the process and is called the disintegration energy. This energy, which is equivalent to the difference in mass between the parent nucleus and product nuclei, appears as kinetic energy of the α particle and the kinetic energy of the product nucleus. The equation also shows that the charge is conserved, because the charge on the parent nucleus is Ze (where e is the electronic charge); on the product nucleus it is (Z – 2)e and on the a particle it is 2e.

A typical example of a decay is the transformation of radium to radon:

$$^{226}_{88}Ra \xrightarrow[1{,}622 \text{ years}]{T\frac{1}{2}} ^{222}_{86}Rn + ^{4}_{2}He + 4.87 \text{ MeV}$$

Since the momentum of the α particle must be equal to the recoil momentum of the radon nucleus and since the radon nucleus is much heavier than the α particle, it can be shown that the kinetic energy possessed by the radon nucleus is negligibly small (0.09 MeV) and that the disintegration energy appears almost entirely as the kinetic energy of the a particle (4.78 MeV).

The α particles emitted by radioactive substances have kinetic energies of about 5 to 10 MeV.

From a specific nuclide, they are emitted with discrete energies.

B. β Particle Decay

The process of radioactive decay, which is accompanied by the ejection of a positive or a negative electron from the nucleus, is called the β decay. The negative electron, or negatron, is denoted by β^-, and the positive electron, or positron, is represented by β^+. Neither of these particles exists as such inside the nucleus, but is created at the instant of the decay process. The basic transformations may be written as:

$$^{1}_{0}\mathrm{n} \rightarrow {}^{1}_{1}\mathrm{p} + {}^{0}_{-1}\beta + \tilde{\nu}(\beta^-\text{decay})$$

$$^{1}_{1}\mathrm{p} \rightarrow {}^{1}_{0}\mathrm{n} + {}^{0}_{+1}\beta + \nu(\beta^+\text{decay})$$

where ${}^{1}_{1}\mathrm{n}$, ${}^{1}_{1}\mathrm{p}$, $\tilde{\nu}$, and ν stand for neutron, proton, antineutrino, and neutrino, respectively. The last two particles, namely antineutrino and neutrino, are identical particles but with opposite spins. They carry no charge and practically no mass.

B.1. Negatron Emission

The radionuclides with an excessive number of neutrons or a high neutron-to-proton (n/p) ratio lie above the region of stability (Fig. 1.1). These nuclei tend to reduce the n/p ratio to achieve stability. This is accomplished by emitting a negative electron. The direct emission of a neutron to reduce the n/p ratio is rather uncommon and occurs with some nuclei produced as a result of fission reactions.

The general equation for the negatron or β^-decay is written as

$$^{A}_{Z}X \rightarrow {}^{A}_{Z+1}Y + {}^{0}_{-1}\beta + \tilde{\nu} + Q$$

where Q is the disintegration energy for the process. This energy is provided by the difference in mass between the initial nucleus $^{A}_{Z}X$ and the sum of the masses of the product nucleus $^{A}_{Z+1}Y$ and the particles emitted.

The energy Q is shared between the emitted particles (including γ rays if emitted by the daughter nucleus) and the recoil nucleus. The kinetic energy possessed by the recoil nucleus is negligible because of its much greater mass compared with the emitted particles. Thus practically the entire disintegration energy is carried by the emitted particles. If there were only one kind of particle involved, all the particles emitted in such a disintegration would have the same energy equal to Q, thus yielding a sharp-line spectrum. However, the observed spectrum in the β decay is continuous, which suggests that there is more than one particle emitted in this process.

For these reasons, Wolfgang Pauli (1931) introduced the hypothesis that a second particle, later known as the neutrino, accompanied each β particle emitted and shared the available energy.

The experimental data show that the β particles are emitted with all energies ranging from zero to the maximum energy characteristic of the β transition. Figure 2.6 shows the distribution of energy among the β particles of ^{32}P. The overall transition is

$$^{32}_{15}P \xrightarrow[14.3\ \text{days}]{T_{\frac{1}{2}}} {}^{32}_{16}S + {}^{0}_{-1}\beta + \tilde{\nu} + 1.7\ \text{MeV}$$

As seen in Figure 2.6, the endpoint energy of the β-ray spectrum is equal to the disintegration energy and is designated by E_{max}, the maximum electron energy. Although the shape of the energy spectrum and the values for E_{max} are characteristic of the particular nuclide, the average energy of the β particles from a β emitter is approximately $E_{max}/3$.

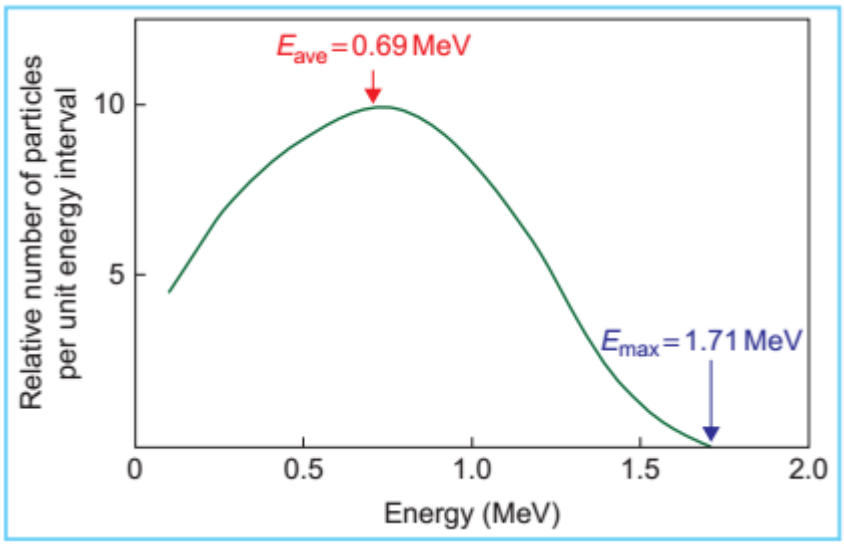

Figure 2.6. β-ray energy spectrum from 32p.

The neutrino has no charge and practically no mass. For that reason the probability of its interaction with matter is very small and its detection is extremely difficult. However, Fermi successfully presented the theoretical evidence of the existence of the neutrino and predicted the shape of the β-ray spectra. The existence of neutrinos has been verified by direct experiments.

B.2. Positron Emission

Positron-emitting nuclides have a deficit of neutrons, and their n/p ratios are lower than those of the stable nuclei of the same atomic number or neutron number (Fig. 1.1). For these nuclides to achieve stability, the decay mode must result in an increase of the n/p ratio. One possible mode is the β decay involving the emission of a positive electron or positron. The overall decay reaction is as follows:

$$^{A}_{Z}X \rightarrow {}^{A}_{Z-1}Y + {}^{0}_{+1}\beta + \nu + Q$$

As in the case of the negatron emission, discussed previously, the disintegration energy Q is shared by the positron, the neutrino, and any γ rays emitted by the daughter nucleus. Also, like the negatrons, the positrons are emitted with a spectrum of energies.

A specific example of positron emission is the decay of $^{22}_{11}Na$:

$$^{22}_{11}\mathrm{Na} \xrightarrow[2.60\ \mathrm{days}]{T_{\frac{1}{2}}} {}^{22}_{10}\mathrm{Ne} + {}^{0}_{+1}\beta + \nu + 1.82\,\mathrm{MeV}$$

The released energy, 1.82 MeV, is the sum of the maximum kinetic energy of the positron، 0.545 MeV, and the energy of the γ ray, 1.275 MeV.

An energy level diagram for the positron decay of $^{22}_{11}Na$ is shown in Figure 2.7. The arrow representing β^+ decay starts from a point $2m_0c^2$ (=1.02 MeV) below the energy state of the parent atom. This excess energy, which is the equivalent of two electron masses, must be available as part of the transition energy for the positron emission to take place. In other words, for the β^+ decay to occur, the mass-energy difference of 1.02 MeV between the parent and daughter atoms is needed to cover the loss of β^+ (0.511 MeV) by the parent nucleus as well as the release of a valence electron (0.511 MeV) by the daughter atom. Also, it can be shown that the energy released in a positron decay process is given by the atomic mass difference between the parent and the daughter nuclides minus the $2m_0c^2$. The positron is unstable and eventually combines with another electron, producing annihilation of the particles. This event results in two γ-ray photons, each of 0.511 MeV, thus converting two electron masses into energy.

The phenomenon of positron-electron annihilation has a practical use in radiology—the development of positron emission tomography (PET). An isotope such as ^{18}F, incorporated into a metabolically active compound, emits positrons which are annihilated by electrons in the body tissues. For

each annihilation two photons of 0.511 MeV are emitted in opposite directions. By detecting these photons by a ring of detectors in a circular geometry surrounding the patient, the site of annihilation events and the intervening anatomy are reconstructed by using computer software (e.g., filtered back projection algorithm).

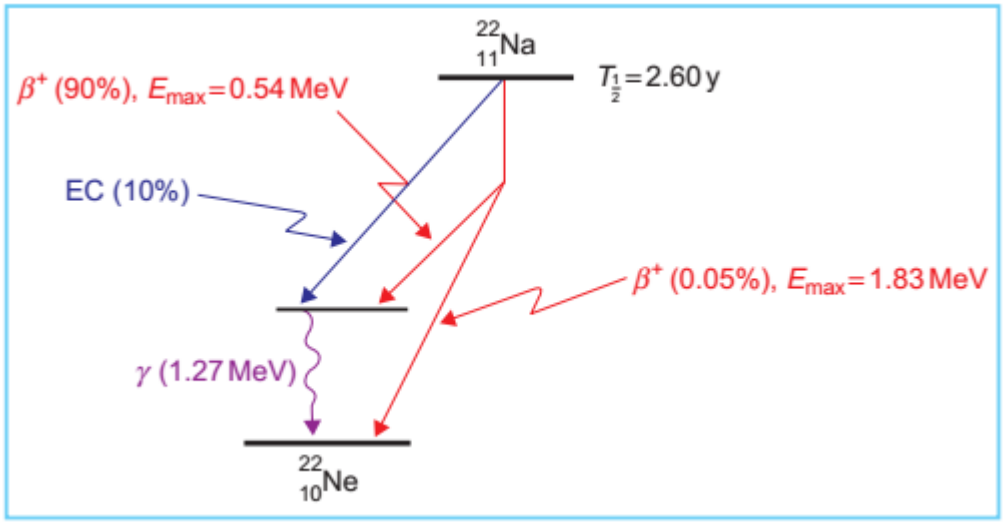

Figure 2.7. Energy level diagram for the positron decay of $^{22}_{11}Na$ to $^{22}_{10}Ne$.

C. Electron Capture

The electron capture is a phenomenon in which one of the orbital electrons is captured by the nucleus, thus transforming a proton into a neutron:

$$^{1}_{1}\mathrm{p} + {}^{0}_{-1}\mathrm{e} \rightarrow {}^{1}_{0}\mathrm{n} + \nu$$

The general equation of the nuclear decay is

$$^{A}_{Z}X + {}^{0}_{-1}\mathrm{e} \rightarrow {}_{Z-1}{}^{A}Y + \nu + Q$$

The electron capture is an alternative process to the positron decay. The unstable nuclei with neutron deficiency may increase their n/p ratio to gain stability by electron capture. As illustrated in Figure 2.7, $^{22}_{11}Na$ decays 10% of the time by K electron capture. The resulting nucleus is still in the excited state and releases its excess energy by the emission of a γ-ray photon. In general, the γ decay follows the particle emission almost instantaneously (less than 10^{-9} seconds).

The electron capture process involves mostly the K shell electron because of its closeness to the nucleus. The process is then referred to as K capture. However, other L or M capture processes are also possible in some cases.

The decay by electron capture creates an empty hole in the involved shell that is then filled with another outer orbit electron, thus giving rise to the characteristic x-rays. There is also the emission of Auger electrons, which

are monoenergetic electrons produced by the absorption of characteristic x-rays by the atom and reemission of the energy in the form of orbital electrons ejected from the atom.

The process can be crudely described as internal photoelectric effect (to be discussed in later chapters) produced by the interaction of the electron capture characteristic x-rays with the same atom.

Another name for characteristic x-rays produced by the interaction of photons with the atom is fluorescent x-rays. The excess energy released by the atom through electron transition from an outer orbit to an inner orbit appears as photons (fluorescent x-rays) or Auger electrons.

The two processes are competing. The probability of fluorescent x-ray emission vs. Auger electrons depends on the atomic number of the atom involved. Fluorescent yield (w), defined as the ratio of the number of characteristic photons emitted to the number of electron shell vacancies، increases with increase in atomic number. For large Z values fluorescent radiation is favored، while for low Z values Auger electrons are more probable. For example, Auger electrons are emitted more frequently in materials of $Z < 30$, while fluorescent yield predominates for higher Z. For soft tissue ($Z \sim 7.64$) $w \sim 0$; for tungsten ($Z = 74$) $w \sim 0.93$.

D. Internal Conversion

The emission of γ rays from the nucleus is one mode by which a nucleus left in an excited state after a nuclear transformation gets rid of excess energy. There is another competing mechanism, called internal conversion, by which the nucleus can lose energy (Fig. 2.8). In this process, the excess nuclear energy is passed on to one of the orbital electrons, which is then ejected from the atom. The process can be crudely likened to an internal photoelectric effect in which the γ ray escaping from the nucleus interacts with an orbital electron of the same atom. The kinetic energy of the internal conversion electron is equal to energy released by the nucleus minus the binding energy of the orbital electron involved.

As discussed in the case of the electron capture, the ejection of an orbital electron by internal conversion will create a vacancy in the involved shell, resulting in the production of characteristic photons or Auger electrons (Fig. 2.9).

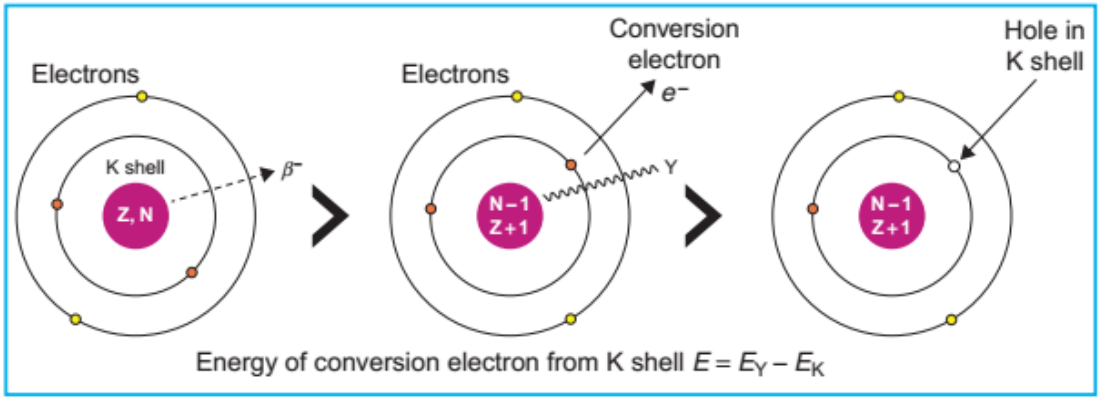

Figure 2.8. Schematic illustration of internal conversion. Left to right: the nucleus undergoes β^- decay and creates a daughter nucleus, which is still in the excited state and decays by γ emission. The γ ray could be absorbed by the atom، ejecting a K-shell electron of energy ($E\gamma$–E_K), thereby creating a vacancy in the K-shell orbit.

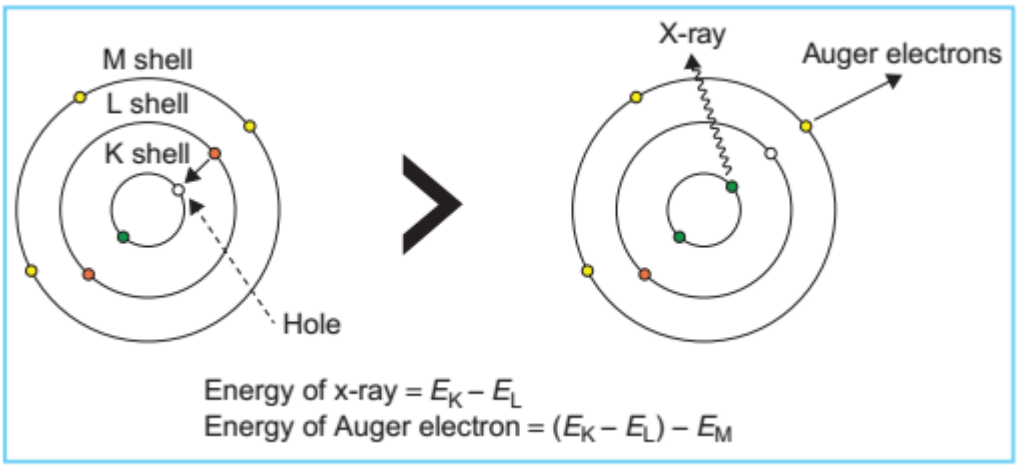

Figure 2.9. Schematic illustration of auger electron emission. the steps involved in the process are as follows: ejection of an orbital electron (e.g., by internal conversion) → creation of a hole in the shell (e.g., K shell) → filling of the hole by an electron from an outer shell (e.g., L shell) → emission of characteristic x-ray of energy ($E_K - E_L$) or→ ejection of auger electron (e.g., from the M shell) with energy [($E_K - E_L$) – E_M].

D.1. Isomeric Transition

In most radioactive transformations, the daughter nucleus loses the excess energy immediately in the form of γ rays or by internal conversion. No radioactive nuclide, however, decays solely by γ emission. In the case of some nuclides, the excited state of the nucleus persists for an appreciable time. In that case, the excited nucleus is said to exist in the metastable state. The metastable nucleus is an isomer of the final product nucleus which has

the same atomic and mass number but different energy state. An example of such a nuclide commonly used in nuclear medicine is 99mTc, which is an isomer of ^{99}Tc. As discussed earlier (Section 2.6), ^{99m}Tc is produced by the decay of ^{99}Mo ($T_{1/2}$ = 67 hours) and itself decays to ^{99}Tc with a half-life of 6 hours.

2.8 .Nuclear Reactions

a. The α, p Reaction

The first nuclear reaction was observed by Rutherford in 1919 in an experiment in which he bombarded nitrogen gas with α particles from a radioactive source. Rutherford's original transmutation reaction can be written as:

$$^{14}_{7}\mathrm{N} + ^{4}_{2}\mathrm{He} \rightarrow ^{17}_{8}\mathrm{O} + ^{1}_{1}\mathrm{H} + Q$$

where Q generally represents the energy released or absorbed during a nuclear reaction. If Q is positive, energy has been released and the reaction is called exoergic, and if Q is negative, energy has been absorbed and the reaction is endoergic. Q is also called nuclear reaction energy or disintegration energy (as defined earlier in decay reactions) and is equal to the difference in the masses of the initial and final particles.

The minimum required energy is called the threshold energy for the reaction and must be available from the kinetic energy of the bombarding particle.

A reaction in which an α particle interacts with a nucleus to form a compound nucleus which، in turn, disintegrates immediately into a new nucleus by the ejection of a proton is called an α,p reaction. The first letter, α, stands for the bombarding particle and the second letter, p, stands for the ejected particle, in this case a proton. The general reaction of this type is written as:

$$^{A}_{Z}X + ^{4}_{2}\mathrm{He} \rightarrow ^{A+3}_{Z+1}Y + ^{1}_{1}\mathrm{H} + Q$$

B. The α, n Reaction

The bombardment of a nucleus by α particles with the subsequent emission of neutrons is designated as an α, n reaction. An example of this type of reaction is $^{9}\mathrm{Be}(a, n)^{12}\mathrm{C}$. This was the first reaction used for producing small neutron sources. A material containing a mixture of radium and beryllium has been commonly used as a neutron source in research

laboratories. In this case, the a particles emitted by radium bombard the beryllium nuclei and eject neutrons.

C. Proton Bombardment

The most common proton reaction consists of a proton being captured by the nucleus with the emission of a γ ray. The reaction is known as p,γ. Examples are $^{7}\mathrm{Li}(p,\gamma)^{8}\mathrm{Be}$ and $^{12}\mathrm{C}(p,\gamma)^{13}\mathrm{N}$. Other possible reactions produced by proton bombardment are of the type p,n; p,d; and p,a. The symbol d stands for the deuteron ($^{2}_{1}H$).

D. Deuteron Bombardment

The deuteron particle is a combination of a proton and a neutron ($^{2}_{1}H$). This combination appears to break down in most deuteron bombardments with the result that the compound nucleus emits either a neutron or a proton. The two types of reactions can be written as:

$$^{A}_{Z}\mathrm{X(d,n)}^{A+1}_{Z+1}\mathrm{Y} \quad \text{and} \quad ^{A}_{Z}\mathrm{X(d,p)}^{A+1}_{Z}\mathrm{X}.$$

An important reaction that has been used as a source of high-energy neutrons is produced by the bombardment of beryllium by deuterons. The equation for the reaction is:

$$^{2}_{1}\mathrm{H} + {}^{9}_{4}\mathrm{Be} \rightarrow {}^{10}_{5}\mathrm{B} + {}^{1}_{0}\mathrm{n}$$

The process is known as stripping. In this process, the deuteron is not captured by the nucleus but passes close to it. The proton is stripped off from the deuteron and the neutron continues to travel with high speed.

E. Neutron Bombardment

Neutrons, because they possess no electric charge, are very effective in penetrating the nuclei and producing nuclear reactions. For the same reason, the neutrons do not have to possess high kinetic energies in order to penetrate the nucleus. As a matter of fact, slow neutrons or thermal neutrons (neutrons with average energy equal to the energy of thermal agitation in a material، which is about 0.025 eV at room temperature) have been found to be extremely effective in producing nuclear transformations. An example of a slow neutron capture is the n,a reaction with boron:

$$^{10}_{5}\mathrm{B} + {}^{1}_{0}\mathrm{n} \rightarrow {}^{7}_{3}\mathrm{Li} + {}^{4}_{2}\mathrm{He}$$

The previous reaction forms the basis of neutron detection. In practice, an ionization chamber is filled with boron gas such as $BF3$. The a particle

released by the n, a reaction with boron produces the ionization detected by the chamber.

The most common process of neutron capture is the n, γ reaction. In this case, the compound nucleus is raised to one of its excited states and then immediately returns to its normal state with the emission of a g-ray photon. These γ rays, called capture γ rays, can be observed coming from a hydrogenous material such as paraffin used to slow down (by multiple collisions with the nuclei) the neutrons and ultimately capture some of the slow neutrons. The reaction can be written as follows:

$$^{1}_{1}\mathrm{H} + {}^{1}_{0}\mathrm{n} \rightarrow {}^{2}_{1}\mathrm{H} + \gamma$$

Because the thermal neutron has negligible kinetic energy, the energy of the capture γ ray can be calculated by the mass difference between the initial particles and the product particles, assuming negligible recoil energy of $^{2}_{1}H$. Products of the n, γ reaction, in most cases, have been found to be radioactive, emitting β particles. Typical examples are

$$^{59}_{27}\mathrm{Co} + {}^{1}_{0}\mathrm{n} \rightarrow {}^{60}_{27}\mathrm{Co} + \gamma$$

followed by

$$^{60}_{27}\mathrm{Co} \xrightarrow[5.3 \text{ years}]{T\frac{1}{2}} {}^{60}_{28}\mathrm{Ni} + {}^{0}_{-1}\beta + \gamma_1 + \gamma_2$$

$$^{197}_{79}\mathrm{Au} + {}^{1}_{0}\mathrm{n} \rightarrow {}^{198}_{79}\mathrm{Au} + \gamma$$

followed by

$$^{198}_{79}\mathrm{Au} \xrightarrow[2.7 \text{ days}]{T\frac{1}{2}} {}^{198}_{80}\mathrm{Hg} + {}^{0}_{-1}\beta$$

Another type of reaction produced by neutrons, namely the n, p reaction, also yields β emitters in most cases. This process with slow neutrons has been observed in the case of nitrogen:

$$^{14}_{7}\mathrm{N} + {}^{1}_{0}\mathrm{n} \rightarrow {}^{14}_{6}\mathrm{C} + {}^{1}_{1}\mathrm{H}$$

followed by

$$^{14}_{6}\mathrm{C} \xrightarrow[5{,}700 \text{ years}]{T\frac{1}{2}} {}^{14}_{7}\mathrm{N} + {}^{0}_{-1}\beta$$

The example of a fast neutron n, p reaction is the production of ^{32}P:

$$^{32}_{16}\mathrm{S} + {}^{1}_{0}\mathrm{n} \rightarrow {}^{32}_{15}\mathrm{P} + {}^{1}_{1}\mathrm{H}$$

followed by

$$^{32}_{15}\mathrm{P} \xrightarrow[14.3 \text{ days}]{T\frac{1}{2}} {}^{32}_{16}\mathrm{S} + {}^{0}_{-1}\beta$$

It should be pointed out that whether a reaction will occur with fast or slow neutrons depends on the magnitude of the mass difference between the expected product nucleus and the bombarded nucleus. For example, in the case of an n, p reaction, if this mass difference exceeds 0.000840 amu

(mass difference between a neutron and a proton), then only fast neutrons will be effective in producing the reaction.

F. Photodisintegration

An interaction of a high-energy photon with an atomic nucleus can lead to a nuclear reaction and to the emission of one or more nucleons. In most cases, this process of photodisintegration results in the emission of neutrons by the nuclei. An example of such a reaction is provided by the nucleus of ^{63}Cu bombarded with a photon beam:

$$^{63}_{29}\mathrm{Cu} + \gamma \rightarrow {}^{62}_{29}\mathrm{Cu} + {}^{1}_{0}\mathrm{n}$$

The above reaction has a definite threshold, 10.86 MeV. This can be calculated by the definition of threshold energy, namely the difference between the rest energy of the target nucleus and that of the residual nucleus plus the emitted nucleon(s). Because the rest energies of many nuclei are known for a very high accuracy, the photodisintegration process can be used as a basis for energy calibration of machines producing high-energy photons.

In addition to the γ, n reaction, other types of photodisintegration processes have been observed.

Among these are γ, p; γ, d; γ, t and γ, α, where d stands for deuteron and t stands for triton ($^{3}_{1}H$).

G. Fission

This type of reaction is produced by bombarding certain high atomic number nuclei by neutrons.

The nucleus, after absorbing the neutron, splits into nuclei of lower atomic number as well as additional neutrons. A typical example is the fission of ^{235}U with slow neutrons:

$$^{235}_{92}\mathrm{U} + {}^{1}_{0}\mathrm{n} \rightarrow {}^{236}_{92}\mathrm{U} \rightarrow {}^{141}_{56}\mathrm{Ba} + {}^{92}_{36}\mathrm{Kr} + 3{}^{1}_{0}\mathrm{n} + Q$$

Thermal neutrons (slow neutrons of average energy ~0.025 eV) are more effective in producing fission reaction. The product nuclei of a fission reaction, called fragments, consist of many possible combinations of A and Z. The fission yield curve (Fig. 2.10) shows maximum yield at approximately A of 90 and 140.

The energy released Q can be calculated, as usual, by the mass difference between the original and the final particles and, in the above reaction, averages more than 200 MeV per reaction.

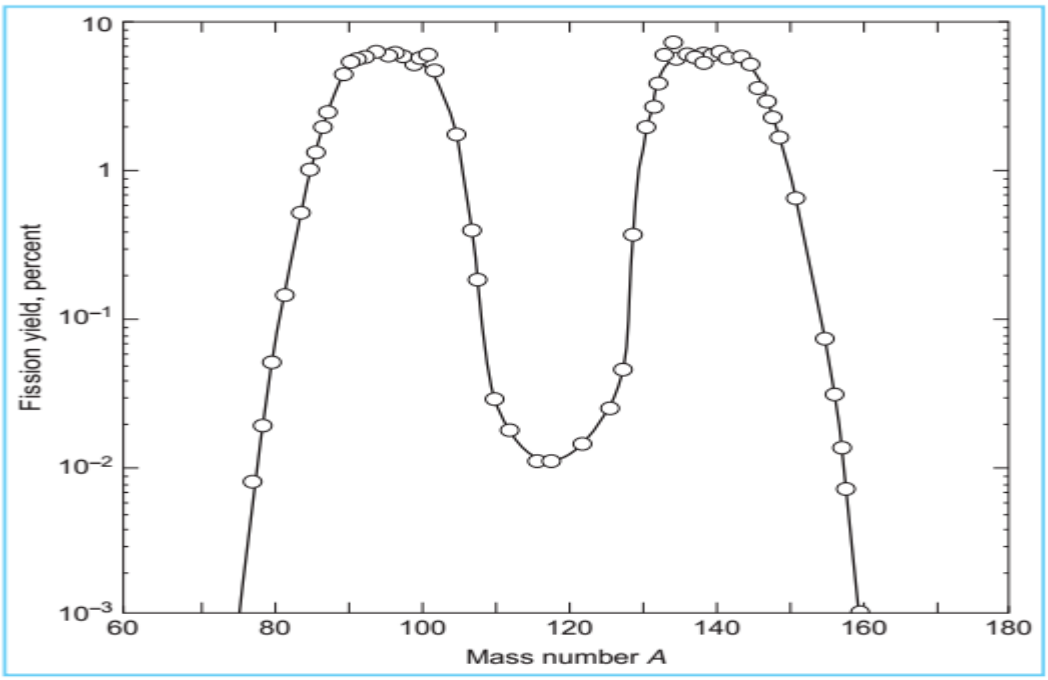

Figure 2.10. plot of nuclear fission yield (%) as a function of mass number of fission nuclei (fragments) produced.

This energy appears as the kinetic energy of the product particles as well as γ rays. The fission fragments carry most this energy (~167 MeV).

The additional neutrons released in the process may also interact with other ^{235}U nuclei, thereby creating the possibility of a chain reaction. To induce a chain reaction, neutrons have to be slowed down to thermal energies by collision with nuclei of low Z material (e.g., graphite، water, heavy water), called moderators. However, a sufficient mass or, more technically, the critical mass of the fissile material (e.g., ^{235}U) is required to sustain a chain reaction.

As seen in the above instance, the energy released per fission reaction is enormous. The process، therefore, has become a major energy source as in the case of nuclear reactors. In a nuclear reactor، the chain reactions are controlled and sustained in a steady state. In a nuclear bomb, on the other hand, the chain reaction is uncontrolled and occurs in a fraction of a second to cause explosion.

H. Fusion

Nuclear fusion may be considered the reverse of nuclear fission; that is, low-mass nuclei are combined to produce one nucleus. A typical reaction is:

$$^{2}_{1}\mathrm{H} + {}^{3}_{1}\mathrm{H} \rightarrow {}^{4}_{2}\mathrm{He} + {}^{1}_{0}\mathrm{n} + Q$$

Because the total mass of the product particles is less than the total mass of the reactants, energy Q is released in the process. In the above example, the loss in mass is about 0.0189 amu, which gives Q = 17.6 MeV.

For the fusion reaction to occur, the nuclei must be brought sufficiently close together so that the repulsive coulomb forces are overcome and the short-range nuclear forces can initiate the fusion reaction. This is accomplished by heating low Z nuclei to very high temperatures (greater than 107 K) which are comparable with the inner core temperature of the sun. In practice, fission reactions have been used as starters for the fusion reactions.

2.9 .Activation of Nuclides

Elements can be made radioactive by various nuclear reactions, some of which have been described in the preceding section. The yield of a nuclear reaction depends on parameters such as the number of bombarding particles, the number of target nuclei, and the probability of the occurrence of the nuclear reaction. This probability is proportional to a quantity called the cross section which is usually given in units of barns, where a barn is 10^{-24} cm^2. The cross section of nuclear reaction depends on the nature of the target material as well as the type of the bombarding particles and their energy.

Another important aspect of activation is the growth of activity. It can be shown that in the activation of isotopes the activity of the transformed sample grows exponentially. If both the activation and decay of the material are considered, the actual growth of activity follows a net growth curve that reaches a maximum value, called saturation activity, after several half-lives.

When that happens, the rate of activation equals the rate of decay.

As mentioned earlier, slow (thermal) neutrons are very effective in activating nuclides. High fluxes of slow neutrons (10^{10} to 10^{14}

neutrons/cm^2/s) are available in a nuclear reactor where neutrons are produced by fission reactions.

2.10 .Nuclear Reactors

In nuclear reactors, the fission process is made self-sustaining by chain reaction in which some of the fission neutrons are used to induce still more fissions. The nuclear "fuel" is usually ^{235}U، although thorium and plutonium are other possible fuels. The fuel, in the form of cylindrical rods, is arranged in a lattice within the reactor core. Because the neutrons released during fission are fast neutrons, they have to be slowed down to thermal energy (about 0.025 eV) by collisions with nuclei of low Z material. Such materials are called moderators. Typical moderators include

graphite, beryllium, water, and heavy water (water with heavy hydrogen ^2_1H as part of the molecular structure). The fuel rods are immersed in the moderators. The reaction is "controlled" by inserting rods of material that efficiently absorbs neutrons, such as cadmium or boron. The position of these control rods in the reactor core determines the number of neutrons available to induce fission and thus control the fission rate or power output. One of the major uses of nuclear reactors is to produce power. In this case, the heat generated by the absorption of γ rays and neutrons is used for the generation of electrical power. In addition, because reactors can provide a large and continuous supply of neutrons, they are extremely valuable for producing radioisotopes used in nuclear medicine, industry, and research.

3 Production of X-Rays

X-rays were discovered by Roentgen in 1895 while studying cathode rays (stream of electrons) in a gas discharge tube. He observed that another type of radiation was produced (presumably by the interaction of electrons with the glass walls of the tube) that could be detected outside the tube.

This radiation could penetrate opaque substances, produce fluorescence, blacken a photographic plate, and ionize a gas. He named the new radiation x-rays.

3.1 .THE X-RAY TUBE

Figure 3.1 is a schematic representation of a conventional x-ray tube. The tube consists of a glass envelope which has been evacuated to high vacuum. At one end is a cathode (negative electrode) and at the other an anode (positive electrode), both hermetically sealed in the tube.

The cathode is a tungsten filament which when heated emits electrons, a phenomenon known as thermionic emission. The anode consists of a thick copper rod, at the end of which is placed a small piece of tungsten target. When a high voltage is applied between the anode and the cathode, the electrons emitted from the filament are accelerated toward the anode and achieve high velocities before striking the target. The x-rays are produced by the sudden deflection or acceleration of the electron caused by the attractive force of the tungsten nucleus. The x-ray beam emerges through a thin glass window in the tube envelope. In some tubes, thin beryllium windows are used to reduce inherent filtration of the x-ray beam.

A. THE ANODE

The choice of tungsten as the target material in conventional x-ray tubes is based on the criteria that the target must have a high atomic number and high melting point. The efficiency of x-ray production depends on the atomic number, and for that reason, tungsten with Z = 74 is a good target material. In addition, tungsten, which has a melting point of 3,370 ˚C, is the element of choice for withstanding intense heat produced in the target by the electronic bombardment.

Efficient removal of heat from the target is an important requirement for the anode design. This has been achieved in some tubes by conduction of heat through a thick copper anode to the outside of the tube where it is cooled by oil, water, or air. Rotating anodes have also been used in diagnostic x-rays to reduce the temperature of the target at any one spot.

The heat generated in the rotating anode is radiated to the oil reservoir surrounding the tube. It should be mentioned that the function of the oil bath surrounding an x-ray tube is to insulate the tube housing from the high voltage applied to the tube as well as absorb heat from the anode.

Some stationary anodes are hooded by a copper and tungsten shield to prevent stray electrons from striking the walls or other nontarget components of the tube. These are secondary electrons produced from the target when it is being bombarded by the primary electron beam. Whereas copper in the hood absorbs the secondary electrons, the tungsten shield surrounding the copper shield absorbs the unwanted x-rays produced in the copper.

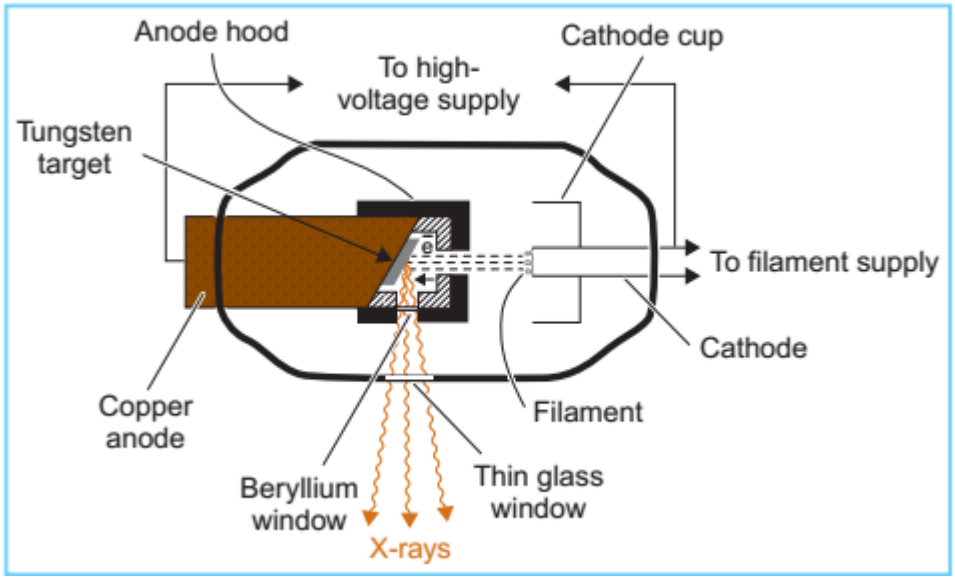

Figure 3.1. Schematic diagram of a therapy x-ray tube with a hooded anode.

An important requirement of the anode design is the optimum size of the target area from which the x-rays are emitted. This area, which is called the focal spot, should be as small as possible for producing sharp radiographic images. However, smaller focal spots generate more heat per unit area of target and, therefore, limit currents and exposure. In therapy tubes, relatively larger focal spots are acceptable since the radiographic image quality is not the overriding concern.

The apparent size of the focal spot can be reduced by the principle of line focus, illustrated in Figure 3.2. The target is mounted on a steeply inclined surface of the anode. The apparent side a is equal to A sin θ, where A is the side of the actual focal spot at an angle θ with respect to the perpendicular to the electron beam direction. Since the other side of the

actual focal spot is perpendicular to the electron, its apparent length remains the same as the original. The dimensions of the actual focal spot are chosen so that the apparent focal spot results in an approximate square. Therefore, by making the target angle θ small, side a can be reduced to a desired size. In diagnostic radiology, the target angles are quite small (6 to 17 degrees) to produce apparent focal spot sizes ranging from 0.1 × 0.1 to 2 × 2 mm^2. In most therapy tubes, however, the target angle is larger (about 30 degrees) and the apparent focal spot ranges between 5 × 5 and 7 × 7 mm^2.

Since the x-rays are produced at various depths in the target, they suffer varying amounts of attenuation in the target. There is greater attenuation for x-rays coming from greater depths than those from near the surface of the target. Consequently, the intensity of the x-ray beam decreases from the cathode to the anode direction of the beam. This variation across the x-ray beam is called the heel effect. The effect is particularly pronounced in diagnostic tubes because of the low x-ray energy and steep target angles. The problem can be minimized by using a compensating filter to provide differential attenuation across the beam in order to compensate for the heel effect and improve the uniformity of the beam.

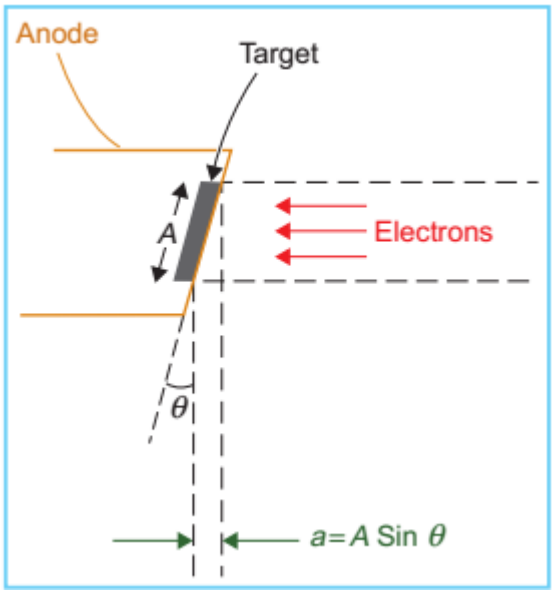

Figure 3.2. Diagram illustrating the principle of line focus. The side A of the actual focal spot is reduced to side a of the apparent focal spot. the other dimension (perpendicular to the plane of the paper) of the focal spot remains unchanged.

B. The Cathode

The cathode assembly in a modern x-ray tube (Coolidge tube) consists of a wire filament, a circuit to provide filament current, and a negatively charged focusing cup. The function of the cathode cup is to direct the electrons toward the anode so that they strike the target in a well-defined area، the focal spot. Since the size of the focal spot depends on filament

size, the diagnostic tubes usually have two separate filaments to provide "dual-focus," namely one small and one large focal spot.

The material of the filament is tungsten, which is chosen because of its high melting point.

3.2 .Basic X-Ray Circuit

The actual circuit of a modern x-ray machine is very complex. In this section, however, we will consider only the basic aspects of the x-ray circuit.

A simplified diagram of a self-rectified therapy unit is shown in Figure 3.3. The circuit can be divided into two parts: the high-voltage circuit to provide the accelerating potential for the electrons and the low-voltage circuit to supply heating current to the filament. Since the voltage applied between the cathode and the anode is high enough to accelerate all the electrons across to the target, the filament temperature or filament current controls the tube current (the current in the circuit due to the flow of electrons across the tube) and hence the x-ray intensity.

The filament supply for electron emission usually consists of 10 V at about 6 A. As shown in Figure 3.3, this can be accomplished by using a step-down transformer in the AC line voltage.

The filament current can be adjusted by varying the voltage applied to the filament. Since a small change in this voltage or filament current produces a large change in electron emission or the current (Fig. 3.12), a special kind of transformer is used which eliminates normal variations in line voltage.

The high voltage to the x-ray tube is supplied by the step-up transformer (Fig. 3.3). The primary of this transformer is connected to an autotransformer and a rheostat. The function of the autotransformer is to provide a stepwise adjustment in voltage. The device consists of a coil of wire wound on an iron core and operates on the principle of inductance. When an alternating line voltage is applied to the coil, potential is divided between the turns of the coil. By using a selector switch, a contact can be made to any turn, thus varying the output voltage which is measured between the first turn of the coil and the selector contact.

The rheostat is a variable resistor, i.e., a coil of wire wound on a cylindrical object with a sliding contact to introduce as much resistance in the circuit as desired and thus vary the voltage in a continuous manner. It may be mentioned that, whereas there is appreciable power loss in the rheostat

because of the resistance of the wires, the power loss is small in the case of the inductance coil since the wires have low resistance.

The voltage input to the high-tension transformer or the x-ray transformer can be read on a voltmeter in the primary part of its circuit. The voltmeter, however, is calibrated so that its reading corresponds to the kilovoltage which will be generated by the x-ray transformer secondary coil in the output part of the circuit and applied to the x-ray tube. The tube voltage can be measured by the sphere gap method in which the voltage is applied to two metallic spheres separated by an air gap. The spheres are slowly brought together until a spark appears. There is a mathematical relationship between the voltage, the diameter of the spheres, and the distance between them at the instant that the spark first appears.

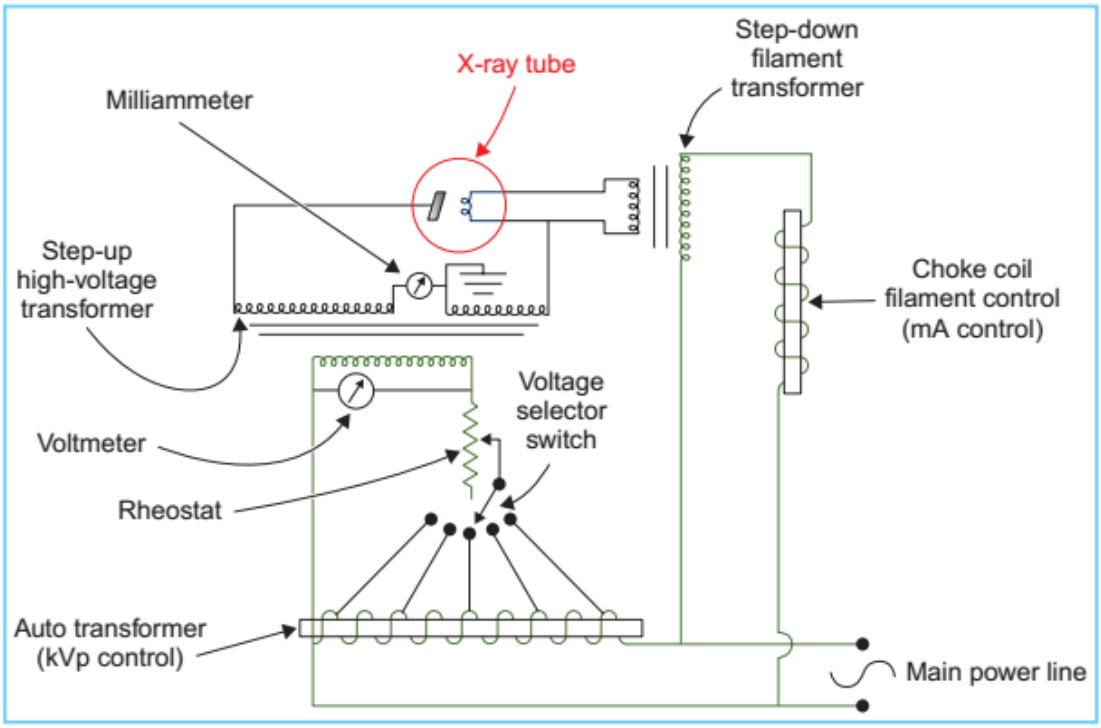

Figure 3.3. Simplified circuit diagram of a self-rectified x-ray unit.

The tube current can be read on a milliammeter in the high-voltage part of the tube circuit.

The meter is actually placed at the midpoint of the x-ray transformer secondary coil, which is grounded. The meter, therefore, can be safely placed at the operator's console.

The alternating voltage applied to the x-ray tube is characterized by the peak voltage and the frequency. For example, if the line voltage is 220 V

at 60 cycles/s, the peak voltage will be 220 $\sqrt{2}$ =311 V, since the line voltage is normally expressed as the root mean square value.

Thus, if this voltage is stepped up by an x-ray transformer of turn ratio 500:1, the resultant peak

voltage applied to the x-ray tube will be 220$\sqrt{2}$ × 500 = 155,564 V = 155.6 kV.

Since the anode is positive with respect to the cathode only through half the voltage cycle، the tube current flows through that half of the cycle. During the next half-cycle, the voltage is reversed and the current cannot flow in the reverse direction. Thus, the tube current as well as the x-rays will be generated only during the half-cycle when the anode is positive. A machine operating in this manner is called the self-rectified unit. The variation with time of the voltage، tube current, and x-ray intensity is illustrated in Figure 3.4.

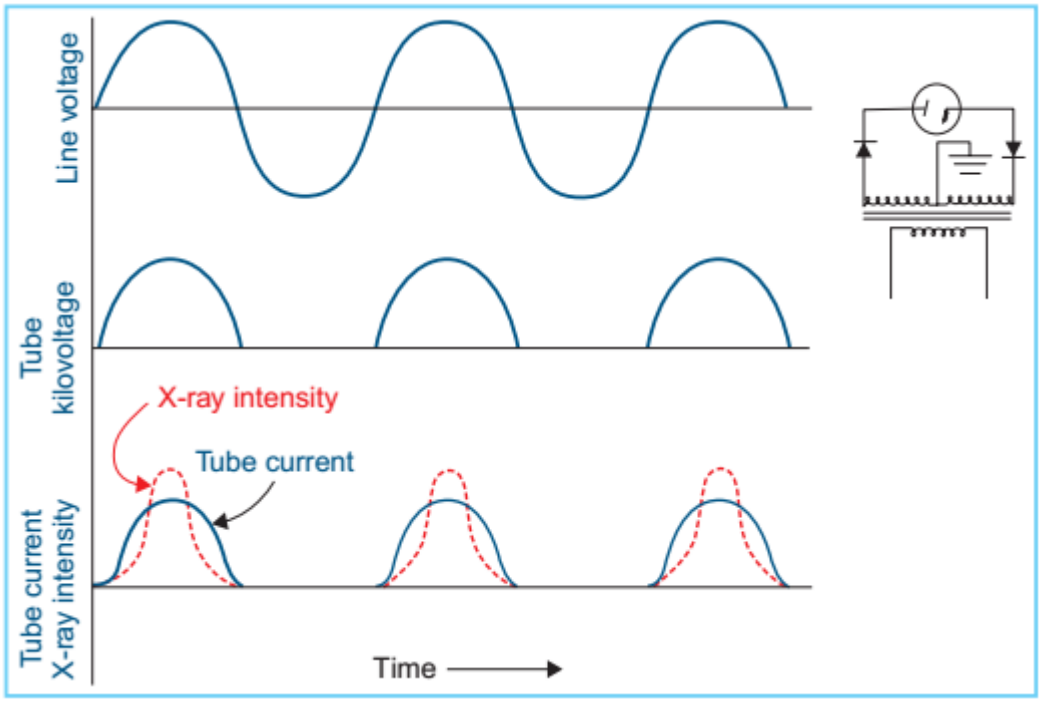

Figure 3.4. Graphs illustrating the variation with time of the line voltage, the tube kilovoltage, the tube current، and the x-ray intensity for self- or half-wave rectification. the half-wave rectifier circuit is shown on the right. Rectifier indicates the direction of conventional current (opposite to the flow of electrons).

3.3 .Voltage Rectification

The disadvantage of the self-rectified circuit is that no x-rays are generated during the inverse voltage cycle (when the anode is negative relative to the cathode), and therefore, the output of the machine is relatively low. Another problem arises when the target gets hot and emits electrons by the process of thermionic emission. During the inverse voltage cycle, these electrons will flow from the anode to the cathode and bombard the cathode filament. This can destroy the filament.

The problem of tube conduction during inverse voltage can be solved by using voltage rectifiers. Rectifiers placed in series in the high-voltage part of the circuit prevent the tube from conducting during the inverse voltage cycle. The current will flow as usual during the cycle when the anode is positive relative to the cathode. This type of rectification is called half-wave rectification and is illustrated in Figure 3.4.

The high-voltage rectifiers are either valve or solid-state type. The valve rectifier is similar in principle to the x-ray tube. The cathode is a tungsten filament and the anode is a metallic plate or cylinder surrounding the filament. The current flows only from the anode to the cathode but the valve will not conduct during the inverse cycle even if the x-ray target gets hot and emits electrons.

A valve rectifier can be replaced by solid state rectifiers. These rectifiers consist of conductors which have been coated with certain semiconducting elements such as selenium, silicon, and germanium. These semiconductors conduct electrons in one direction only and can withstand reverse voltage up to a certain magnitude. Because of their very small size, thousands of these rectifiers can be stacked in series in order to withstand the given inverse voltage.

Rectifiers can also be used to provide full-wave rectification. For example, four rectifiers can be arranged in the high-voltage part of the circuit so that the x-ray tube cathode is negative and the anode is positive during both half-cycles of voltage. This is schematically shown in Figure 3.5. The electronic current flows through the tube via ABCDEFGH when the transformer end A is negative and via HGCDEFBA when A is positive. Thus, the electrons flow from the filament to the target during both half-cycles of the transformer voltage. As a result of full-wave rectification, the effective tube current is higher since the current flows during both half-cycles.

In addition to rectification, the voltage across the tube may be kept nearly constant by a smoothing condenser (high capacitance) placed across the x-ray tube. Such constant potential circuits have been used in x-ray machines for therapy.

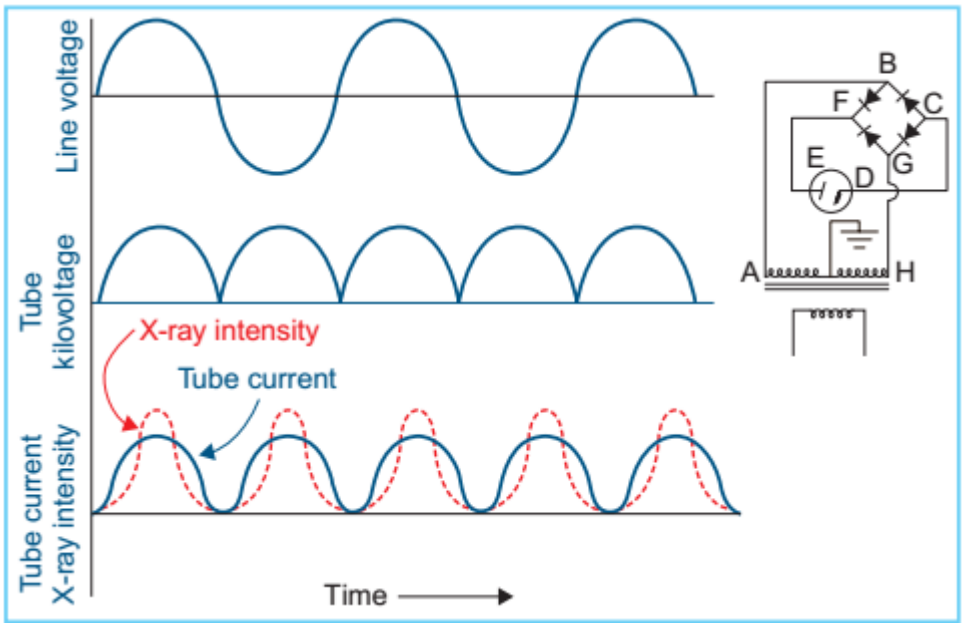

Figure 3.5. Graphs illustrating the variation with time of the line voltage, the tube kilovoltage، the tube current, and the x-ray intensity for full-wave rectification. the rectifier circuit is shown on the right. the arrow symbol on the rectifier diagram indicates the direction of conventional current flow (opposite to the flow of electronic current).

3.4 .High-Output X-Ray Generators

A. Three-Phase Generators

In x-ray imaging, it is important to have high-enough x-ray output in a short time so that the effect of patient motion is minimal and does not create blurring of the image. This can be done through the use of a three-phase x-ray generator in which the high voltage applied to the x-ray tube is in three phases. The three-phase (3φ) power line is supplied through three separate wires and is stepped up by an x-ray transformer with three separate windings and three separate iron cores. The voltage waveform in each wire is kept slightly out of phase with each other, so that the voltage across the tube is always near maximum (Fig. 3.6).

With the three-phase power and full-wave rectification, six voltage pulses are applied to the x-ray tube during each power cycle. This is known as a three-phase, six-pulse system.

The voltage ripple, defined as $[(V_{max} - V_{min})/V_{max}] \times 100$, is 13% to 25% for this system. By creating a slight delay in phase between the three-phase rectified voltage waveforms applied to the anode and the cathode, a three-phase, 12-pulse circuit is obtained. Such a system shows much less ripple (3% to 10%) in the voltage applied to the x-ray tube.

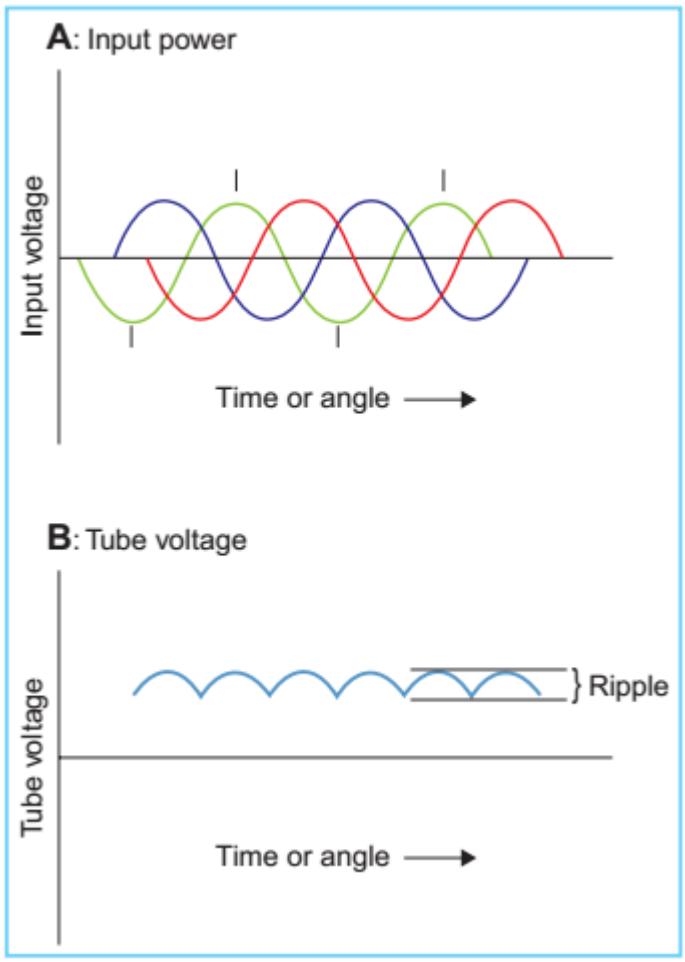

Figure 3.6. Voltage waveforms in a three-phase generator.

B. Constant Potential Generators

The so-called constant potential x-ray generator uses a three-phase line voltage coupled directly to the high-voltage transformer primary. The high voltage thus generated is smoothed and regulated by a circuit involving rectifiers, capacitors, and triode valves. The voltage supplied to the tube is nearly constant, with a ripple of less than 2%. Such a generator provides the highest x-ray output per mAs (milliampere second) exposure. However, it is a very large and expensive generator, used only for special applications.

C. High-Frequency Generators

A much smaller and state-of-the-art generator that provides nearly a constant potential to the x-ray tube is the high-frequency x-ray generator (Fig. 3.7). This generator uses a single-phase line voltage which is rectified and smoothed (using capacitors) and then fed to a chopper and inverter circuit. As a result, the smooth, direct current (DC) voltage is converted into a high frequency (5 to 100 kHz) alternating current (AC) voltage. A step-up transformer converts this high-frequency low-voltage AC into a high-voltage AC which is then rectified and smoothed to provide a nearly constant high-voltage potential (with a ripple of less than 2%) to the x-ray tube.

The principal advantages of a high-frequency generator are (a) reduced weight and size, (b) low voltage ripple, (c) greatest achievable efficiency of x-ray production, (d) maximum x-ray output per mAs, and (e) shorter exposure times.

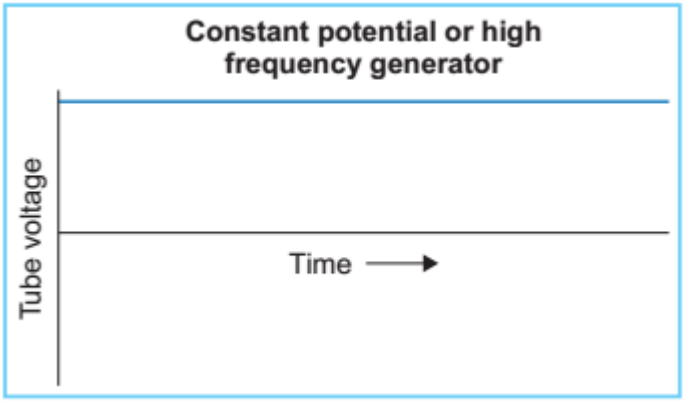

Figure 3.7. Voltage waveforms in a high-frequency generator.

3.5 .Physics of X-Ray Production

There are two different mechanisms by which x-rays are produced. One gives rise to bremsstrahlung x-rays and the other characteristic x-rays.

A. Bremsstrahlung

The process of bremsstrahlung (braking radiation) is the result of radiative "collision" (interaction) between a high-speed electron and a nucleus. The electron while passing near a nucleus may be deflected from its path by the action of Coulomb forces of attraction and lose energy as bremsstrahlung, a phenomenon predicted by Maxwell's general theory of electromagnetic radiation. According to this theory, energy is propagated through space by electromagnetic fields. As the electron, with its associated electromagnetic

field, passes in the vicinity of a nucleus, it suffers a sudden deflection and acceleration. As a result, a part or all of its energy is dissociated from it and propagates in space as electromagnetic radiation. The mechanism of bremsstrahlung production is illustrated in Figure 3.8.

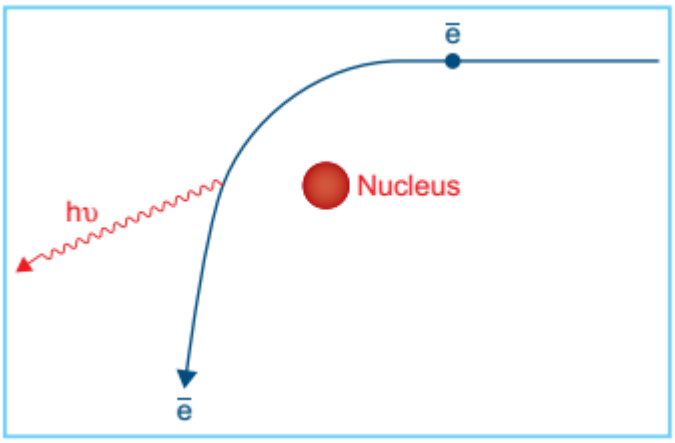

Figure 3.8. Illustration of the bremsstrahlung process.

Since an electron may have one or more bremsstrahlung interactions in the material and an interaction may result in partial or complete loss of electron energy, the resulting bremsstrahlung photon may have any energy up to the initial energy of the electron. Also, the direction of emission of bremsstrahlung photons depends on the energy of the incident electrons (Fig. 3.9).

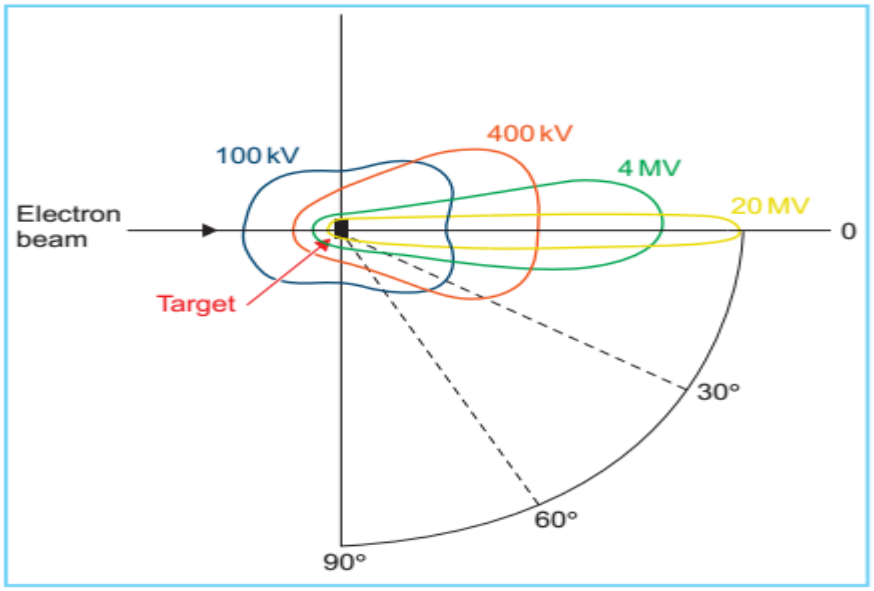

Figure 3.9. Schematic illustration of spatial distribution of x-rays around a thin target.

At electron energies below about 100 keV, x-rays are emitted more or less equally in all directions.

As the kinetic energy of the electrons increases, the direction of x-ray emission becomes increasingly forward. Therefore, transmission-type targets are used in megavoltage x-ray tubes (accelerators) in which the electrons bombard the target from one side and the x-ray beam is obtained on the other side. In the low-voltage x-ray tubes, it is technically advantageous to obtain the x-ray beam on the same side of the target, i.e., at 90 degrees with respect to the electron beam direction.

The energy loss per atom by electrons depends on the square of the atomic number (Z^2). Thus, the probability of bremsstrahlung production varies with Z^2 of the target material. However، the efficiency of x-ray production depends on the first power of atomic number and the voltage applied to the tube. The term efficiency is defined as the ratio of output energy emitted as x-rays to the input energy deposited by electrons. It can be shown that Efficiency = 9×10^{-10} ZV.

where V is tube voltage in volts. From the above equation, it can be shown that the efficiency of x-ray production with tungsten target (Z = 74) for electrons accelerated through 100 kV is less than 1%. The rest of the input energy (~99%) appears as heat. Efficiency improves considerably for high-energy x-rays, reaching 30% to 95% for accelerator beams depending upon energy. The accuracy of above equation is limited to a few megavolts.

B. Characteristic X-Rays

Electrons incident on the target also produce characteristic x-rays. The mechanism of their production is illustrated in Figure 3.10. An electron, with kinetic energy E_0, may interact with the atoms of the target by ejecting an orbital electron, such as a K, L, or M electron, leaving the atom ionized. The original electron will recede from the collision with energy $E_0 - \Delta E$, where ΔE is the energy given to the orbital electron. A part of ΔE is spent in overcoming the binding energy of the electron and the rest is carried by the ejected electron. When a vacancy is created in an orbit, an outer orbital electron will fall down to fill that vacancy. In so doing, the energy is radiated in the form of electromagnetic radiation. This is called characteristic radiation, i.e‹. characteristic of the atoms in the target and of the shells between which the transitions took place. With higher atomic number targets and the transitions involving inner shells such as K and L, the characteristic radiations emitted are of energies high enough to be

considered in the x-ray part of the electromagnetic spectrum. Table 3.1 gives the major characteristic radiation energies produced in a tungsten target. It should be noted that, unlike bremsstrahlung, characteristic x-rays are emitted at discrete energies. If the transition involved an electron descending from the L shell to the K shell, then the photon emitted will have energy $hv = E_K - E_L$, where E_K and E_L are the electron-binding energies of the K shell and the L shell, respectively.

The threshold energy that an incident electron must possess in order to first strip an electron from the atom is called critical absorption energy. These energies for some elements are given in Table 3.2.

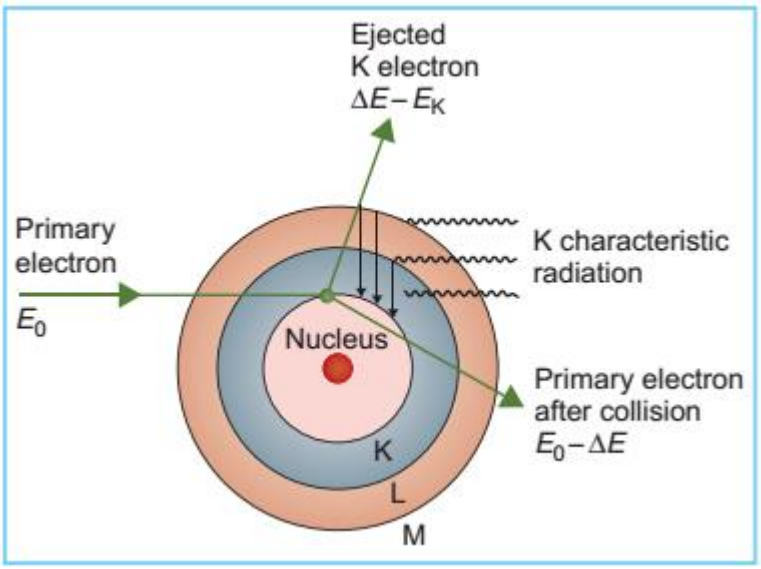

Figure 3.10. Diagram to explain the production of characteristic radiation.

TABLE 3.1 Principal Characteristic X-Ray Energies for Tungsten

Series	Lines	Transition	Energy (keV)
K	$K\beta_2$	N_{III}–K	69.09
	$K\beta_1$	M_{III}–K	67.23
	$K\alpha_1$	L_{III}–K	59.31
	$K\alpha_2$	L_{II}–K	57.97
L	$L\gamma_1$	N_{IV}–L_{II}	11.28
	$L\beta_2$	N_V–L_{III}	9.96
	$L\beta_1$	M_{IV}–L_{II}	9.67
	$L\alpha_1$	M_V–L_{III}	8.40
	$L\alpha_2$	M_{IV}–L_{III}	8.33

TABLE 3.2 Critical Absorption Energies (keV)

	Element											
Level	H	C	O	Al	Ca	Cu	Sn	I	Ba	W	Pb	U
Z	1	6	8	13	20	29	50	53	56	74	82	92
K	0.0136	0.283	0.531	1.559	4.038	8.980	29.190	33.164	37.41	69.508	88.001	115.59
L				0.087	0.399	1.100	4.464	5.190	5.995	12.090	15.870	21.753

3.6 .X-Ray Energy Spectra

X-ray photons produced by an x-ray machine are heterogeneous in energy. The energy spectrum shows a continuous distribution of energies for the bremsstrahlung photons superimposed by characteristic radiation of discrete energies. A typical spectral distribution is shown in Figure 3.11. If no filtration, inherent or added, of the beam is assumed, the calculated energy spectrum will be a straight line (shown as dotted lines in Fig. 3.11) and mathematically given by Kramer's equation:

$$I_E = KZ(E_m - E) \tag{3.1}$$

where I_E is the intensity of photons with energy E, Z is the atomic number of the target, E_m is the maximum photon energy, and K is a constant. As pointed out earlier, the maximum possible energy that a bremsstrahlung photon can have is equal to the energy of the incident electron.

The maximum energy in kiloelectron volts (keV) is numerically equal to the voltage difference between the anode and the cathode in kilovolts peak (kV_p). However, the intensity of such photons is zero as predicted by the previous equation, that is, $I_E = 0$ when $E = E_m$.

The unfiltered energy spectrum discussed previously is considerably modified as the photons experience inherent filtration (absorption in the target, glass walls of the tube, or thin beryllium window). The inherent filtration in conventional x-ray tubes is usually equivalent to about 0.5 -to 1 mm aluminum. Added filtration, placed externally to the tube, further modifies the spectrum. It should be noted that the filtration affects primarily the initial low-energy part of the spectrum and does not affect significantly the high-energy photon distribution.

The purpose of the added filtration is to enrich the beam with higher-energy photons by absorbing the lower-energy components of the spectrum. As the filtration is increased, the transmitted beam hardens, i.e., it achieves higher average energy and therefore greater penetrating power. Thus, the addition of filtration is one way of improving the penetrating power of the beam. The other method, of course, is by increasing the voltage across the tube. Since the total intensity of the beam (area under the curves in Fig. 3.11) decreases with increasing filtration and increases with voltage, a proper combination of voltage and filtration is required to achieve desired hardening of the beam as well as acceptable intensity.

The shape of the x-ray energy spectrum is the result of the alternating voltage applied to the tube, multiple bremsstrahlung interactions within the

target, and filtration in the beam. However, even if the x-ray tube were to be energized with a constant potential, the x-ray beam would still be heterogeneous in energy because of the multiple bremsstrahlung processes that result in different energy photons.

Because of the x-ray beam having a spectral distribution of energies, which depends on voltage as well as filtration, it is difficult to characterize the beam quality in terms of energy, penetrating power, or degree of beam hardening. A practical rule of thumb is often used which states that the average x-ray energy is approximately one-third of the maximum energy or kV_p.

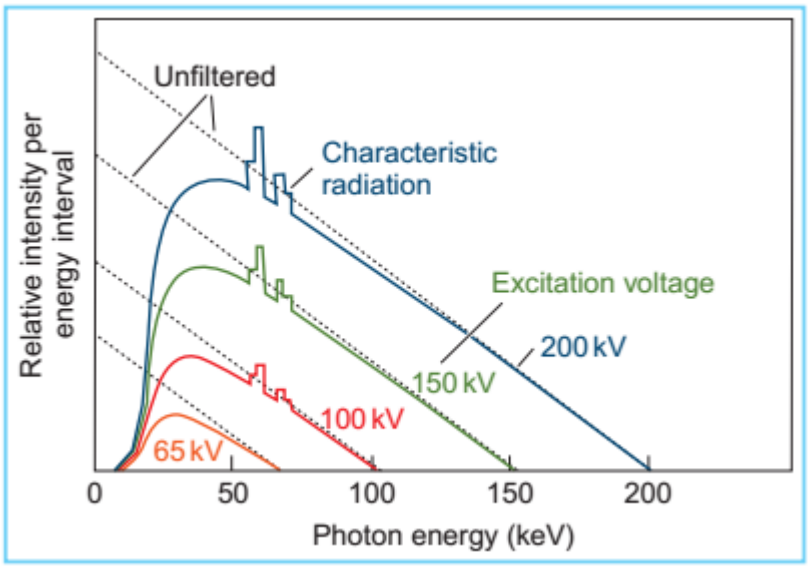

Figure 3.11. Spectral distribution of x-rays calculated for a thick tungsten target using equation 3.1. Dotted curves are for no filtration and the solid curves are for a filtration of 1-mm aluminum.

Of course, the one-third rule is a rough approximation since filtration significantly alters the average energy. Another quantity, known as half-value layer, has been defined to describe the quality of an x-ray beam.

3.7 .Operating Characteristics

In this section, the relationships between x-ray output, filament current, tube current, and tube voltage are briefly discussed. The output of an x-ray machine can also be expressed in terms of the ionization it produces in air. This quantity, which is a measure of ionization per unit mass of air, is called exposure.

The filament current affects the emission of electrons from the filament and, therefore, the tube current. Figure 3.12a shows the typical relationship

between the relative exposure rate and the filament current measured in amperes (A). The figure shows that under typical operating conditions (filament current of 5 to 6 A), a small change in filament current produces a large change in relative exposure rate. This means that the constancy of filament current is critical to the constancy of the x-ray output.

In Figure 3.12b, the exposure rate is plotted as a function of the tube current. There is a linear relationship between exposure rate and tube current. As the current or milliamperage is doubled، the output is also doubled.

The increase in the x-ray output with increase in voltage, however, is much greater than that given by a linear relationship. Although the actual shape of the curve (Fig. 3.12c) depends on the filtration, the output of an x-ray machine varies approximately as a square of kilovoltage.

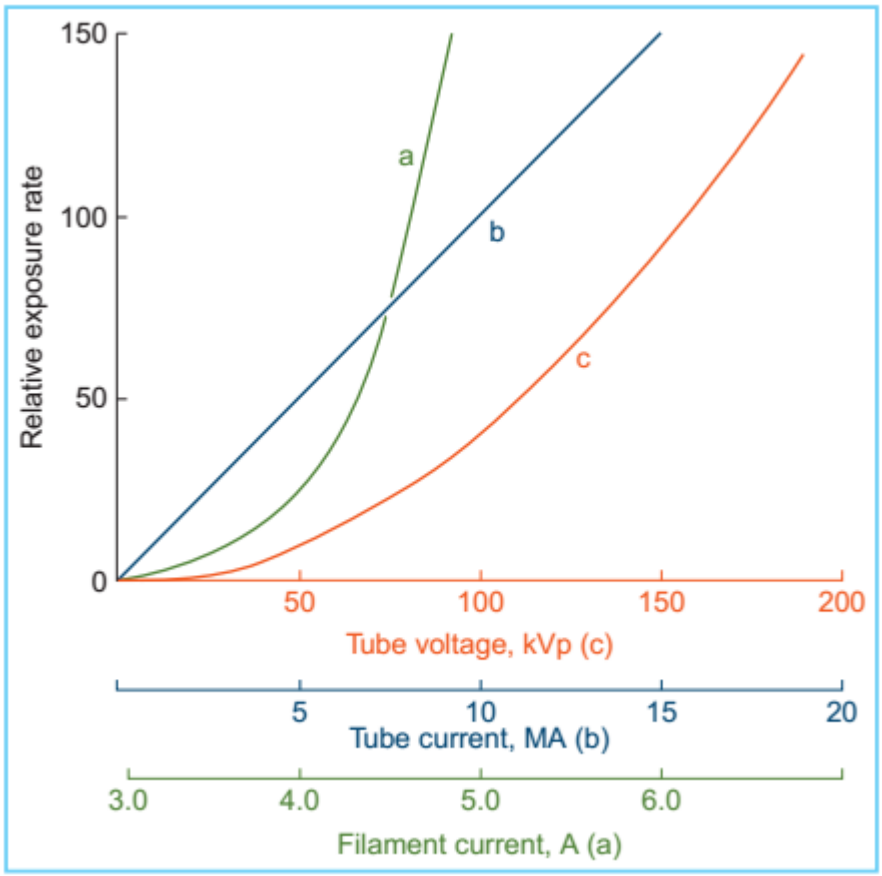

Figure 3.12. Illustration of typical operating characteristics. plots of relative exposure rate versus (a) filament current at a given kV_p, (b) tube current at a given kVp, and (c) tube voltage at a given tube current.

4 Clinical Radiation Generators

4.1 .Kilovoltage Units

Up to about 1950, most of the external beam radiotherapy was carried out with x-rays generated at voltages up to 300 kVp. Subsequent development of higher-energy machines and the increasing popularity of the cobalt-60 units in the 1950s and the 1960s resulted in a gradual demise of the conventional kilovoltage machines. However, these machines have not completely disappeared. Even in the present era of the megavoltage beams, there is still some use for the lower-energy beams, especially in the treatment of superficial skin lesions.

In this chapter, we will consider in particular the salient features of the therapy machines.

On the basis of beam quality and their use, the x-ray therapy in the kilovoltage range has been divided into subcategories. The following ranges are more in accordance with the National Council on Radiation Protection and Measurements (NCRP).

A. Grenz-Ray Therapy

The term Grenz-ray therapy is used to describe treatment with beams of very soft (low-energy) x-rays produced at potentials below 20 kV. Because of the very low depth of penetration (Fig. 4.1, line a), such radiations are no longer used in radiation therapy.

B. Contact Therapy

A contact therapy or endocavitary machine operates at potentials of 40 to 50 kV and facilitates irradiation of accessible lesions at very short source (focal spot) to surface distances (SSD). The machine operates typically at a tube current of 2 mA. Applicators available with such machines can provide an SSD of 2.0 cm or less. A filter of 0.5- to 1.0-mm thick aluminum is usually interposed in the beam to absorb the very soft component of the energy spectrum.

Because of very short SSD and low voltage, the contact therapy beam produces a very rapidly decreasing depth dose in tissue. For that reason, if the beam is incident on a patient, the skin surface is maximally irradiated but the underlying tissues are spared to an increasing degree with depth. The dose versus depth curve or simply the depth–dose curve of a typical contact therapy beam is shown in Figure 4.1, line b. It is readily seen that this quality of radiation is useful for tumors not deeper than 1 to 2 mm. The

beam is almost completely absorbed with 2 cm of soft tissue. Endocavitary x-ray machines have been used in the treatment of superficial rectal cancers.

C. Superficial Therapy

The term superficial therapy applies to treatment with x-rays produced at potentials ranging from 50 to 150 kV. Varying thicknesses of filtration (usually 1- to 6-mm aluminum) are added to harden the beam to a desired degree. As mentioned in Section 3.6, the degree of hardening or beam quality can be expressed as the half-value layer (HVL). The HVL is defined as the thickness of a specified material that, when introduced into the path of the beam, reduces the exposure rate by one-half. Typical HVLs used in the superficial range are 1.0- to 8.0-mm Al.

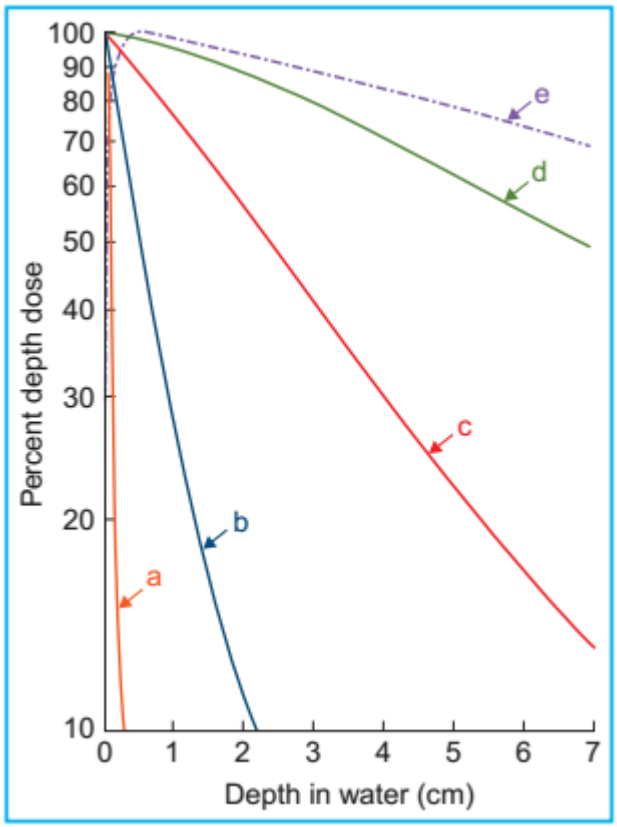

Figure 4.1. Depth–dose curves in water or soft tissues for various quality beams. Line a: Grenz rays, HVL = 0.04 mm al، field diameter = 33 cm, SSD = 10 cm. Line b: Contact therapy، HVL = 1.5 mm al, field diameter = 2.0 cm, SSD = 2 cm. Line c :Superficial therapy, HVL = 3.0 mm al, field diameter = 3.6 cm، SSD = 20 cm. Line d: Orthovoltage, HVL = 2.0 mm Cu, field size = 10 × 10 cm, SSD = 50 cm. Line e: Cobalt-60 γ rays, field size = 10 × 10 cm, SSD = 80 cm.

The superficial treatments are usually given with the help of applicators or cones attachable to the diaphragm of the machine. The SSD typically ranges between 15 and 20 cm. The machine is usually operated at a tube current of 5 to 8 mA. As seen in Figure 4.1, line c, a superficial beam of the quality shown is useful for irradiating tumors confined to about 5-mm depth (~90% depth dose). Beyond this depth, the dose dropoff is too severe to deliver adequate depth dose without considerable overdosing of the skin surface.

D. Orthovoltage Therapy or Deep Therapy

The term orthovoltage therapy, or deep therapy, is used to describe treatment with x-rays produced at potentials ranging from 150 to 500 kV. Most orthovoltage equipment is operated at 200 to 300 kV and 10 to 20 mA. Various filters have been designed to achieve HVLs between 1 -and 4-mm Cu. An orthovoltage machine is shown in Figure 4.2.

Although cones can be used to collimate the beam into a desired size, a movable diaphragm، consisting of lead plates, permits a continuously adjustable field size. The SSD is usually set at 50 cm.

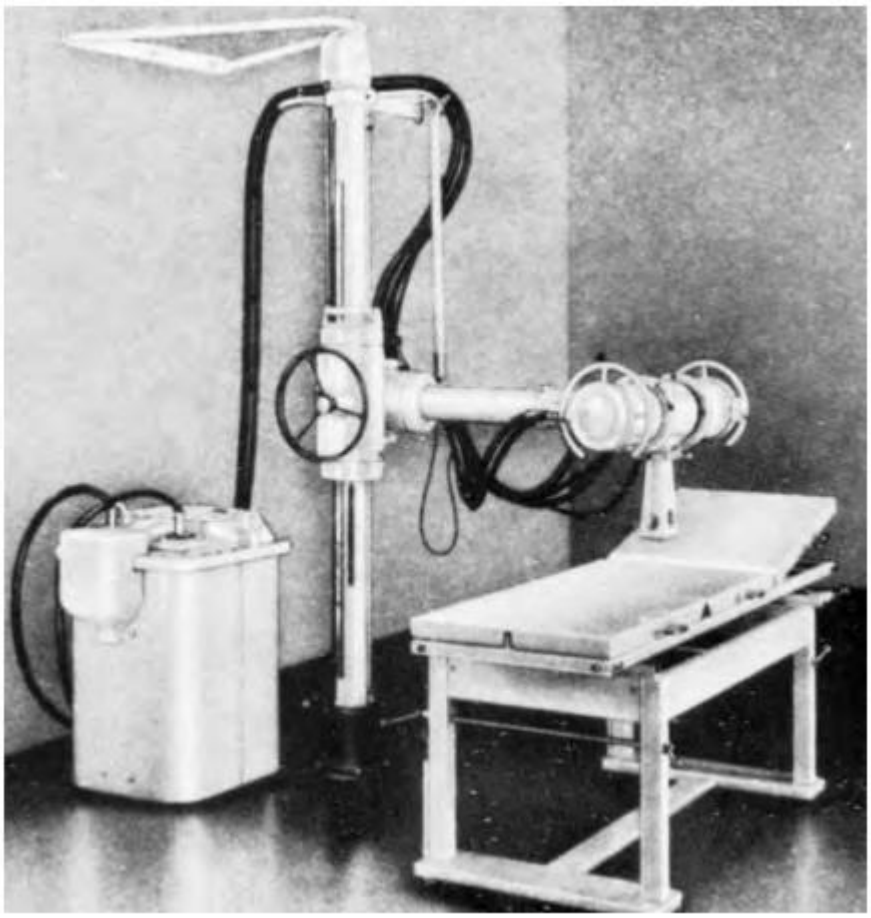

Figure 4.2. Photograph of Siemens Stabilapan.

Figure 4.1, line d, shows a depth–dose curve for a moderately filtered orthovoltage beam.

Although the actual depth–dose distribution would depend on many conditions such as kilovoltage، HVL, SSD, and field size, some generalizations can be made from this curve about the orthovoltage beam characteristics. The maximum dose occurs close to the skin surface, with 90% of that value occurring at a depth of about 2 cm. Thus, in a single field

treatment, adequate dose cannot be delivered to a tumor beyond this depth. However, by increasing beam filtration or HVL and combining two or more beams directed at the tumor from different directions, a higher dose to deeper tumors is delivered. As will be discussed in further detail in Chapter 11, there are severe limitations

to the use of orthovoltage beam in treating lesions deeper than 2 to 3 cm. The greatest limitation is the skin dose, which becomes prohibitively large when adequate doses are to be delivered to deep-seated tumors. In the early days of radiation therapy, when orthovoltage was the highest energy available, treatments were given until radiation tolerance of the skin was reached. Although methods were developed to use multiple beams and other techniques to keep the skin dose under tolerance limits, the problem of high skin dose remained an overriding concern in the orthovoltage era. With the availability of cobalt teletherapy, the skin-sparing properties of higher-energy radiation (Fig. 4.1, line e) became the major reason for the modern trend to megavoltage beams.

Although skin dose and depth–dose distribution have been presented here as two examples of the limitations posed by low-energy beams, there are other properties such as increased absorbed dose in bone and increased scattering that make orthovoltage beams unsuitable for the treatment of tumors behind bone.

E. Supervoltage Therapy

X-ray therapy in the range of 500 to 1,000 kV has been designated as high-voltage therapy or supervoltage therapy. In a quest for higher-energy x-ray beams, considerable progress was made in the 1950s and 1960s toward developing higher-voltage machines. The major problem at that time was insulating the high-voltage transformer. It soon became apparent that conventional transformer systems were not suitable for producing potential much above 300 kVp. However، with the rapidly advancing technology of the times, new approaches to the design of high-energy machines were found. One of these machines is the resonant transformer, in which the voltage is stepped up in a very efficient manner.

E.1. Resonant Transformer Units

Resonant transformer units have been used to generate x-rays from 300 to 2,000 kV. The schematic diagram of the apparatus is shown in Figure 4.3. In this apparatus, the secondary of the high-voltage transformer (without the iron core) is connected in parallel with capacitors distributed

lengthwise inside the x-ray tube. The combination of the transformer secondary and the capacitance in parallel exhibits the phenomenon of resonance. At the resonant frequency, the oscillating potential attains very high amplitude. Thus, the peak voltage across the x-ray tube becomes very large when the transformer is tuned to resonate at the input frequency. Since the electrons attain high energies before striking the target, a transmission-type target (Section 3.4) may be used to obtain the x-ray beam on the other side of the target. The electrical insulation is provided by pressurized Freon gas.

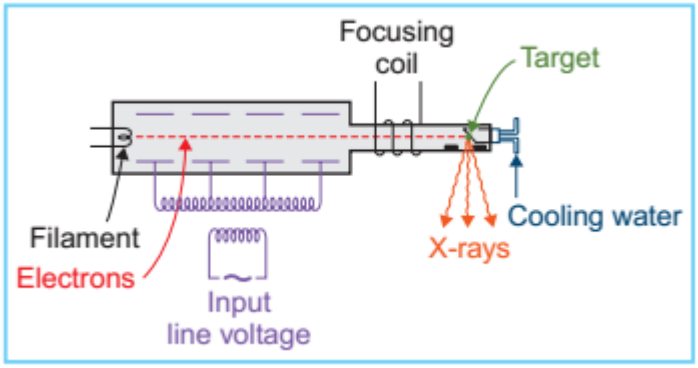

Figure 4.3. Diagram of a resonant transformer unit.

F. Megavoltage Therapy

X-ray beams of energy 1 MV or greater can be classified as megavoltage beams. Although the term strictly applies to the x-ray beams, the γ-ray beams produced by radionuclides are also commonly included in this category if their energy is 1 MeV or greater. Examples of clinical megavoltage machines are accelerators such as Van de Graaff generator, linear accelerator, betatron and microtron, and teletherapy γ-ray units such as cobalt-60.

4.2 .Van De Graaff Generator

The Van de Graaff machine is an electrostatic accelerator designed to accelerate charged particles.

In radiotherapy, the unit accelerates electrons to produce high-energy x-rays, typically at 2 MV.

Figure 4.4 shows a schematic diagram illustrating the basic principle of a Van de Graaff generator. In this machine, a charge voltage of 20 to 40 kV is applied across a moving belt of insulating material. A corona discharge takes place and electrons are sprayed onto the belt. These electrons are

carried to the top where they are removed by a collector connected to a spherical dome.

As the negative charges collect on the sphere, a high potential is developed between the sphere and the ground. This potential is applied across the x-ray tube consisting of a filament, a series of metal rings, and a target. The rings are connected to resistors to provide a uniform drop of potential from the bottom to the top. X-rays are produced when the electrons strike the target.

Van de Graaff machines are capable of reaching voltages up to 25 MV, limited only by size and required high-voltage insulation. Normally the insulation is provided by a mixture of nitrogen and CO_2 or sulfur hexafluoride (SF_6). The generator is enclosed in a steel tank and is filled with the gas mixture at a pressure of about 20 atm.

Van de Graaff and resonant transformer (Section 4.1.E) units for clinical use are no longer produced commercially. The reason for their demise is the emergence of technically better machines such as cobalt-60 units and linear accelerators.

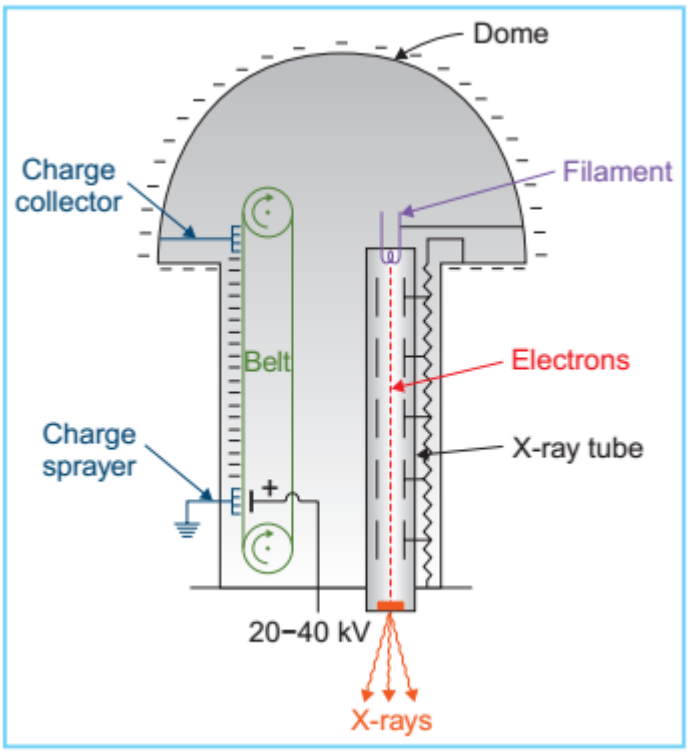

Figure 4.4. a Van de Graaff generator.

4.3 .Linear Accelerator

The linear accelerator (linac) is a device that uses high-frequency electromagnetic waves to accelerate charged particles such as electrons to high energies through a linear tube. The high-energy electron beam itself can be used for treating superficial tumors, or it can be made to strike a target to produce x-rays for treating deep-seated tumors.

There are several types of linear accelerator designs, but the ones used in radiation therapy accelerate electrons either by traveling or stationary electromagnetic waves of frequency in the microwave region (~3,000 megacycles/s). The difference between traveling wave and stationary wave accelerators is the design of the accelerator structure. Functionally, the traveling wave structures require a terminating, or "dummy," load to absorb the residual power at the end of the structure, thus preventing a backward reflected wave. On the other hand, the standing wave structures provide maximum reflection of the waves at both ends of the structure so that the combination of forward and reverse traveling waves will give rise to stationary waves. In the standing wave design, the microwave power is coupled into the structure via side coupling cavities rather than through the beam aperture. Such a design tends to be more efficient than the traveling wave designs since axial, beam transport cavities, and the side cavities can be independently optimized. However, it is more expensive and requires installation of a circulator (or isolator) between the power source and the structure to prevent reflections from reaching the power source.

Figure 4.5 is a block diagram of a medical linear accelerator showing major components and auxiliary systems. A power supply provides direct current (DC) power to the modulator، which includes the pulse-forming network and a switch tube known as hydrogen thyratron. High voltage pulses from the modulator section are flat-topped DC pulses of a few microseconds in duration. These pulses are delivered to the magnetron or klystron and simultaneously to the electron gun. Pulsed microwaves produced in the magnetron or klystron are injected into the accelerator tube or structure via a waveguide system. At the proper instant electrons, produced by an electron gun, are also pulse injected into the accelerator structure. Figure 4.6 shows the time duration of klystron (or magnetron) voltage pulse, microwave pulse, electron gun voltage pulse، and radiation pulse. The pulse duration in each case is the same (~5 ms). The interpulse duration is longer (~5 ms).

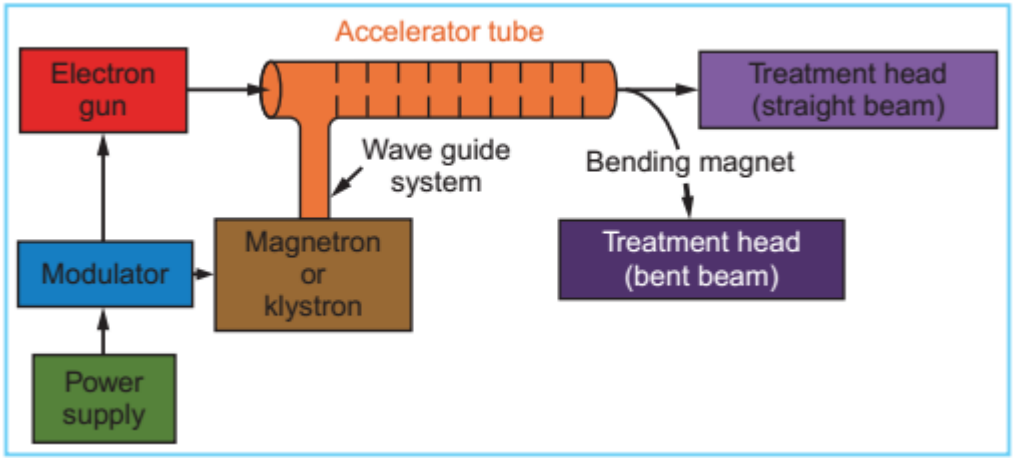

Figure 4.5. a block diagram of typical medical linear accelerator.

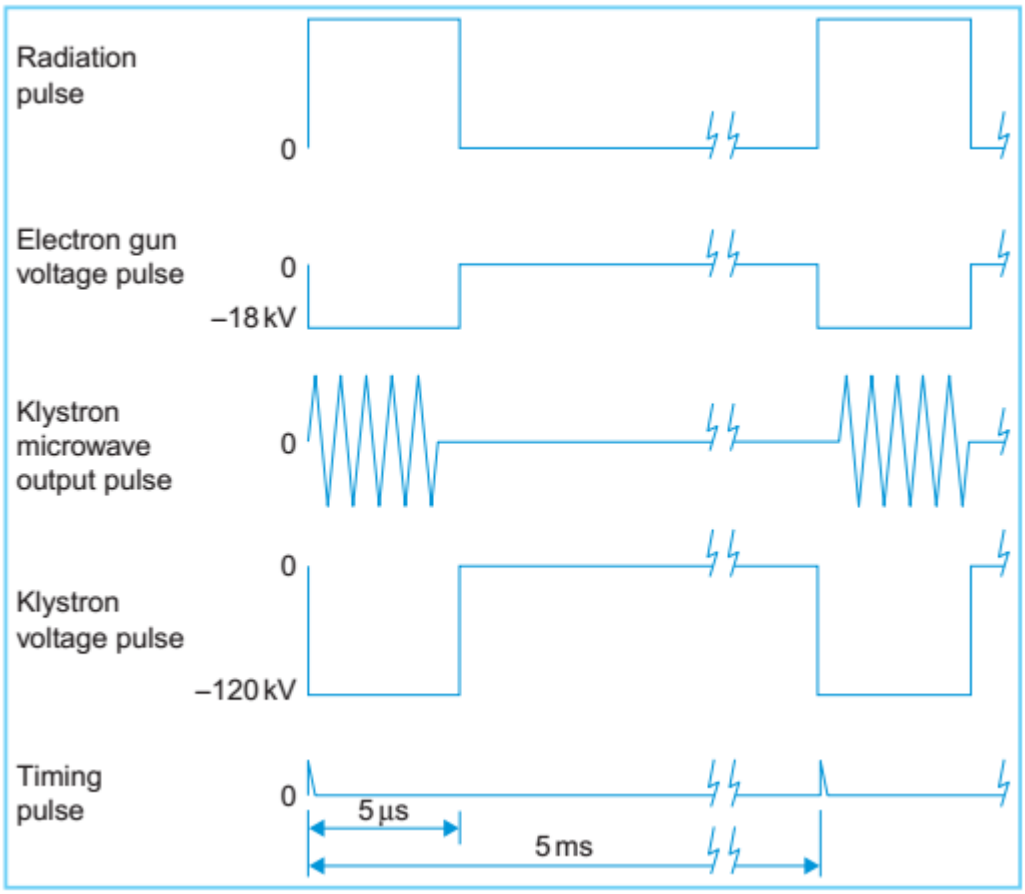

Figure 4.6. timing diagram for voltage, microwave, and radiation pulses.

The accelerator structure (or accelerator waveguide) consists of a copper tube with its interior divided by copper disks or diaphragms of varying aperture and spacing. This section is evacuated to a high vacuum. As the electrons are injected into the accelerator structure with an initial energy of about 50 keV, the electrons interact with the electromagnetic field of the microwaves. The electrons gain energy from the sinusoidal electric field by an acceleration process analogous to that of a surf rider.

As the high-energy electrons emerge from the exit window of the accelerator structure, they are in the form of a pencil beam of about 3 mm in diameter. In the low-energy linacs (up to 6 MV) with relatively short accelerator tube, the electrons are allowed to proceed straight on and strike a target for x-ray production. In the higher-energy linacs, however, the accelerator structure is too long and, therefore, is placed horizontally or at an angle with respect to the horizontal. The electrons are then bent through a suitable angle (usually about 90 or 270 degrees) between the accelerator structure and the target. The precision bending of the electron beam is accomplished by the beam transport system consisting of bending magnets, focusing coils, and other components.

A. The Magnetron

The magnetron is a device that produces microwaves. It functions as a high-power oscillator، generating microwave pulses of several microseconds' duration and with a repetition rate of several hundred pulses per second. The frequency of the microwaves within each pulse is about 3,000 MHz.

The magnetron has a cylindrical construction, having a central cathode and an outer anode with resonant cavities machined out of a solid piece of copper (Fig. 4.7). The space between the cathode and the anode is evacuated. The cathode is heated by an inner filament and the electrons are generated by thermionic emission. A static magnetic field is applied perpendicular to the plane of the cross section of the cavities and a pulsed DC electric field is applied between the cathode and the anode. The electrons emitted from the cathode are accelerated toward the anode by the action of the pulsed DC electric field. Under the simultaneous influence of the magnetic field, the electrons move in complex spirals toward the resonant cavities, radiating energy in the form of microwaves. The generated microwave pulses are led to the accelerator structure via the waveguide.

Typically, magnetrons operate at a 2-MW peak power output to power low-energy linacs (6 MV or less). Although most higher-energy linacs use klystrons, accelerators of energy as high as 25 MeV have been designed to use magnetrons of about 5 MW power.

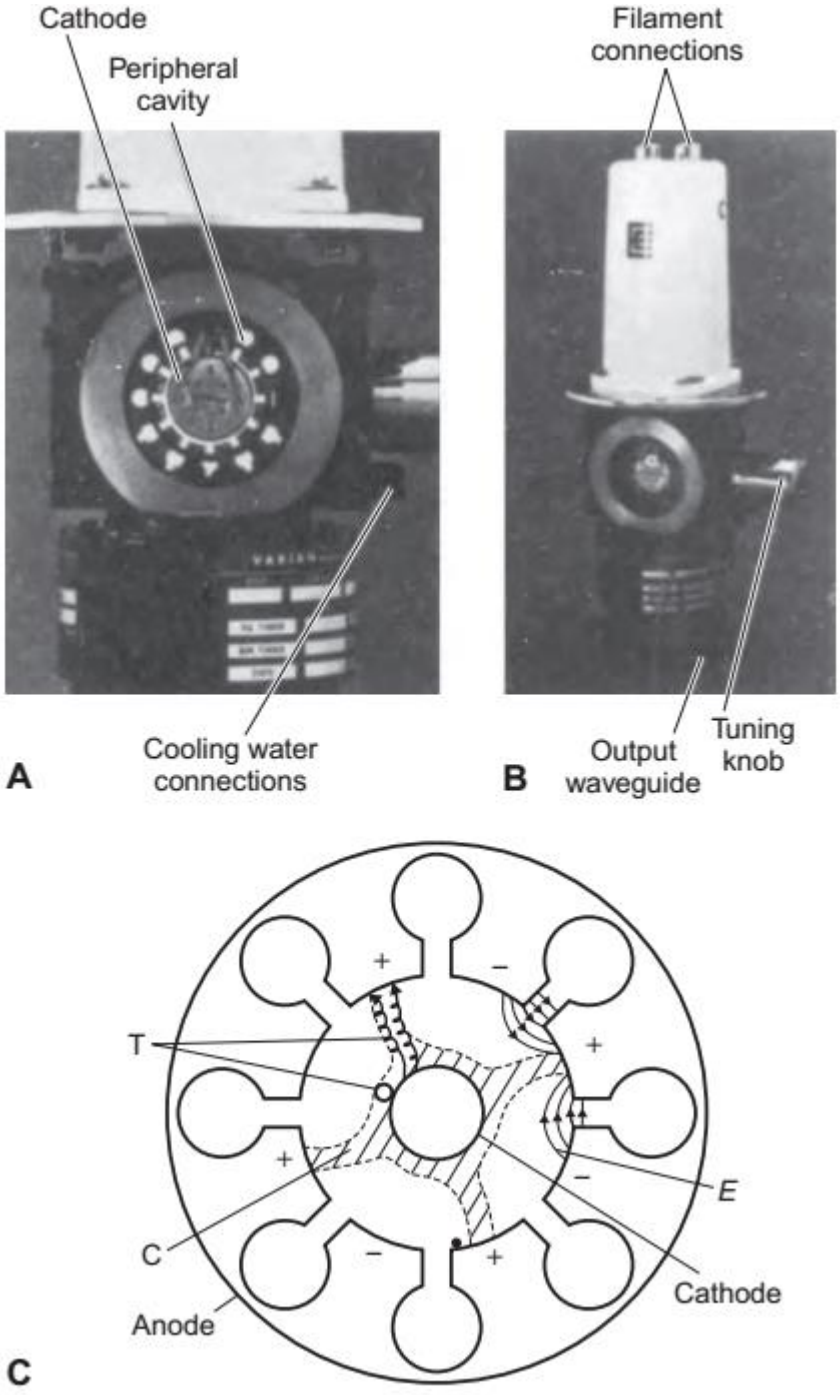

Figure 4.7. A, B: Cutaway magnetron pictures. C: Cross-sectional diagram showing principle of magnetron operation.

B. The Klystron

The klystron is not a generator of microwaves but rather a microwave amplifier. It needs to be driven by a low-power microwave oscillator. Figure 4.8 shows a cross-sectional drawing of an elementary two-cavity klystron. The electrons produced by the cathode are accelerated by a

negative pulse of voltage into the first cavity, called the buncher cavity, which is energized by low-power microwaves. The microwaves set up an alternating electric field across the cavity. The velocity of the electrons is altered by the action of this electric field to a varying degree by a process known as velocity modulation. Some electrons are speeded up while others are slowed down and some are unaffected. This results in bunching of electrons as the velocity-modulated beam passes through a field-free space in the drift tube.

As the electron bunches arrive at the catcher cavity (Fig. 4.8), they induce charges on the ends of the cavity and thereby generate a retarding electric field. The electrons suffer deceleration, and by the principle of conservation of energy, the kinetic energy of electrons is converted into high-power microwaves.

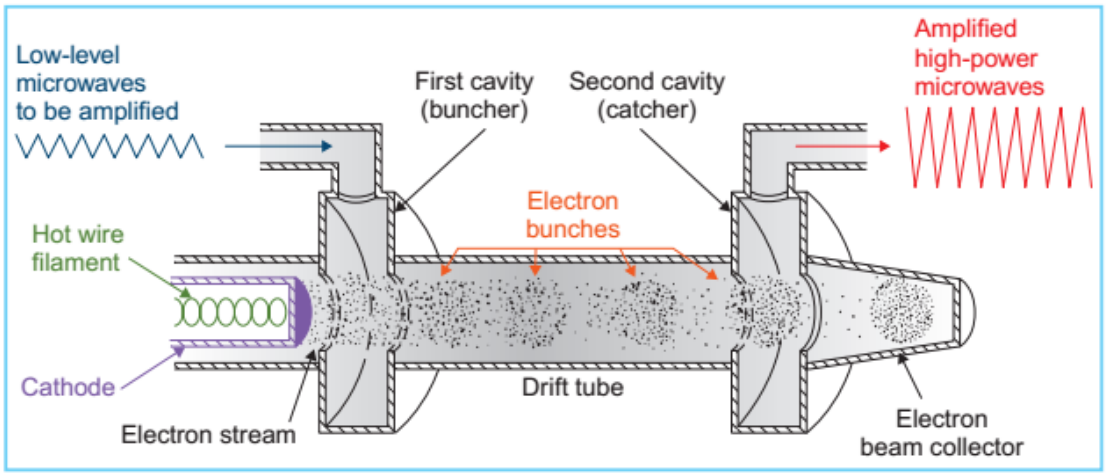

Figure 4.8. Cross-sectional drawing of a two-cavity klystron.

C. The Linac X-Ray Beam

Bremsstrahlung x-rays are produced when the electrons are incident on a target of a high-Z material such as tungsten. The target is water cooled, and it is thick enough to absorb the incident electrons. As a result of bremsstrahlung-type interactions (Section 3.4.A), the electron energy is converted into a spectrum of x-ray energies with maximum energy equal to the incident electron energy. The average photon energy of the beam is approximately one-third of the maximum energy.

D. The Electron Beam

As mentioned previously, the electron beam, as it exits the window of the accelerator tube, is a narrow pencil about 3 mm in diameter. In the electron mode of linac operation, this beam، instead of striking the target, is made

to strike an electron scattering foil to spread the beam as well as get a uniform electron fluence across the treatment field. The scattering foil consists of a thin high-Z metallic foil (e.g., lead, tantalum). The thickness of the foil is such that most of the electrons are scattered instead of suffering bremsstrahlung. However, a small fraction of the total energy is still converted into bremsstrahlung and appears as x-ray contamination of the electron beam. Most systems also employ a secondary low-Z foil of variable thickness to flatten the electron beam. The low atomic number material is chosen to minimize additional bremsstrahlung radiation produced in the beam.

In some linacs, the broadening of the electron beam is accomplished by electromagnetic scanning of the electron pencil beam over a large area. Although this minimizes the x-ray contamination, some x-rays are still produced by electrons striking the collimator walls or other high atomic number materials in the electron collimation system.

E. Treatment Head

The treatment head (Fig. 4.9A–C) consists of a thick shell of high-density shielding material such as lead, tungsten, or lead–tungsten alloy. It contains an x-ray target, scattering foil, flattening filter, ion chamber, fixed and movable collimator, and light localizer system. The head provides sufficient shielding against leakage radiation in accordance with radiation protection Guidelines.

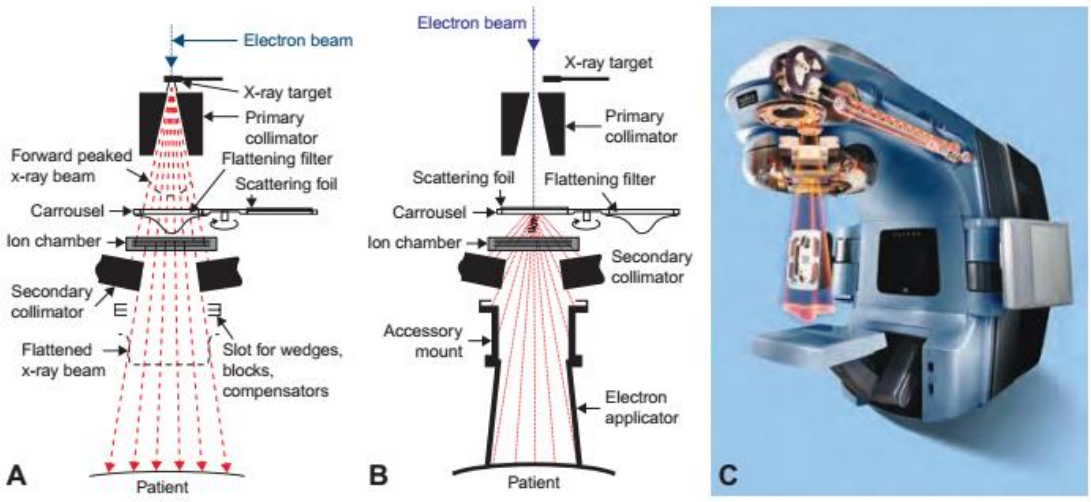

Figure 4.9. Components of treatment head. A: X-ray therapy mode. B: Electron therapy mode. C: a cut-away diagram of the linac.

F. Target and Flattening Filter

In Section 3.4.A, we discussed the angular distribution of x-rays produced by electrons of various energies incident on a target. Since linear accelerators produce electrons in the megavoltage range، the x-ray intensity is peaked in the forward direction. To make the beam intensity uniform across the field, a flattening filter is inserted in the beam (Fig. 4.9A). This filter is usually made of lead، although tungsten, uranium, steel, aluminum, or a combination has also been used or suggested.

G. Beam Collimation and Monitoring

The treatment beam is first collimated by a fixed primary collimator located immediately beyond the x-ray target. In the case of x-rays, the collimated beam then passes through the flattening filter. In the electron mode, the filter is moved out of the way (Fig. 4.9B).

The flattened x-ray beam or the electron beam is incident on the dose monitoring chambers.

The monitoring system consists of several ion chambers or a single chamber with multiple plates.

Although the chambers are usually transmission type, i.e., flat parallel plate chambers to cover the entire beam, cylindrical thimble chambers have also been used in some linacs.

The function of the ion chamber is to monitor dose rate, integrated dose, and field symmetry.

Since the chambers are in a high-intensity radiation field and the beam is pulsed, it is important to make sure that the ion collection efficiency of the chambers remains unchanged with changes in the dose rate. Bias voltages in the range of 300 to 1,000 V are applied across the chamber electrodes, depending on the chamber design. Contrary to the beam calibration chambers, the monitor chambers in the treatment head are usually sealed so that their response is not influenced by temperature and pressure of the outside air. In some linacs (e.g., Elekta), however, the monitor chambers are not sealed but have automatic pressure and temperature compensation system. In either case, these chambers have to be periodically checked to ensure that their response is independent of environmental temperature and pressure.

After passing through the ion chambers, the beam is further collimated by a continuously movable x-ray collimator. This collimator consists of two

pairs of lead or tungsten blocks (jaws) which provide a rectangular opening from 0 × 0 to the maximum field size (40 × 40 cm2 or a little less) projected at a standard distance such as 100 cm from the x-ray source (focal spot on the target). The collimator blocks are constrained to move so that the block edge is always along a radial line passing through the x-ray source position.

In addition to the x-ray jaws, modern accelerators are equipped with multileaf collimators to provide irregularly shaped field blocking and intensity modulation for intensity-modulated radiation therapy (IMRT).

The field size definition is provided by a light localizing system in the treatment head.

A combination of mirror and a light source located in the space between the chambers and the jaws projects a light beam as if emitting from the x-ray focal spot. Thus, the light field is congruent with the radiation field. Frequent checks are required to ensure this important requirement of field alignment.

Whereas the x-ray collimation systems of most medical linacs are similar, the electron collimation systems vary widely. Since electrons scatter readily in air, the beam collimation must be achieved close to the skin surface of the patient. There is a considerable scattering of electrons from the collimator surfaces including the movable jaws. Dose rate can change by a factor of two or three as the collimator jaws are opened to maximum field size limits. If the electrons are collimated by the same jaws, as for x-rays, there will be an extremely stringent requirement on the accuracy of the jaw opening, since output so critically depends on the surface area of the collimator. This problem has been solved by keeping the x-ray collimator wide open and attaching an auxiliary collimator for electrons in the form of trimmers extended down to the skin surface. In other systems, the auxiliary electron collimator consists of a set of attachable cones of various sizes.

The dose distribution in an electron field is significantly influenced by the collimation system provided with the machine because of electron scattering.

H. Gantry

Most of the linear accelerators currently produced are so constructed that the source of radiation can rotate about a horizontal axis (Fig. 4.10). As the gantry rotates, the collimator axis (supposedly coincident with the central axis of the beam) moves in a vertical plane. The point of intersection of the

collimator axis and the axis of rotation of the gantry is known as the isocenter.

Modern accelerators, like the one shown in Figure 4.10, are also equipped with gantry-mounted imaging systems for image-guided radiation therapy.

Figure 4.10. Photograph of Varian trilogy linear accelerator.

4.4 .Betatron

The operation of the betatron is based on the principle that an electron in a changing magnetic field experiences acceleration in a circular orbit. Figure 4.11 shows a schematic drawing of the machine. The accelerating tube is shaped like a hollow doughnut and is placed between the poles of an alternating current magnet. A pulse of electrons is introduced into this evacuated doughnut by an injector at the instant that the alternating current cycle begins. As the magnetic field rises, the electrons experience acceleration continuously and spin with increasing velocity around the tube. By the end of the first quarter cycle of the alternating magnetic field, the electrons have made several thousand revolutions and achieved maximum energy. At this instant or earlier, depending on the energy desired, the electrons are made to spiral out of the orbit by an additional attractive force. The high-energy electrons then strike a target to produce x-rays or a scattering foil to produce a broad beam of electrons.

Betatrons were first used for radiotherapy in the early 1950s. They preceded the introduction of linear accelerators by a few years. Although the betatrons can provide x-ray and electron therapy beams over a wide range of energies, from less than 6 to more than 40 MeV, they are

inherently low-electron-beam current devices. The x-ray dose rates and field size capabilities of medical betatrons are low compared with medical linacs and even modern cobalt units. However, in the electron therapy mode, the beam current is adequate to provide a high dose rate. The reason for this difference between x-ray and electron dose rates is that the x-ray production via bremsstrahlung as well as beam flattening requires a much larger primary electron beam current (about 1,000 times) than that required for the electron therapy beam.

The availability of medium energy linacs with high x-ray dose rates, large field sizes, and electron therapy energies up to 20 MeV has given the linacs a considerable edge in popularity over the betatrons. Moreover, many radiation therapists regard the small field size and dose rate capabilities of the betatron as serious disadvantages to the general use of the device. Thus, a significant increase in betatron installations in this country, paralleling medical linacs, seems unlikely.

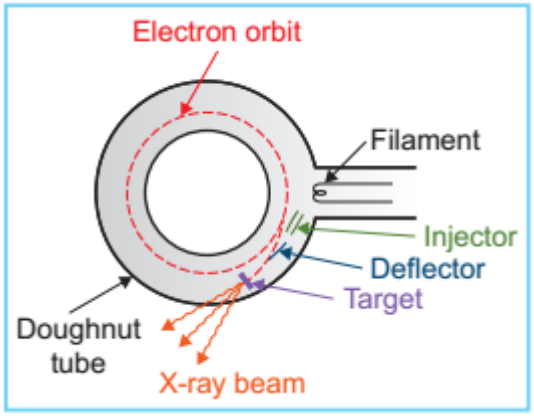

Figure 4.11. Diagram illustrating the operation of a betatron.

4.5 .Microtron

The microtron is an electron accelerator that combines the principles of both the linear accelerator and the cyclotron (Section 4.6). In the microtron, the electrons are accelerated by the oscillating electric field of one or more microwave cavities (Fig. 4.12A, B). A magnetic field forces the electrons to move in a circular orbit and return to the cavity. As the electrons receive higher and higher energy by repeated passes through the cavity, they describe orbits of increasing radius in the magnetic field. The cavity voltage, frequency, and magnetic field are so adjusted that the electrons arrive each time in the correct phase at the cavity. Because the electrons travel with an approximately constant velocity (almost the speed of light),

the above condition can be maintained if the path length of the orbits increases with one microwave wavelength per revolution.

The microwave power source is either a klystron or a magnetron.

The extraction of the electrons from an orbit is accomplished by a narrow deflection tube of steel that screens the effect of the magnetic field. When the beam energy is selected, the deflection tube is automatically moved to the appropriate orbit to extract the beam.

The principal advantages of the microtron over a linear accelerator of comparable energy are its simplicity, easy energy selection, and small beam energy spread as well as the smaller size of the machine. Because of the low energy spread of the accelerated electrons and small beam emittance (product of beam diameter and divergence), the beam transport system is greatly simplified. These characteristics have encouraged the use of a single microtron to supply a beam to several treatment rooms.

Although the method of accelerating electrons used in the microtron was proposed as early as in 1944 by Veksler, the first microtron for radiotherapy (a 10-MeV unit) was described by Reistad and Brahme in 1972. Later, a 22-MeV microtron was developed by AB Scanditronix and installed at the University of Umeå, Sweden. This particular model (MM 22) produced two x-rays beams of energy 6 or 10 and 21 MV and 10 electron beams of 2, 5, 7, 9, 11, 13, 16، 18 ،20 ،and 22 MeV.

The circular microtron, as described above and shown schematically in Figure 4.11A, is a bulky structure because it requires a large magnetic gap to accommodate accelerating cavity and large diameter magnetic field to accommodate the large number of spaced orbits with limited energy gain per orbit. These constraints are removed by a racetrack microtron, which uses a standing wave linac structure (instead of a single cavity) to accelerate the electrons (Fig. 4.12B).

The parameters of a 50-MeV racetrack microtron developed at the Royal Institute of Technology, Stockholm, are given by Rosander et al. A review is also provided by Karzmark et al.

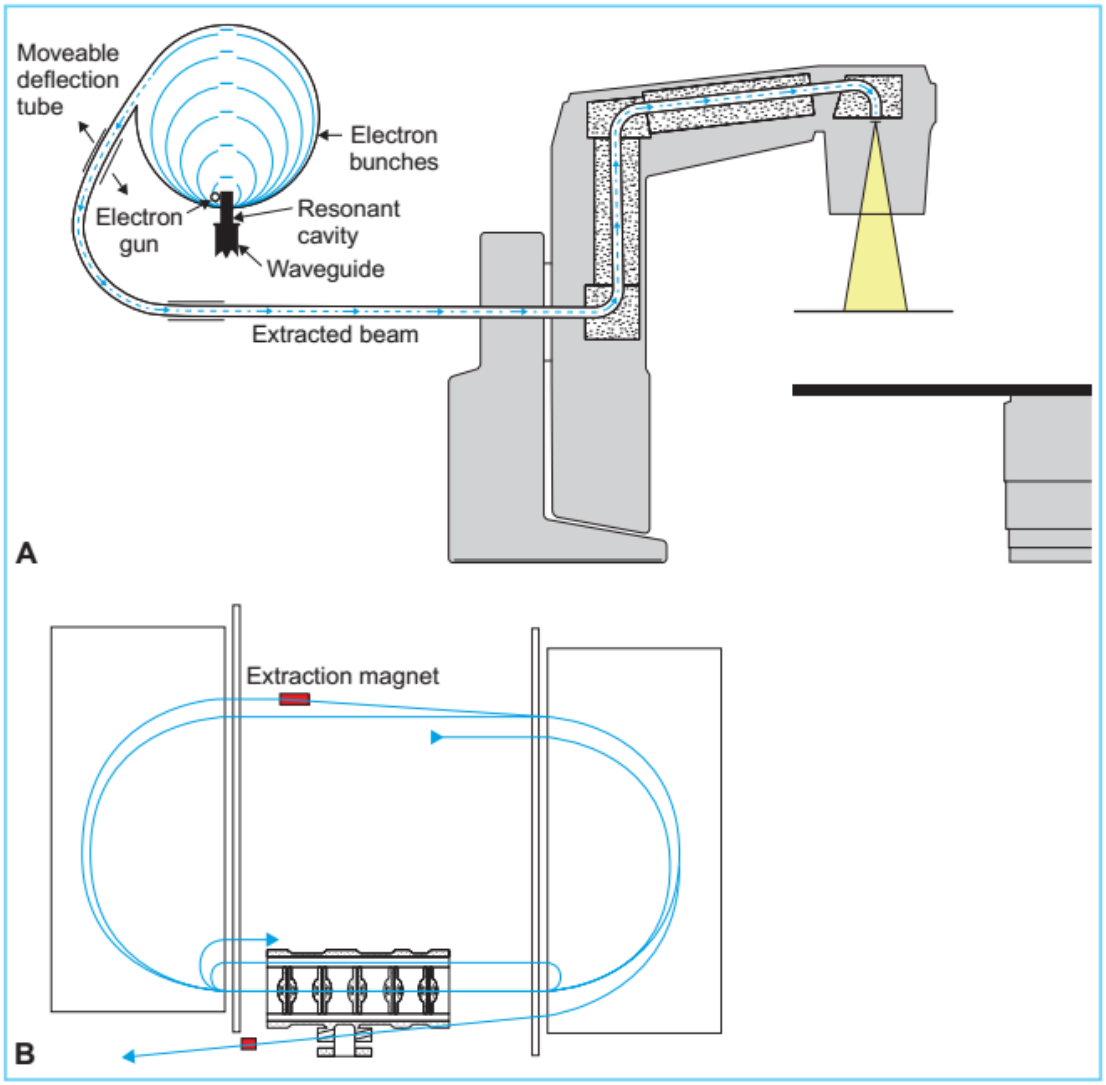

Figure 4.12. A: Schematic diagram of a circular microtron unit. B: Electron orbits and accelerating cavities in a racetrack microtron.

4.6 .Cyclotron

The cyclotron is a charged particle accelerator, mainly used for nuclear physics research. In radiation therapy, these machines have been used as a source of high-energy protons for proton beam therapy. More recently, the cyclotrons have been adopted for generating neutron beams.

In the latter case, the deuterons (^2_1H)are accelerated to high energies and then made to strike a suitable target to produce neutrons by nuclear reactions. One such reaction occurs when a beam of deuterons, accelerated to a high energy (~15 to 50 MeV), strikes a target of low atomic number, such as beryllium. Neutrons are produced by a process called stripping (Section 2.8.D). Another important use of the cyclotron in medicine is as a particle accelerator for the production of certain radionuclides.

A schematic diagram illustrating the principle of cyclotron operation is shown in Figure 4.13. The machine consists essentially of a short metallic cylinder divided into two sections, usually referred to as Ds. These Ds are highly evacuated and placed between the poles of a DC magnet (not shown), producing a constant magnetic field. An alternating potential is applied between the two Ds. Positively charged particles such as protons or deuterons are injected into the chamber at the center of the two Ds. Under the action of the magnetic field, the particles travel in a circular orbit. The frequency of the alternating potential is adjusted such that as the particle passes from one D to the other, it is accelerated by the electric field of the right polarity. With each pass between the Ds, the particle receives an increment of energy and the radius of its orbit increases. Thus, by making many revolutions, the particle such as a deuteron achieves kinetic energy as high as 30 MeV.

There is a limit to the energy that a particle can attain by the above process. According to the theory of relativity, as the particle reaches high velocity (in the relativistic range), further acceleration causes the particle to gain in mass. This causes the particle to get out of step with the frequency of the alternating potential applied to the Ds. This problem has been solved in the synchrotrons where the frequency of the potential is adjusted to compensate for the increase in particle mass.

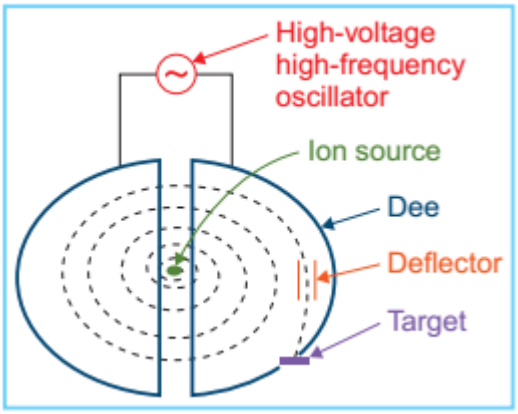

Figure 4.13. Diagram illustrating the principle of operation of a cyclotron.

4.7 .Machines Using Radionuclides

Radionuclides such as radium-226, cesium-137, and cobalt-60 have been used as sources of g rays for teletherapy. These γ rays are emitted from the radionuclides as they undergo radioactive disintegration.

Of all the radionuclides, ^{60}Co has proved to be the most suitable for external beam radiotherapy. The reasons for its choice over radium and cesium are higher possible specific activity (curies per gram), greater radiation output per curie, and higher average photon energy. These characteristics for the three radionuclides are compared in Table 4.1. In addition, radium is much more expensive and has greater self-absorption of its radiation than either cesium or cobalt.

A. Cobalt-60 Unit

A.1. Source

The ^{60}Co source is produced by irradiating ordinary stable ^{59}Co with neutrons in a reactor. The nuclear reaction can be represented by ^{59}Co(n,γ) ^{60}Co.

The ^{60}Co source, usually in the form of a solid cylinder, disks, or pallets, is contained inside a stainless-steel capsule and sealed by welding. This capsule is placed into another steel capsule which is again sealed by welding. The double-welded seal is necessary to prevent any leakage of the radioactive material.

TABLE 4.1 Teletherapy Source Characteristics

Radionuclide	Half-Life (y)	γ-Ray Energy (MeV)	Γ-Value[a] $\left(\frac{Rm^2}{Ci-h}\right)$	Specific Activity Achieved in Practice (Ci/g)
Radium-226 (filtered by 0.5 mm Pt)	1,622	0.83 (avg.)	0.825	~0.98
Cesium-137	30.0	0.66	0.326	~50
Cobalt-60	5.26	1.17, 1.33	1.30	~200

The ^{60}Co source decays to ^{60}Ni with the emission of β particles (E_{max} =0.32 MeV) and two photons per disintegration of energies 1.17 and 1.33 MeV (decay scheme given in Fig. 1.5).

These γ rays constitute the useful treatment beam. The β particles are absorbed in the cobalt metal and the stainless-steel capsules resulting in the emission of bremsstrahlung x-rays and a small number of characteristic x-rays. However, these x-rays of average energy around 0.1 MeV do not contribute appreciably to the dose in the patient because they are strongly attenuated in the material of the source and the capsule. The other "contaminants" to the treatment beam are the lower-energy γ rays produced by the interaction of the primary γ radiation with the source itself, the surrounding capsule, the source housing, and the collimator system.

The scattered components of the beam contribute significantly (~10%) to the total intensity of the beam. All these secondary interactions thus, to some extent, result in heterogeneity of the beam.

In addition, electrons are also produced by these interactions and constitute what is usually referred to as the electron contamination of the photon beam.

A typical teletherapy ^{60}Co source is a cylinder of diameter ranging from 1.0 to 2.0 cm and is positioned in the cobalt unit with its circular end facing the patient. The fact that the radiation source is not a point source complicates the beam geometry and gives rise to what is known as the geometric penumbra.

A.2. Source Housing

The housing for the source is called the source head (Fig. 4.14). It consists of a steel shell filled with lead for shielding purposes and a device for bringing the source in front of an opening in the head from which the useful beam emerges.

Also, a heavy metal alloy sleeve is provided to form an additional primary shield when the source is in the off position.

Figure 4.14. Photograph of cobalt unit, theratron 780. Illustration of transmission penumbra: A: Nondivergent collimating block. B: Divergent collimating block.

A number of methods have been developed for moving the source from the off position to the on position. These methods have been discussed in detail by Johns and Cunningham. It will suffice here to mention briefly four different mechanisms: (a) the source mounted on a rotating wheel inside the sourcehead to carry the source from the off position to the on position؛ (b) the source mounted on a heavy metal drawer plus its ability to slide horizontally through a hole running through the sourcehead—in the on position the source faces the aperture for the treatment beam and in the off position the source moves to its shielded location and a light source mounted on the same drawer occupies the on position of the source; (c) mercury is allowed to flow into the space immediately below the source to shut off the beam; and (d) the source is fixed in front of the aperture and the beam can be turned on and off by a shutter consisting of heavy metal jaws. All of the above mechanisms incorporate a safety feature in which the source is returned automatically to the off position in case of a power failure.

A.3. Beam Collimation and Penumbra

A collimator system is designed to vary the size and shape of the beam to meet the individual treatment requirements. The simplest form of a continuously adjustable diaphragm consists of two pairs of heavy metal blocks. Each pair can be moved independently to obtain a square or a rectangleshaped field. Some collimators are multivane type, i.e., multiple blocks to control the size of the beam. In either case, if the inner surface of the blocks is made parallel to the central axis of the beam, the radiation will pass through the edges of the collimating blocks resulting in what is known as the transmission penumbra (illustrated in Fig. 4.15A). The extent of this penumbra will be more pronounced for larger collimator openings because of greater obliquity of the rays at the edges of the blocks. This effect has been minimized in some designs by shaping the collimator blocks so that the inner surface of the blocks remains always parallel to the edge of the beam (Fig. 4.15B). In these collimators, the blocks are hinged to the top of the collimator housing so that the slope of the blocks is coincident with the included angle of the beam. Although the transmission penumbra can be minimized with such an arrangement, it cannot be completely removed for all field sizes.

The term penumbra, in a general sense, means the region, at the edge of a radiation beam، over which the dose rate changes rapidly as a function of distance from the beam axis. The transmission penumbra, mentioned

above, is the region irradiated by photons which are transmitted through the edge of the collimator block.

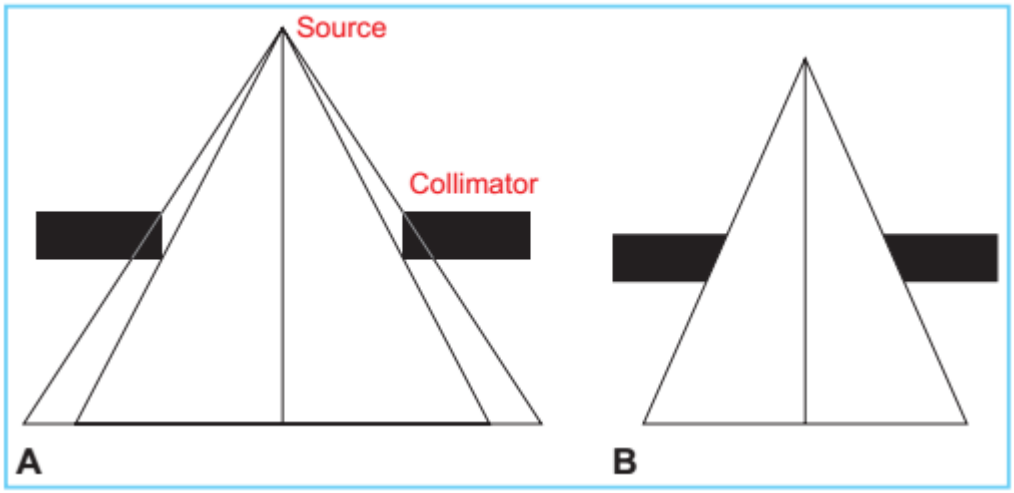

Figure 4.15. Illustration of transmission penumbra: A: Nondiverging collimating block. B: Diverging collimating block.

Another type of penumbra, known as the geometric penumbra, is illustrated in Figure 4.16.

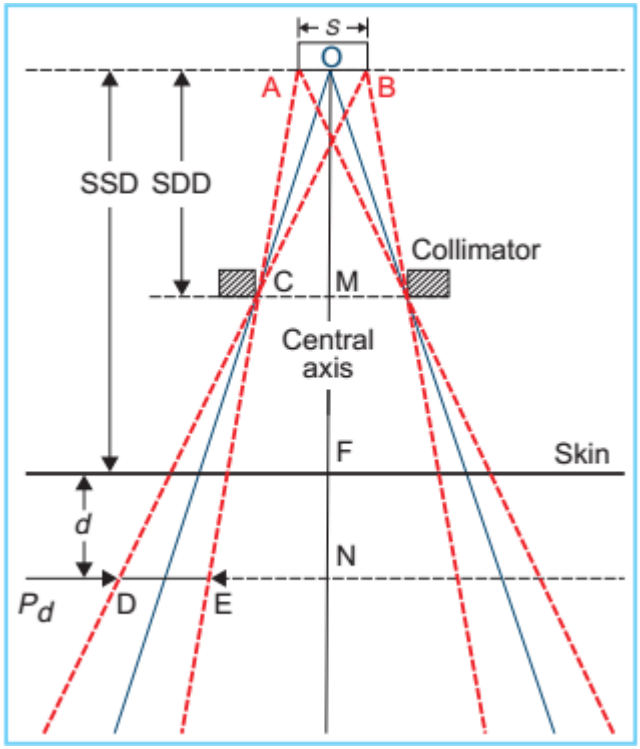

Figure 4.16. Diagram for calculating geometric penumbra.

The geometric width of the penumbra (P_d) at any depth (d) from the surface of a patient can be determined by considering similar triangles ABC and DEC. From geometry, we have

$$\frac{DE}{AB} = \frac{CE}{CA} = \frac{CD}{CB} = \frac{MN}{OM} = \frac{OF + FN - OM}{OM} \tag{4.1}$$

If AB = s, the source diameter, OM = SDD, the source to diaphragm distance, OF = SSD, the source to surface distance, then from the previous equation, the penumbra (DE) at depth d is given by

$$P_d = \frac{s(SSD + d - SDD)}{SDD} \tag{4.2}$$

The penumbra at the surface can be calculated by substituting d = 0 in Equation 4.2.

As Equation 4.2 indicates, the penumbra width increases with increase in source diameter، SSD, and depth but decreases with an increase in SDD. The geometric penumbra, however, is independent of field size as long as the movement of the diaphragm is in one plane, that is, SDD stays constant with increase in field size.

Because SDD is an important parameter in determining the penumbra width, this distance can be increased by extendable penumbra trimmers. These trimmers consist of heavy metal bars to attenuate the beam in the penumbra region, thus "sharpening" the field edges. The penumbra, however, is not eliminated completely but reduced since SDD with the trimmers extended is increased. The new SDD is equal to the source to trimmer distance. An alternative way of reducing the penumbra is to use secondary blocks, placed close to the patient, for redefining or shaping the field. As will be discussed in Chapter 13, the blocks should not be placed closer than 15 to 20 cm from the patient because of excessive electron contaminants produced by the block carrying tray.

The combined effect of the transmission and geometric penumbras is to create a region of dose variation at the field edges. A dose profile of the beam measured across the beam in air at a given distance from the source would show dosimetrically the extent of the penumbra. However، at a depth in the patient the dose variation at the field border is a function of not only geometric and transmission penumbras but also the scattered radiation produced in the patient. Thus, dosimetrically, the term physical penumbra width has been defined as the lateral distance between two specified isodose curves4 at a specified depth.

4.8 .Heavy Particle Beams

Whereas x-rays and electrons are the main radiations used in radiotherapy, heavy particle beams offer special advantages with regard to dose localization and therapeutic gain (greater effect on tumor than on normal tissue). These particles include neutrons, protons, deuterons, a particles، negative pions, and heavy ions accelerated to high energies. Their use in radiation therapy is still experimental, and because of the enormous cost involved, only a few institutions have been able to acquire these modalities for clinical trials. From the literature, which is full of encouraging as well as discouraging reports about their efficacy, it appears that the role of heavy particles in radiation therapy is not yet established. However, the radiobiologic interest in the field remains as strong as ever.

A. Neutrons

High-energy neutron beams for radiotherapy are produced by deuterium–tritium (D–T) generators, cyclotrons, or linear accelerators. The bombarding particles are either deuterons or protons and the target material is usually beryllium, except in the D–T generator in which tritium is used as the target.

A.1. D–T Generator

A low-energy deuteron beam (100 to 300 keV) incident on a tritium target yields neutron by the following reaction:

$$^{2}_{1}\mathrm{H} + {}^{3}_{1}\mathrm{H} \rightarrow {}^{4}_{2}\mathrm{He} + {}^{1}_{0}n + 17.6\ \mathrm{MeV} \qquad (4.3)$$

The disintegration energy of 17.6 MeV is shared between the helium nucleus (a particle) and the neutron, with about 14 MeV given to the neutron. The neutrons thus produced are essentially monoenergetic and isotropic (same yield in all directions). The major problem is the lack of sufficient dose rate at the treatment distance. The highest dose rate that has been achieved so far is about 15 cGy/min at 1 m. The advantage of D–T generators over other sources is that its size is small enough to allow isocentric mounting on a gantry.

A.2. Cyclotron

Deuterons accelerated to high energies (~15 to 50 MeV) by a cyclotron bombard a low atomic number target such as beryllium to produce neutrons according to a stripping reaction (see Section 2.8.D):

$$^{2}_{1}\mathrm{H} + {}^{9}_{4}\mathrm{Be} \rightarrow {}^{10}_{5}\mathrm{B} + {}^{1}_{0}n$$

Neutrons are produced mostly in the forward direction with a spectrum of energies, as shown in Figure 4.15. The average neutron energy is about 40% to 50% of the deuteron energy.

The bombarding particles can also be protons accelerated to high energies by a cyclotron or a linear accelerator. The neutron spectrum produced by 41 MeV protons is shown in Figure 4.17.

A hydrogenous material filter (e.g., polyethylene) is used to reduce the number of low-energy neutrons in the spectrum.

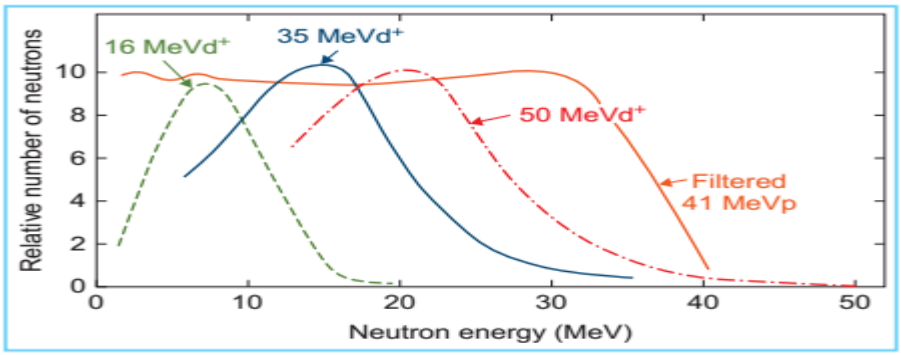

Figure 4.17. Neutron spectra produced by deuterons on the beryllium target.

B. Protons and Heavy Ions

Proton beams for therapeutic application range in energy from 150 to 250 MeV. These beams can be produced by a cyclotron, synchrocyclotron, or a linear accelerator. The major advantage of high-energy protons and other heavy charged particles is their characteristic distribution of dose with depth (Fig. 4.18). As the beam traverses the tissues, the dose deposited is approximately constant with depth until near the end of the range where the dose peaks out to a high value followed by a rapid falloff to zero. The region of high dose at the end of the particle range is called the Bragg peak.

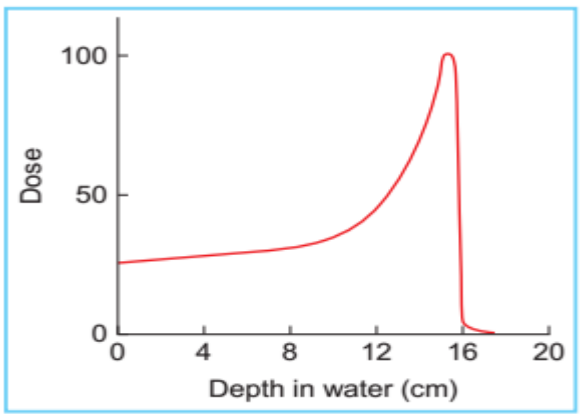

Figure 4.18. Depth–dose distribution characteristic of heavily charged particles, showing the Bragg peak.

Figure 14.19 shows the range–energy relationship for protons. The approximate range for other particles with the same initial velocity can be calculated by the following relationship:

$$R_1/R_2 = (M_1/M_2) \cdot (Z_2/Z_1)^2 \qquad (4.4)$$

where R_1 and R_2 are particle ranges, M_1 and M_2 are the masses, and Z_1 and Z_2 are the charges of the two particles being compared. Thus, from the range energy data for protons one can calculate the range of other particles. The energy of heavily charged particles or stripped nuclei is often expressed in terms of kinetic energy per nucleon (specific kinetic energy) or MeV/u where u is the mass number of the nucleus. Particles with the same MeV/u have approximately the same velocity. For example, 150 MeV protons, 300 MeV deuterons, and 600 MeV helium ions all have approximately the same velocity and ranges of about 16 cm, 32 cm, and 16 cm in water, respectively.

However, for ions heavier than helium, the range for the same MeV/u is somewhat less than that for protons. As predicted by Equation 4.4, the range is dependent on A/Z^2, where A is the mass number and Z is the nuclear charge. Since A/Z^2 decreases as the ions get heavier, the range of heavier ions is less than the range of lighter ions for the same MeV/u with the exception of protons.

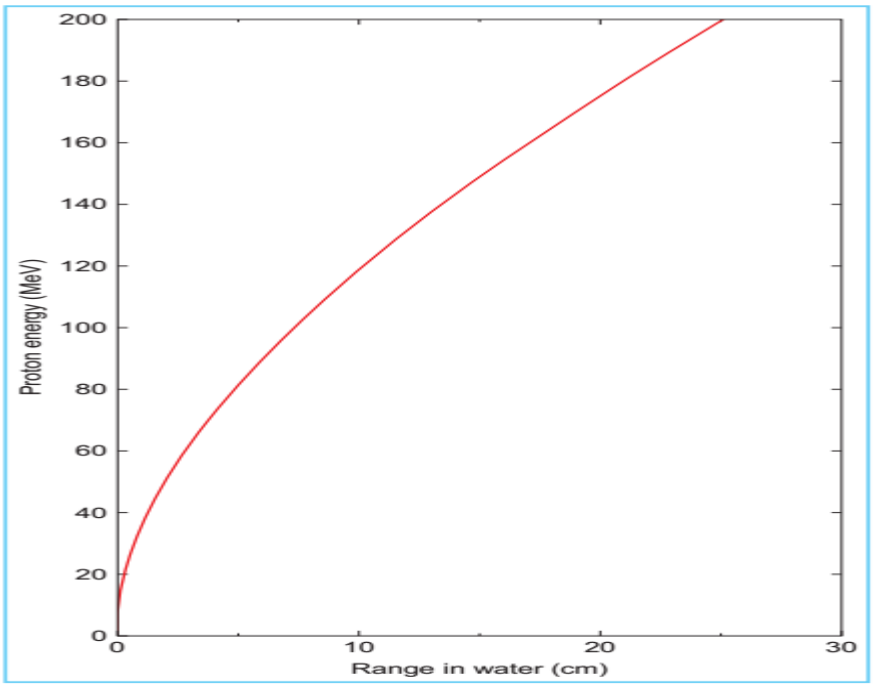

Figure 4.19. range–energy relationship for protons.

C. Negative Pions

The existence of pi mesons was theoretically predicted by Yukawa in 1935 when he postulated that protons and neutrons in the nucleus are held together by a mutual exchange of pi mesons.

A pi meson (or pion) has a mass 273 times that of electron and may have a positive charge, a negative charge, or may be neutral. The charged pions decay into mu mesons and neutrinos with a mean life of 2.54×10^{-8} seconds and the neutral pions decay into pairs of photons with a mean life of about 10^{-16} seconds.

$$\pi^+ \rightarrow \mu^+ + \nu$$
$$\pi^- \rightarrow \mu^- + \tilde{\nu}$$
$$\pi^0 \rightarrow h\nu_1 + h\nu_2$$

Only negative pions have been used for radiation therapy.

Beams of negative pions can be produced in a nuclear reaction. Protons of energy in the range of 400 to 800 MeV, produced in a cyclotron or a linear accelerator, are usually used for pion beam production for radiotherapy. Beryllium is a suitable target material. Pions of positive، negative, and zero charge with a spectrum of energies are produced and negative pions of suitable energy are extracted from the target using bending and focusing magnets. Pions of energy close to 100 MeV are of interest in radiation therapy, providing a range in water of about 24 cm.

The Bragg peak exhibited by pions is more pronounced than other heavy particles because of the additional effect of nuclear disintegration by $\pi-$ capture. This phenomenon, commonly known as star formation, occurs when a pion is captured by a nucleus in the medium near the end of its range. A pion capture results in the release of several other particles such as protons, neutrons, and α particles.

Although pion beams have attractive radiobiologic properties, they suffer from the problems of low dose rates, beam contamination, and high cost.

5 Interactions of Ionizing Radiation

When an x- or γ-ray beam passes through a medium, interaction between photons and matter can take place with the result that energy is transferred to the medium. The initial step in the energy transfer involves the ejection of electrons from the atoms of the absorbing medium.

These high-speed electrons transfer their energy by producing ionization and excitation of the atoms along their paths. If the absorbing medium consists of body tissues, sufficient energy may be deposited within the cells, destroying their reproductive capacity. However, most of the absorbed energy is converted into heat, producing no biologic effect.

5.1 .Ionization

Ionization is the process by which a neutral atom acquires a positive or a negative charge. Ionizing radiations can strip electrons from atoms as they travel through media. An atom from which electron has been removed is a positive ion. In some cases, the stripped electron may subsequently combine with a neutral atom to form a negative ion. The combination of a positively charged ion and a negatively charged ion (usually a free electron) is called an ion pair.

Charged particles such as electrons, protons, and α-particles are known as directly ionizing radiation provided, they have sufficient kinetic energy to produce ionization by collision as they penetrate matter. The energy of the incident particle is lost in a large number of small increments along the ionization track in the medium, with an occasional interaction in which the ejected electron receives sufficient energy to produce a secondary track of its own, known as a δ ray. If، on the other hand, the energy lost by the incident particle is not sufficient to eject an electron from the atom but is used to raise the electrons to higher-energy levels, the process is termed excitation.

Uncharged particles such as neutrons and photons are indirectly ionizing radiation because they liberate directly ionizing particles from matter when they interact with matter. Ionizing photons interact with the atoms of a material or absorber to produce high-speed electrons by three major processes: photoelectric effect, Compton effect, and pair production. Before considering each process in detail, we shall discuss the mathematical aspects of radiation absorption.

5.2 .Photon Beam Description

An x-ray beam emitted from a target or a γ-ray beam emitted from a radioactive source consists of a large number of photons, usually with a variety of energies. A beam of photons can be described by many terms, some of which are defined as follows:

1. The fluence (Φ) of photons is the quotient dN by da, where dN is the number of photons that enter an imaginary sphere of cross-sectional area da:

$$\Phi = \frac{dN}{da} \tag{5.1}$$

2. Fluence rate or flux density (f) is the fluence per unit time:

$$\phi = \frac{d\Phi}{dt} \tag{5.2}$$

where dt is the time interval.

3. Energy fluence (Ψ) is the quotient of dE_{fl} by da, where dE_{fl} is the sum of the energies of all the photons that enter a sphere of cross-sectional area da:

$$\Psi = \frac{dE_{fl}}{da} \tag{5.3}$$

For a monoenergetic beam, dE_{fl} is just the number of photons dN times energy $h\upsilon$ carried by each photon:

$$dE_{fl} = dN \cdot h\upsilon \tag{5.4}$$

4. Energy fluence rate, energy flux density, or intensity (ψ) is the energy fluence per unit time:

$$\psi = \frac{d\Psi}{dt} \tag{5.5}$$

5.3 .Photon Beam Attenuation

An experimental arrangement designed to measure the attenuation characteristics of a photon beam is shown in Figure 5.1. A narrow beam of monoenergetic photons is incident on an absorber of variable thickness. A detector is placed at a fixed distance from the source and sufficiently farther away from the absorber so that only the primary photons (those photons that passed through the absorber without interacting) are measured by the detector. Any photon scattered by the absorber is not supposed to be measured in this arrangement. Thus, if a photon interacts with an atom, it is either completely absorbed or scattered away from the detector.

Under these conditions, the reduction in the number of photons (dN) is proportional to the number of incident photons (N) and to the thickness of the absorber (dx). Mathematically,

$$dN \propto Ndx$$
$$dN = -\mu Ndx \tag{5.6}$$

where μ is the constant of proportionality, called the attenuation coefficient. The minus sign indicates that the number of photons decreases as the absorber thickness increases. The above equation can also be written in terms of intensity (I):

$$dI = -\mu Idx$$

or

$$\frac{dI}{I} = -\mu dx \tag{5.7}$$

If thickness x is expressed as a length, then μ is called the linear attenuation coefficient. For example, if the thickness is measured in centimeters, the units of μ are 1/cm, or cm^{-1}.

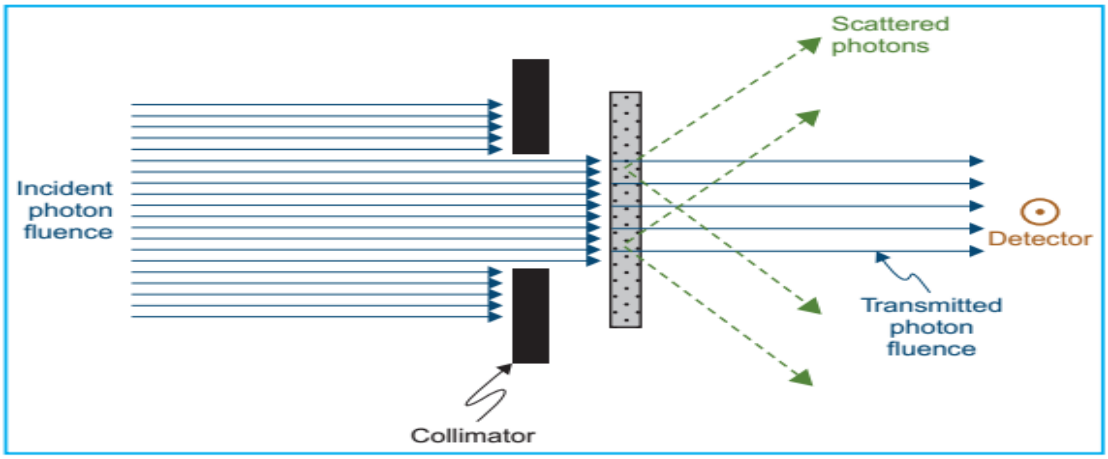

Figure 5.1. Diagram to illustrate an experimental arrangement for studying narrow-beam attenuation through an absorber. Measurements are under "good geometry".

Equation 5.7 is identical to Equation 2.1, which describes radioactive decay, and μ is analogous to decay constant λ. As before, the differential equation for attenuation can be solved to yield the following equation:

$$I(x) = I_0 e^{-\mu x} \tag{5.8}$$

where I(x) is the intensity transmitted by a thickness x and I_0 is the intensity incident on the absorber. If I(x) is plotted as a function of x for a narrow monoenergetic beam, a straight line will be obtained on semilogarithmic

paper (Fig. 5.2A), showing that the attenuation of a monoenergetic beam is described by an exponential function.

The term analogous to half-life (Section 2.4) is the half-value layer (HVL) defined as the thickness of an absorber required to attenuate the intensity of the beam to half its original value. That means that when x = HVL, I/I_0 = 1/2, by definition. Thus, from Equation 5.8 it can be shown that:

$$\text{HVL} = \frac{\ln 2}{\mu} \approx \frac{0.693}{\mu} \qquad (5.9)$$

As mentioned previously, exponential attenuation strictly applies to a monoenergetic beam.

Figure 5.2B is a general attenuation curve for a monoenergetic beam or a beam whose HVL does not change with absorber thickness. Such a curve may be used to calculate the number of HVLs required to reduce the transmitted intensity to a given percentage of the incident intensity.

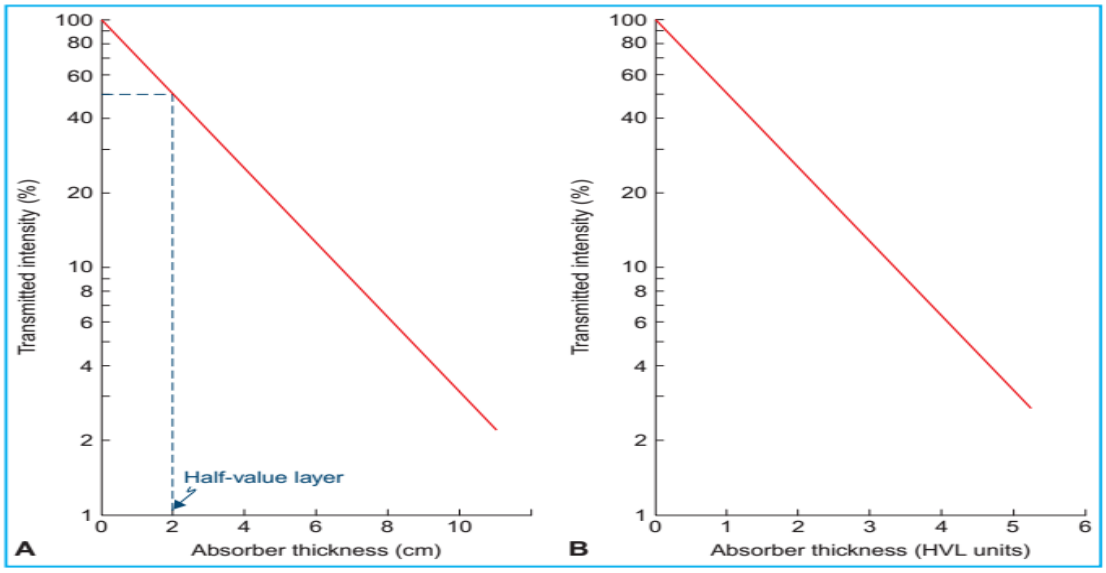

Figure 5.2. A: Graph showing percent transmission of a narrow monoenergetic photon beam as a function of absorber thickness. For this quality beam and absorber material, HVL = 2 cm and m = 0.347 cm^{-1}.

B: Universal attenuation curve showing percent transmission of a narrow monoenergetic beam as a function of absorber thickness in units of half-value layer (HVL).

A practical beam produced by an x-ray generator, however, consists of a spectrum of photon energies. Attenuation of such a beam is no longer exponential. This effect is seen in Figure 5.3، in which the plot of transmitted intensity on semilogarithmic paper is not a straight line.

The slope of the attenuation curve decreases with increasing absorber thickness because the absorber or filter preferentially removes the lower-energy photons. As shown in Figure 5.3, the first HVL is defined as that thickness of material which reduces the incident beam intensity by 50% . The second HVL reduces the beam to 50% of its intensity after it has been transmitted through the first HVL. Similarly, the third HVL represents the quality of the beam after it has been transmitted through the absorber of thickness equal to two HVLs. In general, for a heterogeneous beam, the first HVL is less than the subsequent HVLs. As the filter thickness increases، the average energy of the transmitted beam increases or the beam becomes increasingly harder.

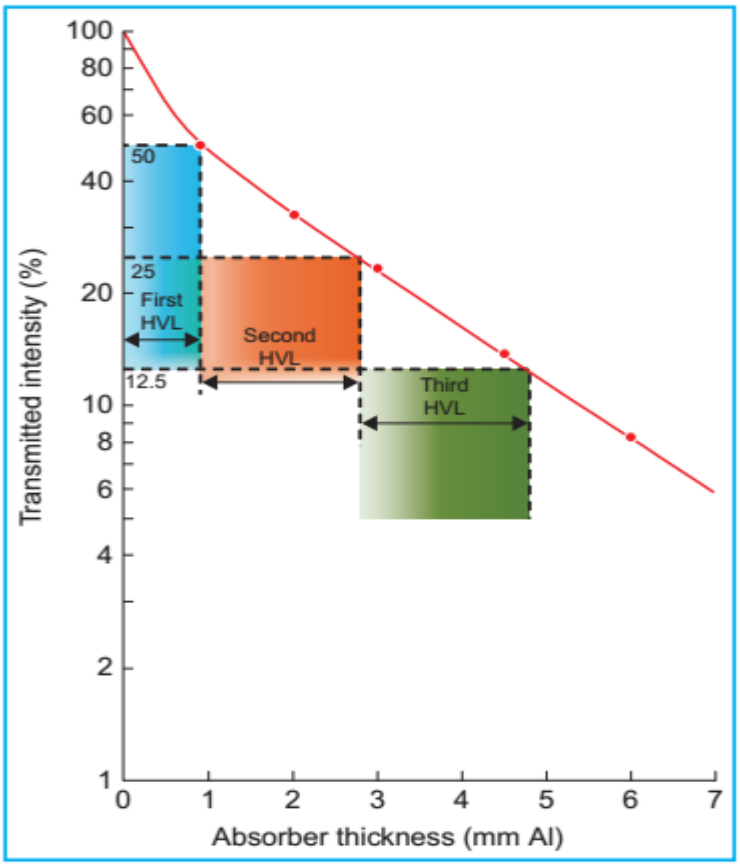

Figure 5.3. Schematic graph showing transmission of an x-ray beam with a spectrum of photon energies through an aluminum absorber. First half-value layer (HVL) = 0.99 mm Al, second HVL = 1.9 mm Al, and third HVL = 2.0 mm Al.

Thus, by increasing the filtration in such an x-ray beam, one increases the penetrating power or the HVL of the beam.

5.4 .Coefficients

A. Attenuation Coefficient

In the previous section, we discussed the linear attenuation coefficient μ, which has units of length^{-1} (e.g., cm^{-1}). In general, this coefficient depends on the energy of the photons and the nature of the material. Since the attenuation produced by a thickness x depends on the number of electrons presented in that thickness, m depends on the density of the material. Thus, by dividing μ by density ρ, the resulting coefficient ($\frac{\mu}{\rho}$) will be independent of density; $\frac{\mu}{\rho}$ is known as the mass attenuation coefficient. This is a more fundamental coefficient than the linear coefficient, since the density has been factored out and its dependence on the nature of the material does not involve density but rather the atomic composition.

If ρ is measured in g/cm^3, then the mass attenuation coefficient has units of cm^2/g. When using μ/ρ in the attenuation Equation 5.8, the thickness should be expressed as ρx, which has units of g/cm^2, because $\mu x = (\mu/\rho)(\rho x)$ and ρx = (g/cm^3)(cm).

In addition to the cm and g/cm^2 units, the absorber thickness can also be expressed in units of electrons/cm^2 and atoms/cm^2. The corresponding coefficients for the last two units are electronic attenuation coefficient ($_e\mu$) and atomic attenuation coefficient ($_a\mu$), respectively:

$$_e\mu = \frac{\mu}{\rho} \cdot \frac{1}{N_0} \text{ cm}^2/\text{electron} \tag{5.10}$$

$$_a\mu = \frac{\mu}{\rho} \cdot \frac{Z}{N_0} \text{ cm}^2/\text{atom} \tag{5.11}$$

where Z is the atomic number and N_0 is the number of electrons per gram and N_0 is given by:

$$N_0 = \frac{N_A \cdot Z}{A_W} \tag{5.12}$$

where N_A is Avogadro's number and A_W is the atomic weight.

The attenuation coefficient represents the fraction of photons removed per unit thickness.

The transmitted intensity I(x) in Equation 5.8 is caused by photons that did not interact with the material. Those photons that produced interactions will transfer part or all of their energy to the material and result in part or all of that energy being absorbed.

B. Energy Transfer Coefficient

When a photon interacts with the electrons in the material, a part or all of its energy is converted into kinetic energy of electrons. If only a part of the photon energy is given to the electron, the photon itself is scattered with reduced energy. The scattered photon may interact again with a partial or complete transfer of energy to the electrons. Thus, a photon may experience one or multiple interactions in which the energy lost by the photon is converted into kinetic energy of electrons.

If we consider a photon beam traversing a material, the fraction of photon energy transferred into kinetic energy of charged particles per unit thickness of absorber is given by the energy transfer coefficient (μ_{tr}). This coefficient is related to μ as follows:

$$\mu_{tr} = \frac{\bar{E}_{tr}}{h\nu}\mu \qquad (5.13)$$

where $\bar{E}_{tr}$ is the average energy transferred into kinetic energy of charged particles per interaction. The mass energy transfer coefficient is given by $\frac{\overline{\mu_{tr}}}{\rho}$.

C. Energy Absorption Coefficient

Most of the electrons set in motion by the photons will lose their energy by inelastic collisions (ionization and excitation) with atomic electrons of the material. A few, depending on the atomic number of the material, will lose energy by bremsstrahlung interactions with the nuclei. The bremsstrahlung energy is radiated out of the local volume as x-rays and is not included in the calculation of locally absorbed energy.

The energy absorption coefficient (μ_{en}) is defined as the product of energy transfer coefficient and (1 – g) where g is the fraction of the energy of secondary charged particles that is lost to bremsstrahlung in the material.

$$\mu_{en} = \mu_{tr}(1 - g) \qquad (5.14)$$

As before, the mass energy absorption coefficient is given by $\frac{\mu_{en}}{\rho}$.

For most interactions involving soft tissues or other low-Z material in which electrons lose energy almost entirely by ionization collisions, the bremsstrahlung component is negligible.

Thus, $\mu_{en} = \mu_{tr}$ under those conditions. These coefficients can differ appreciably when the kinetic energies of the secondary particles are high and the material traversed has a high atomic number. The energy absorption coefficient is an important quantity in radiotherapy since it allows the evaluation of energy absorbed in the tissues, a quantity of interest in predicting the biologic effects of radiation.

5.5 .Interactions of Photons with Matter

Attenuation of a photon beam by an absorbing material is caused by five major types of interactions. One of these, photodisintegration, was considered in Section 2.8F. This reaction between photon and nucleus is only important at very high photon energies (>10 MeV). The other four processes are coherent scattering, the photoelectric effect, the Compton effect, and the pair production. Each of these processes can be represented by its own attenuation coefficient, which varies in its particular way with the energy of the photon and with the atomic number of the absorbing material. The total attenuation coefficient is the sum of individual coefficients for these processes:

$$\mu/\rho = \sigma_{\text{coh}}/\rho + \tau/\rho + \sigma_c/\rho + \pi/\rho \qquad (5.15)$$

where σ_{coh}, τ, σ_c, and π are attenuation coefficients for coherent scattering, photoelectric effect, Compton effect, and pair production, respectively.

5.6 .Coherent Scattering

The coherent scattering, also known as classical scattering or Rayleigh scattering, is illustrated in Figure 5.4. The process can be visualized by considering the wave nature of electromagnetic radiation. This interaction consists of an electromagnetic wave passing near the electron and setting it into oscillation. The oscillating electron reradiates the energy at the same frequency as the incident electromagnetic wave. These scattered x-rays have the same wavelength as the incident beam. Thus, no energy is changed into electronic motion and no energy is absorbed in the medium. The only effect is the scattering of the photon at small angles. The coherent scattering is probable in high-atomic-number materials and with photons of low energy. The process is only of academic interest in radiation therapy.

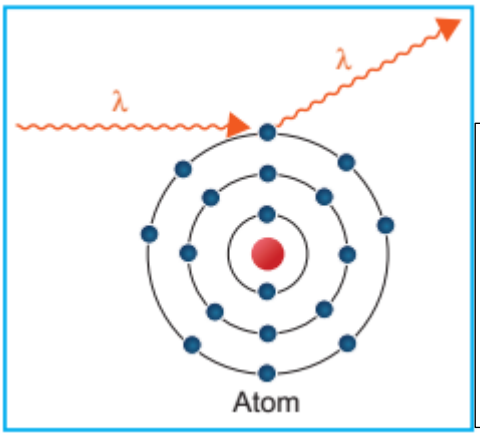

Figure 5.4. Diagram illustrating the process of coherent scattering. The scattered photon has the same wavelength as the incident photon. No energy is transferred.

5.7 .Photoelectric Effect

The photoelectric effect is a phenomenon in which a photon is absorbed by an atom, and as a result one of its orbital electrons is ejected (Fig. 5.5). In this process, the entire energy ($h\upsilon$) of the photon is first absorbed by the atom and then essentially all of it is transferred to the atomic electron. The kinetic energy of the ejected electron (called the photoelectron) is equal to $h\upsilon - E_B$‘ where E_B is the binding energy of the electron. Interactions of this type can take place with electrons in the K, L, M, or N shells.

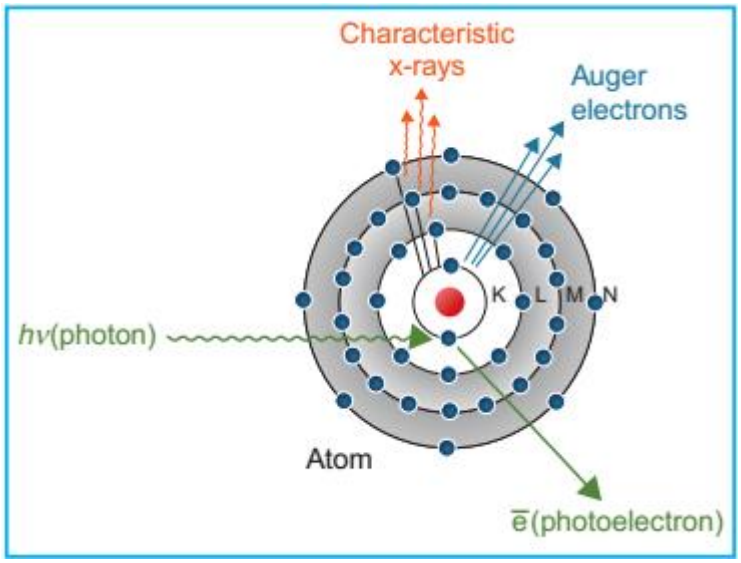

Figure 5.5. Illustration of the photoelectric effect.

After the electron has been ejected from the atom, a vacancy is created in the shell, thus leaving the atom in an excited state. The vacancy can be filled by an outer orbital electron with the emission of a characteristic x-ray (Section 3.4B). There is also the possibility of emission of Auger

electrons (Section 2.7C), which occurs when the energy released as a result of the outer electron filling the vacancy is given to another electron in a higher shell, which is subsequently ejected. Because the K-shell binding energy of soft tissues is only about 0.5 keV, the energy of the characteristic photons produced in biologic absorbers is very low and can be considered to be locally absorbed. For higher-atomic-number materials, the characteristic photons are of higher energy and may deposit energy at large distances compared with the range of the photoelectron.

In such cases, the local energy absorption is reduced by the energy emitted as characteristic radiation (also called fluorescent radiation), which is considered to be remotely absorbed.

The probability of photoelectric absorption depends on the photon energy as illustrated in Figure 5.6, where the mass photoelectric attenuation coefficient ($\frac{\tau}{\rho}$) is plotted as a function of photon energy. Data are shown for water, representing a low-atomic-number material similar to tissue, and for lead, representing a high-atomic-number material. On logarithmic paper, the graph is almost a straight line with a slope of approximately –3; therefore, we get the following relationship between t/r and photon energy:

$$\tau/\rho \propto 1/E^3 \qquad (5.16)$$

The graph for lead has discontinuities at about 15 and 88 keV. These are called absorption edges, and correspond to the binding energies of L and K shells. A photon with energy less than 15 keV does not have enough energy to eject an L electron. Thus, below 15 keV, the interaction is limited to the M- or higher-shell electrons. When the photon has an energy that just equals the binding energy of the L shell, resonance occurs and the probability of photoelectric absorption involving the L shell becomes very high. Beyond this point, if the photon energy is increased, the probability of photoelectric attenuation decreases approximately as $1/E^3$ until the next discontinuity, the K absorption edge. At this point on the graph, the photon has 88 keV energy, which is just enough to eject the K electron. As seen in Figure 5.6, the absorption probability in lead at this critical energy increases dramatically, by a factor of about 10.

The discontinuities or absorption edges for water are not shown in the graph because the K absorption edge for water occurs at very low photon energies (~0.5 keV).

The data for various materials indicates that photoelectric attenuation depends strongly on the atomic number of the absorbing material. The following approximate relationship holds:

$$\tau/\rho \propto Z^3 \tag{5.17}$$

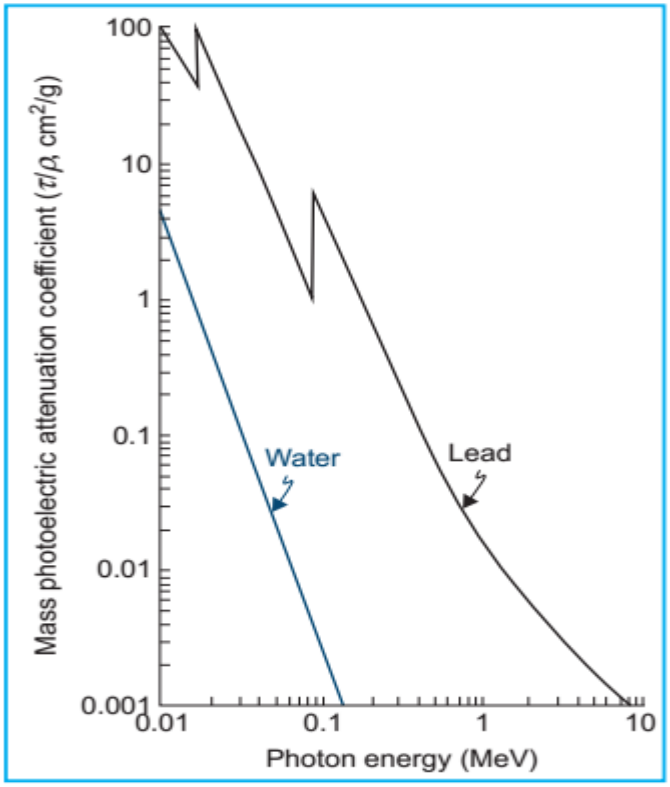

Figure 5.6. Mass photoelectric attenuation coefficient ($\frac{\tau}{\rho}$) plotted against photon energy. Curves for water (Z_{eff} = 7.42) and lead (Z = 82). X-ray Attenuation Coefficients from 10 keV to 100 MeV.

This relationship forms the basis of many applications in diagnostic radiology. The difference in Z of various tissues such as bone, muscle, and fat amplify differences in x-ray absorption ،provided the primary mode of interaction is photoelectric. This Z^3 dependence is also exploited when using contrast materials such as $BaSO_4$ mix and Hypaque. In therapeutic radiology, the low-energy beams produced by superficial and orthovoltage machines cause unnecessary high absorption of x-ray energy in bone as a result of this Z^3 dependence; this problem will be discussed later in Section 5.10. By combining Equations 5.16 and 5.17, we have

$$\tau/\rho \propto Z^3/E^3 \tag{5.18}$$

The angular distribution of electrons emitted in a photoelectric process depends on the photon energy. For a low-energy photon, the photoelectron

is emitted most likely at 90 degrees relative to the direction of the incident photon. As the photon energy increases, the photoelectrons are emitted in a more forward direction.

5.8 .Compton Effect

In the Compton process, the photon interacts with an atomic electron as though it were a "free" electron, that is, the binding energy of the electron is much less than the energy of the bombarding photon. In this interaction, the electron receives some energy from the photon and is emitted at an angle u (Fig. 5.7). The photon, with reduced energy, is scattered at an angle ϕ.

The Compton process can be analyzed in terms of a collision between two particles, a photon and an electron. By applying the laws of conservation of energy and momentum, one can derive the following relationships:

$$E = h\nu_0 \frac{\alpha(1 - \cos\phi)}{1 + \alpha(1 - \cos\phi)} \tag{5.19}$$

$$h\nu' = h\nu_0 = \frac{1}{1 + \alpha(1 - \cos\phi)} \tag{5.20}$$

$$\cot\theta = (1 + \alpha)\tan\phi/2 \tag{5.21}$$

where $h\upsilon_0$ ،$h\upsilon^-$, and E are the energies of the incident photon, scattered photon, and electron ،respectively, and $\alpha = h\nu_0/m_0c^2$, where m_0c^2 is the rest energy of the electron (0.511 MeV). If $h\upsilon_0$ is expressed in MeV, then $\alpha = h\upsilon_0/0.511$.

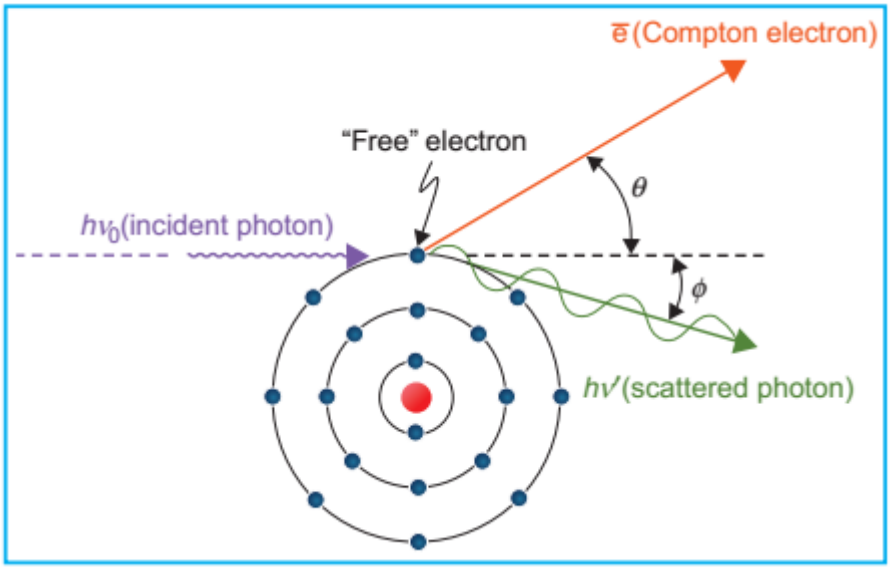

Figure 5.7. Diagram illustrating the Compton effect.

A. Special Cases of Compton Effect

Direct Hit

If a photon makes a direct hit with the electron, the electron will travel forward (θ = 0 degrees) and the scattered photon will travel backward (ϕ = 180 degrees) after the collision. In such a collision, the electron will receive maximum energy E_{max} and the scattered photon will be left with minimum energy $h\nu'$ min. One can calculate Emax and $h\nu'$ min by substituting cos ϕ = cos 180 degrees = –1 in Equations 5.19 and 5.20:

$$E_{max} = h\nu_0 \frac{2\alpha}{1+2\alpha} \tag{5.22}$$

$$h\nu'_{min} = h\nu_0 \frac{1}{1+2\alpha} \tag{5.23}$$

Grazing Hit

If a photon makes a grazing hit with the electron, the electron will be emitted at right angles (θ = 90 degrees) and the scattered photon will go in the forward direction (ϕ = 0 degrees). By substituting cos ϕ = cos 0 degrees = 1 in Equations 5.19 and 5.20, one can show that for this collision E = 0 and $h\nu' = h\nu_0$.

90-Degree Photon Scatter

If a photon is scattered at right angles to its original direction (ϕ = 90 degrees), one can calculate E and $h\nu'$ from Equations 5.19 and 5.20 by substituting cos ϕ = cos 90 degrees = 0. The angle of the electron emission in this case will depend on a, according to Equation 5.21.

Examples. Some useful examples will now be given to illustrate application of the Compton effect to practical problems.

a. Interaction of a low-energy photon. If the incident photon energy is much less than the rest energy of the electron, only a small part of its energy is imparted to the electron, resulting in a scattered photon of almost the same energy as the incident photon. For example, suppose $h\nu_0$ = 51.1 keV; then $\alpha = h\nu_0/m_0c^2$ = 0.0511 MeV/0.511 MeV = 0.1. From Equations 5.22 and 5.23:

$$E_{max} = 51.1\,(\text{keV})\frac{2(0.1)}{1+2(0.1)} = 8.52\,\text{keV} \tag{5.24}$$

$$h\nu'_{min} = 51.1\,(\text{keV})\frac{1}{1+2(0.1)} = 42.58\,\text{keV} \tag{5.25}$$

Thus, for a low-energy photon beam, the Compton scattered photons have approximately the same energy as the original photons. Indeed, as the incident photon energy approaches zero, the Compton effect becomes the classical scattering process described in Section 5.6.

b. Interaction of a high-energy photon. If the incident photon has a very high energy (much greater than the rest energy of the electron), the photon loses most of its energy to the Compton electron and the scattered photon has much less energy. Suppose $h\nu_0$= 5.11 MeV; then α = 10.0. From Equations 5.22 and 5.23,

$$E_{max} = 5.11\,(\text{MeV})\frac{2(10)}{1+2(10)} = 4.87\,\text{MeV} \tag{5.26}$$

$$h\nu'_{min} = 5.11\,(\text{keV})\frac{1}{1+2(10)} = 0.24\,\text{MeV} \tag{5.27}$$

In contrast to example (a) above, the scattered photons produced by high-energy photons carry away only a small fraction of the initial energy. Thus, at high photon energy, the Compton effect causes a large amount of energy absorption compared with the Compton interactions involving low-energy photons.

c. Compton scatter at ϕ = 90 degrees and 180 degrees. In designing radiation protection barriers (walls) to attenuate scattered radiation, one

needs to know the energy of the photons scattered at different angles. The energy of the photons scattered by a patient under treatment at 90 degrees with respect to the incident beam is of particular interest in calculating barrier or wall thicknesses against scattered radiation.

By substituting ϕ = 90 degrees in Equation 5.20, we obtain

$$h\nu' = \frac{h\nu_0}{1+\alpha} \tag{5.28}$$

For high-energy photons with a >> 1, the previous equation reduces to

$$h\nu' \approx \frac{h\nu_0}{\alpha} \tag{5.29}$$

or

$$h\nu' = m_0c^2 = 0.511 \text{ MeV}$$

Similar calculations for scatter at ϕ = 180 degrees will indicate $h\nu'$ = 0.255 MeV. Thus, if the energy of the incident photon is high (a >> 1), we have the following important generalizations:

a. the radiation scattered at right angles is independent of incident energy and has a maximum value of 0.511 MeV؛

b. the radiation scattered backward is independent of incident energy and has a maximum value of 0.255 MeV.

The maximum energy of radiation scattered at angles between 90 and 180 degrees will lie between the above energy limits. However, the energy of the photons scattered at angles less than 90 degrees will be greater than 0.511 MeV and will approach the incident photon energy for the condition of forward scatter. Because the energy of the scattered photon plus that of the electron must equal the incident energy, the electron may acquire any energy between zero and E_{max} given by Equation 5.22.

B. Dependence of Compton Effect on Energy and Atomic Number

It was mentioned previously that the Compton effect is an interaction between a photon and a free electron. Practically, this means that the energy of the incident photon must be large compared with the electron-binding energy. This is in contrast to the photoelectric effect, which becomes most probable when the energy of the incident photon is equal to or slightly greater than the binding energy of the electron. Thus, as the photon energy increases beyond the binding energy of the K electron, the photoelectric effect decreases rapidly with energy (Equation 5.16) (Fig. 5.6) and the Compton effect becomes more and more important. However,

as shown in Figure 5.8, the Compton effect also decreases with increasing photon energy.

Because the Compton interaction involves essentially free electrons in the absorbing material، it is independent of atomic number Z. It follows that the Compton mass attenuation coefficient $\frac{\sigma_c}{\rho}$ is independent of Z and depends only on the number of electrons per gram. Although the number of electrons per gram of elements decreases slowly but systemically with atomic number, most materials except hydrogen can be considered as having approximately the same number of electrons per gram (Table 5.1). Thus, $\frac{\sigma_c}{\rho}$ is nearly the same for all materials.

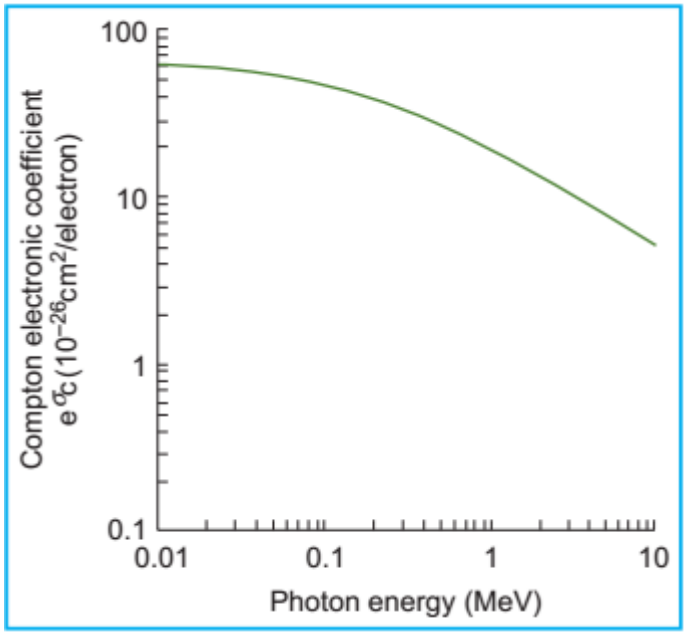

Figure 5.8. a plot of Compton electronic coefficient ${}_e\sigma_c$ against photon energy. the mass coefficient ($\frac{\sigma_c}{\rho}$) is obtained by multiplying the electronic coefficient with the number of electrons per gram for a given material.

TABLE 5.1 Number of Electrons per Gram of Various Materials

Material	Density (g/cm³)	Atomic Number	Number of Electrons per Gram
Hydrogen	0.0000899	1	6.00×10^{23}
Carbon	2.25	6	3.01×10^{23}
Oxygen	0.001429	8	3.01×10^{23}
Aluminum	2.7	13	2.90×10^{23}
Copper	8.9	29	2.75×10^{23}
Lead	11.3	82	2.38×10^{23}
		Effective Atomic Number	
Fat	0.916	6.46	3.34×10^{23}
Muscle	1.04	7.64	3.31×10^{23}
Water	1.00	7.51	3.34×10^{23}
Air	0.001293	7.78	3.01×10^{23}
Bone	1.65	12.31	3.19×10^{23}

From the previous discussion, it follows that if the energy of the beam is in the region where the Compton effect is the only possible mode of interaction, approximately the same attenuation of the beam will occur in any material of equal density thickness, expressed as g/cm^2. For example, in the case of a ^{60}Co γ-ray beam that interacts by Compton effect, the attenuation per g/cm^2 for bone is nearly the same as that for soft tissue. However, 1 cm of bone will attenuate more than 1 cm of soft tissue, because bone has a higher electron density, ρ_e (number of electrons per cubic centimeter), which is given by density times the number of electrons per gram. If the density of bone is assumed to be 1.65 g/cm^3 and that of soft tissue 1.04 g/cm^3, then the attenuation produced by 1 cm of bone will be equivalent to that produced by 1.53 cm of soft tissue:

$$(1\text{ cm})\frac{(\rho_e)_{\text{bone}}}{(\rho_e)_{\text{muscle}}} = (1\text{ cm}) \times \frac{1.65\ (\text{g/cm}^3) \times 3.19 \times 10^{23}\ (\text{electrons/g})}{1.04\ (\text{g/cm}^3) \times 3.31 \times 10^{23}\ (\text{electrons/g})} = 1.53\text{ cm}$$

5.9 .Pair Production

If the energy of the photon is greater than 1.02 MeV, the photon may interact with matter through the mechanism of pair production. In this process (Fig. 5.9), the photon interacts strongly with the electromagnetic field of an atomic nucleus and gives up all its energy in the process of creating a pair consisting of a negative electron (e^-) and a positive electron (e^+). Because the rest mass energy of the electron is equivalent to 0.51 MeV, a minimum energy of 1.02 MeV is required to create the pair of electrons. Thus, the threshold energy for the pair production process is 1.02 MeV. The photon energy in excess of this threshold is shared between

the particles as kinetic energy. The total kinetic energy available for the electron–positron pair is given by ($h\upsilon$ – 1.02) MeV. The particles tend to be emitted in the forward direction relative to the incident photon.

The most probable distribution of energy is for each particle to acquire half the available kinetic energy, although any energy distribution is possible. For example, in an extreme case, it is possible that one particle may receive all the energy, while the other receives no energy.

The pair production process is an example of an event in which energy is converted into mass، as predicted by Einstein's equation $E = mc^2$. The reverse process, namely the conversion of mass into energy, takes place when a positron combines with an electron to produce two photons، called the annihilation radiation.

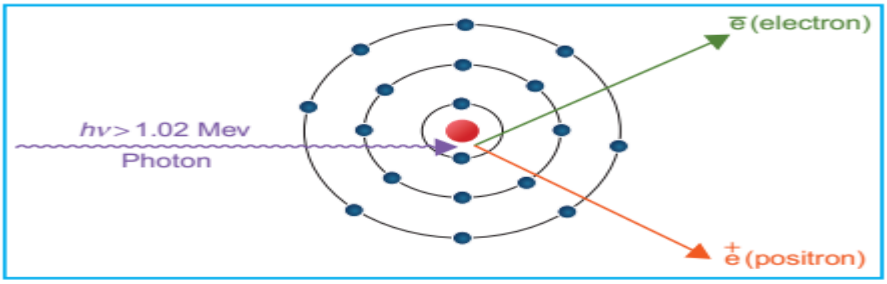

Figure 5.9. Diagram illustrating the pair production process.

A. Annihilation Radiation

The positron created as a result of pair production process loses its energy as it traverses the matter by the same type of interactions as an electron does, namely by ionization, excitation، and bremsstrahlung. Near the end of its range, the slowly moving positron combines with one of the free electrons in its vicinity to give rise to two annihilation photons, each having 0.51 MeV energy. Because momentum is conserved in the process, the two photons are ejected in opposite directions (Fig. 5.10).

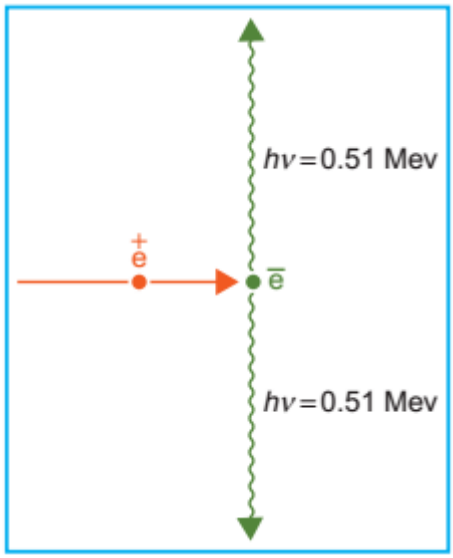

Figure 5.10. Diagram illustrating the production of annihilation radiation.

B. Variation of Pair Production with Energy and Atomic Number

Because the pair production results from an interaction with the electromagnetic field of the nucleus, the probability of this process increases rapidly with atomic number. The attenuation coefficient for pair production (Π) varies with Z^2 per atom, Z per electron, and approximately Z per gram. In addition, for a given material, the likelihood of this interaction increases as the logarithm of the incident photon energy above the threshold energy; these relationships are shown in Figure 5.11. To remove the major dependence of the pair production process on atomic number, the coefficients per atom have been divided by Z^2 before plotting. For energies up to about 20 MeV, the curves are almost coincident for all materials, indicating that a $\Pi \propto Z^2$.

At higher energies, the curves for high-Z materials fall below the low-Z materials because of the screening of the nuclear charge by the orbital electrons.

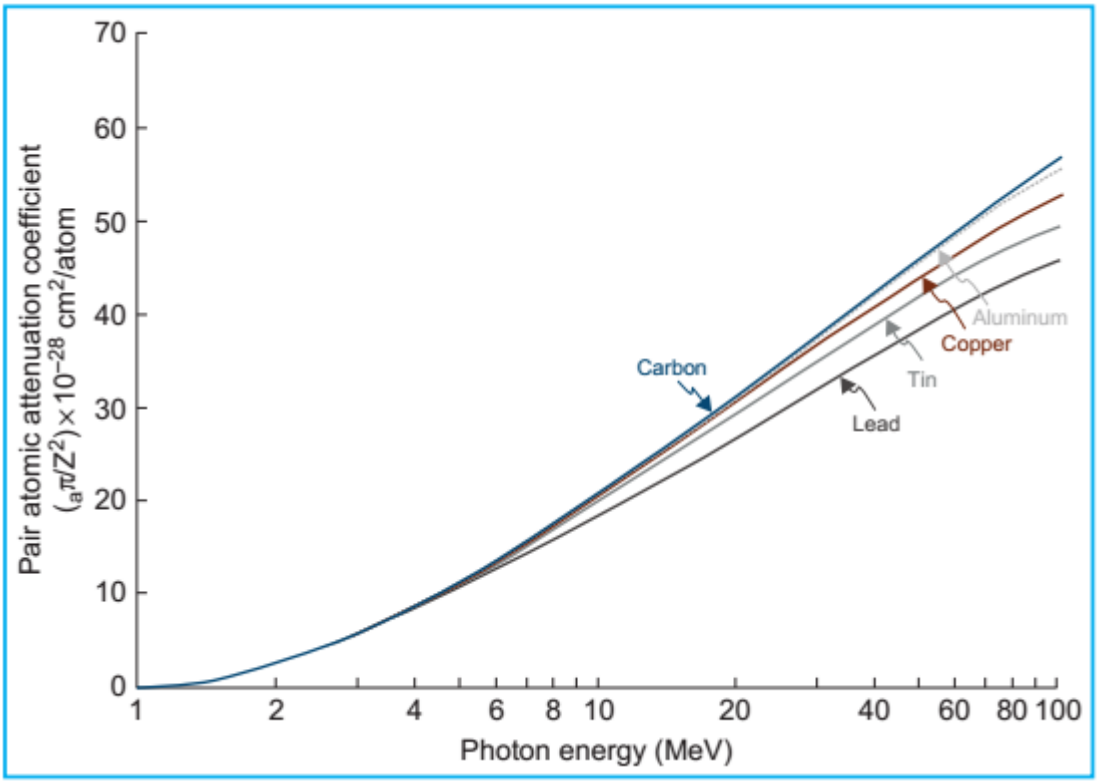

Figure 5.11. plot of the pair atomic attenuation coefficient divided by the square of the atomic number as a function of photon energy for carbon (Z = 6) and lead (Z = 82). the mass attenuation coefficient can be obtained by multiplying a π/ Z^2 obtained from the graph, first by Z^2 and then by the number of atoms per gram of the absorber.

5.10 .Relative Importance of Various Types of Interactions

The total mass attenuation coefficient $(^{\mu}/_{\rho})$ is the sum of the four individual coefficients:

$$\underset{\text{total}}{(\mu/\rho)} = \underset{\text{photoelectric}}{(\tau/\rho)} + \underset{\text{coherent}}{(\sigma_{coh}/\rho)} + \underset{\text{Compton}}{(\sigma_c/\rho)} + \underset{\text{pair}}{(\pi/\rho)} \qquad (5.30)$$

As noted previously, coherent scattering is only important for very low photon energies (<10 keV) and high-Z materials. At therapeutic energies, it is often omitted from the sum.

Figure 5.12 is the plot of total coefficient $(^{\mu}/_{\rho})$ total versus energy for two different materials، water and lead, representative of low- and high-atomic-number materials. The mass attenuation coefficient is large for low energies and high-atomic-number media because of the predominance of photoelectric interactions under these conditions.

The attenuation coefficient decreases rapidly with energy until the photon energy far exceeds the electron-binding energies and the Compton effect becomes the predominant mode of interaction. In the Compton range of energies, the μ/ρ of lead and water do not differ greatly, since this type of interaction is independent of atomic number. The coefficient, however, decreases with energy until pair production begins to become important. The dominance of pair production occurs at energies much greater than the threshold energy of 1.02 MeV.

The relative importance of various types of interactions is presented in Table 5.2. These data for water will also be true for soft tissue. The photon energies listed in column 1 of Table 5.2 represent monoenergetic beams. As discussed in Chapter 3, an x-ray tube operating at a given peak voltage produces radiation of all energies less than the peak energy. As a rough approximation and for the purposes of Table 5.2, one may consider the average energy of an x-ray beam to be equivalent to one-third of the peak energy. Thus, a 26-keV monoenergetic beam in column 1 should be considered as equivalent to an x-ray beam produced by an x-ray tube operated at about 78 kVp. Of course, the accuracy of this approximation is limited by the effects of filtration on the energy spectrum of the beam.

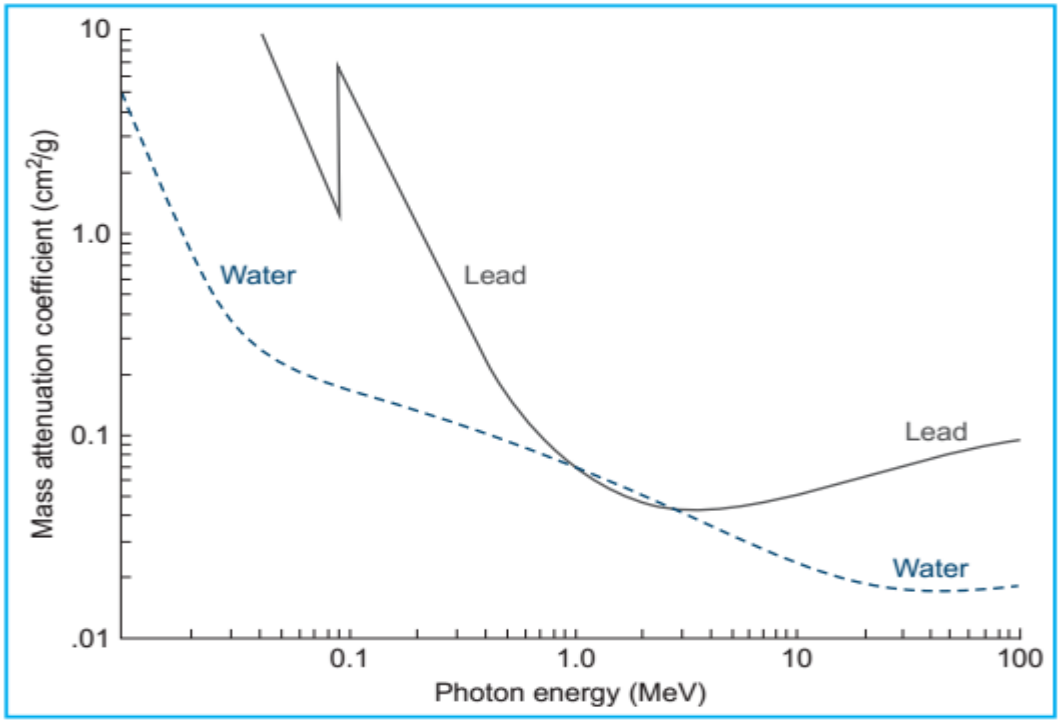

Figure 5.12. plot of the total mass attenuation coefficient (μ/ρ) as a function of photon energy for lead and water.

TABLE 5.2 Relative Importance of Photoelectric (τ), Compton (σ), and Pair Production (π) Processes in Water

	Relative Number of Interactions (%)		
Photon Energy (MeV)	τ	σ	π
0.01	95	5	0
0.026	50	50	0
0.060	7	93	0
0.150	0	100	0
4.00	0	94	6
10.00	0	77	23
24.00	0	50	50
100.00	0	16	84

5.11 .Interactions of Charged Particles

Whereas photons interact with matter by photoelectric, Compton, or pair production processes، charged particles (electrons, protons, α-particles, and nuclei) interact principally by ionization and excitation. Radiative collisions in which the charged particle interacts by the bremsstrahlung process are possible but are much more likely for electrons than for heavier charged particles.

The charged particle interactions or collisions are mediated by Coulomb force between the electric field of the traveling particle and electric fields of orbital electrons and nuclei of atoms of the material. Collisions between the particle and the atomic electrons result in ionization and excitation of the atoms. Collisions between the particle and the nucleus result in radiative loss of energy or bremsstrahlung. Particles also suffer scattering without significant loss of energy. Because of much smaller mass, electrons suffer greater multiple scattering than do heavier particles.

In addition to the Coulomb force interactions, heavy charged particles give rise to nuclear reactions, thereby producing radioactive nuclides. For example, a proton beam passing through tissue produces short-lived radioisotopes ^{11}C, ^{13}N, and ^{15}O, which are positron emitters.

The rate of kinetic energy loss per unit path length of the particle (dE/dx) is known as the stopping power (S). The quantity S/ρ is called the mass stopping power, where ρ is the density of the medium and is usually expressed in MeV cm^2/g.

A. Heavy Charged Particles

Charged particles may be classified as light or heavy, depending upon their masses. Electrons and positrons are called "light" particles because of their very tiny mass (~1/1840 of mass of a proton). A charged particle is called "heavy" if its rest mass is large compared to the rest mass of an electron. Examples include protons, mesons, α-particles, and atomic nuclei.

The rate of energy loss per unit path length or stopping power caused by ionization interactions for charged particles is proportional to the square of the particle charge and inversely proportional to the square of its velocity. Thus, as the particle slows down, its rate of energy loss increases and so does the ionization or absorbed dose to the medium. As was seen in Figure 4.16, the dose deposited in water increases at first very slowly with depth and then very sharply near the end of the range, before dropping to an almost zero value. This peaking of dose near the end of the particle range is called the Bragg peak.

Because of the Bragg peak effect and minimal scattering, protons and heavier charged particle beams provide a much sought-after advantage in radiotherapy—the ability to concentrate dose inside the target volume and minimize dose to surrounding normal tissues. Clinical applications of proton beams are discussed in Chapter 26.

B. Electrons

Interactions of electrons when passing through matter are quite similar to those of heavy particles. However, because of their relatively small mass, the electrons suffer greater multiple scattering and changes in the direction of motion. As a consequence, the Bragg peak is not observed for electrons. Multiple changes in direction during the slowing down process smear out the Bragg peak.

In water or soft tissue, electrons, like other charged particles, lose energy predominantly by ionization and excitation. This results in deposition of energy or absorbed dose in the medium. As stated earlier, the ionization process consists of stripping electrons from the atoms. If the energy transferred to the orbital electron is not sufficient to overcome the binding energy, it is displaced from its stable position and then returns to it; this effect is called excitation. Furthermore, in the process of ionization, occasionally the stripped electron receives sufficient energy to produce an

ionization track of its own. This ejected electron is called a secondary electron, or a δ ray.

Again, because of its small mass, an electron may interact with the electromagnetic field of a nucleus and be decelerated so rapidly that a part of its energy is lost as bremsstrahlung. The rate of energy loss as a result of bremsstrahlung increases with the increase in the energy of the electron and the atomic number of the medium. Electron interactions and the clinical applications of electron beams will be discussed in Chapter 14.

5.12 .Interactions of Neutrons

Like x-rays and γ-rays, neutrons are indirectly ionizing. However, their mode of interaction with matter is different. Neutrons interact basically by two processes: (a) recoiling protons from hydrogen and recoiling heavy nuclei from other elements, and (b) nuclear disintegrations. The first process may be likened to a billiard-ball collision in which the energy is redistributed after the collision between the colliding particles. The energy transfer is very efficient if the colliding particles have the same mass (e.g., a neutron colliding with a hydrogen nucleus). On the other hand, the neutron loses very little energy when colliding with a heavier nucleus. Thus, the most efficient absorbers of a neutron beam are the hydrogenous materials such as paraffin wax or polyethylene. Lead, which is a very good absorber for x-rays, is a poor shielding material against neutrons.

Dose deposited in tissue from a high-energy neutron beam is predominantly contributed by recoil protons. Because of the higher hydrogen content, the dose absorbed in fat exposed to a neutron beam is about 20% higher than in muscle. Nuclear disintegrations produced by neutrons result in the emission of heavy charged particles, neutrons, and γ-rays and give rise to about 30% of the tissue dose. Because of such diverse secondary radiation produced by neutron interactions، the neutron dosimetry is relatively more complicated than the other types of clinical beams.

5.13 .Comparative Beam Characteristics

No one kind of radiation beam is ideal for radiation therapy. Whereas x-rays and electrons are currently the most used beams, particle beams have some unique physical and radiobiologic characteristics that have attracted the attention of many investigators.

Physical advantages of a radiation therapy beam are derived from the depth dose distributions and scatter characteristics. Figures 5.13, 5.14, and 5.15 compare the depth dose characteristics of various beams. It is seen that the depth dose distribution of neutron beams is qualitatively similar to the ^{60}Co γ-rays. The heavy charged particle beams, the Bragg peaks of which were modulated using filters (as is typically done in clinical situations), show a flat dose distribution at the peak region and a sharp dose drop-off beyond the range. Electron beams also show a constant dose region up to about half the particle range and a sharp dose drop-off beyond that point. However، for higher electron energies, the characteristic falloff in dose becomes more gradual. Protons, on the other hand, maintain a sharp cutoff in dose beyond the range, irrespective of energy.

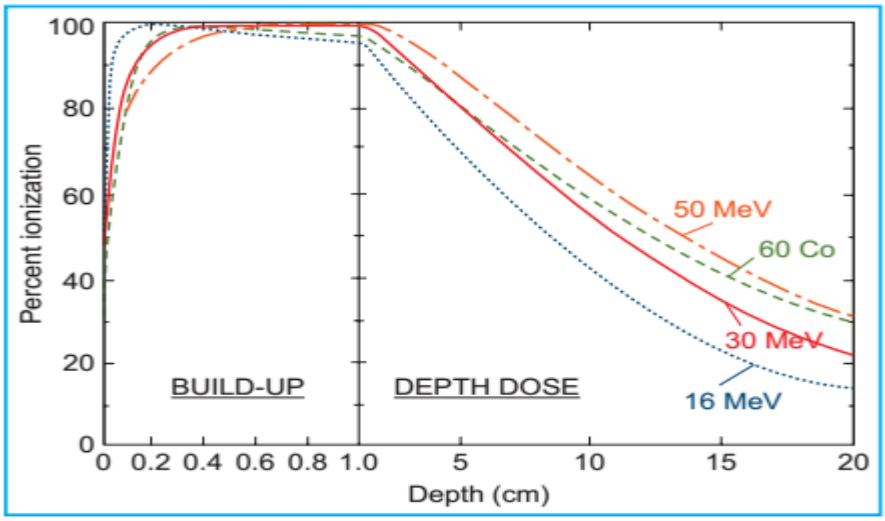

Figure 5.13. Depth dose distribution of neutrons produced by deutrons on beryllium, compared with a cobalt-60 γ beam.

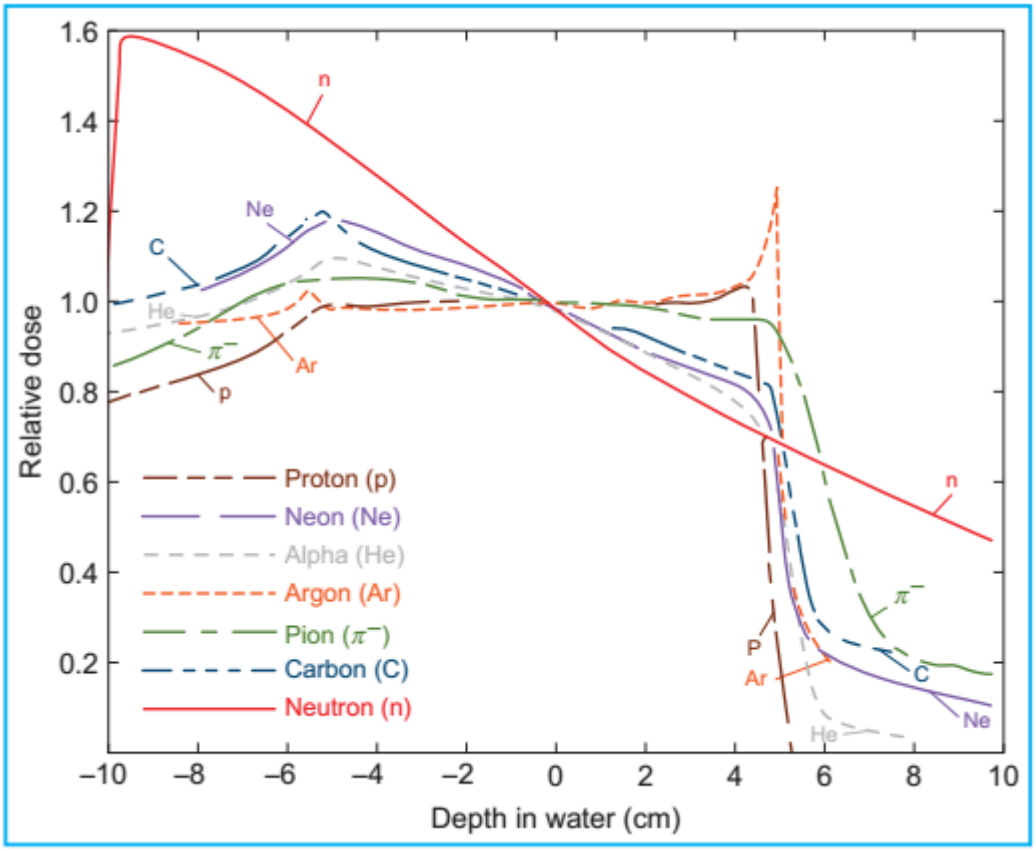

Figure 5.14. Depth dose distribution for various heavy particle beams with modulated Bragg peak at a depth of 10 cm and normalized at the peak center.

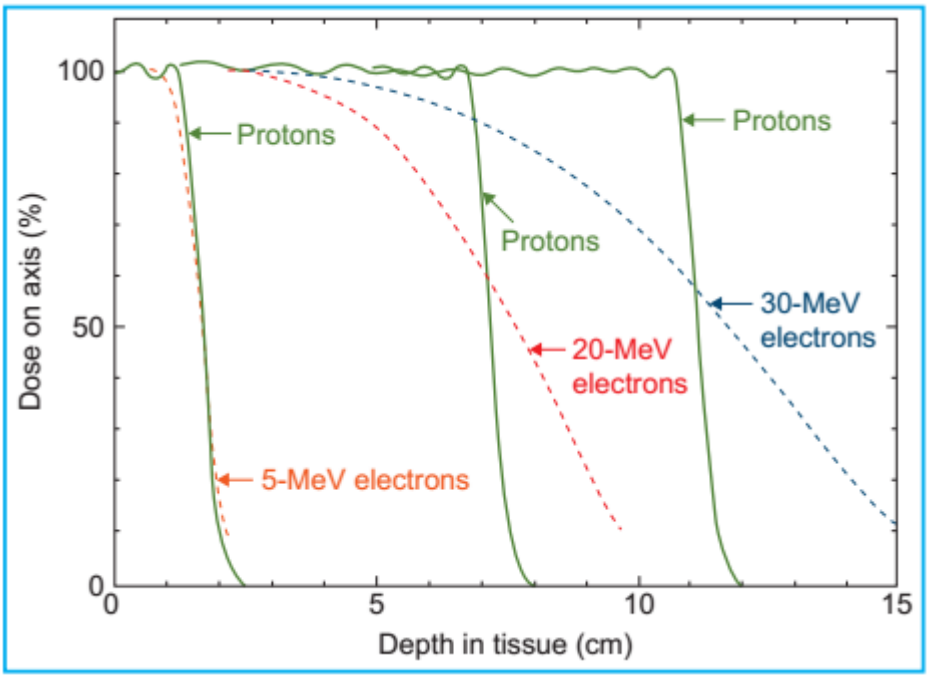

Figure 5.15. Comparison of depth dose distribution for protons and electrons.